1970

Thermal, radiation and mechanical analysis of cylindrical oxide fuel elements of fast reactor in unsteady state

Chi-kang Cheng
Iowa State University

THERMAL, RADIATION AND MECHANICAL ANALYSIS OF CYLINDRICAL OXIDE FUEL ELEMENTS OF FAST REACTOR IN UNSTEADY STATE

by

Chi-kang Cheng

A Dissertation Submitted to the
Graduate Faculty in Partial Fulfillment of
The Requirements for the Degree of
DOCTOR OF PHILOSOPHY

Major Subject: Nuclear Engineering

Approved:

Signature was redacted for privacy.

In Charge of Major Work

Signature was redacted for privacy.

Head of Major Department

Signature was redacted for privacy.

Dean of Graduate College

Iowa State University
Ames, Iowa

1970

TABLE OF CONTENTS

LIST OF TABLES

LIST OF FIGURES

NOMENCLATURE

Primary English Letter Symbol

b	Van der Waals correction term
c	coolant specific heat
C_6	average volumetric contribution of solid fission products per fission per unit volume
d	diameter of gas bubble
d_{cg}	critical diameter of bubble for movement in grain
D	grain size after an annealing time t
D_e	equivalent diameter of coolant channel
D_o	initial grain size; coefficient
D_s	surface diffusion coefficient
e	mean strain
e_c, e_f	emissivities of clad and fuel
e_r, e_θ, e_z	radial, tangential and axial elastic strain deviators
e_{tr}, $e_{t\theta}$, e_{tz}	radial, tangential and axial total strain deviators
e'_{tr}, $e'_{t\theta}$, e'_{tz}	radial, tangential and axial modified total strain deviators
E	modulus of elasticity
E_c, E_f	modulus of elasticity for clad and fuel
$\dot{F}$	fissions per unit volume per unit time
F_{gb}	maximum retarding force of grain boundary
F_s	driving force on bubbles due to thermal gradient

g	defined variable $g = \frac{1}{3}(\varepsilon_r - \varepsilon_\theta - 3\,\varepsilon_R)$
h	heat transfer coefficient between coolant and clad
k	Boltzmann constant
k_o	constant
K	coolant thermal conductivity
K_c	clad thermal conductivity
K_{gap}	gap thermal conductivity
K_{gas}	bonding gas thermal conductivity
K_I, K_{II}, K_{III}	fuel thermal conductivity in region I, II, and III
L	average length across a grain
L_g	thickness of fuel-clad gap
m	number of fission-gas atoms in a bubble
M_1, M_2	molecular weights of fuel and primary vapor constituent in pore
n	number of time intervals for bubble migrating in grain
N	Avogadro's number
$N_{i,n}$	number of bubbles per unit area on grain boundary having been collided i times and having passed n time intervals
N_o	number of bubbles per unit volume
N_t	total number of bubbles per unit volume moving away from grain boundaries
Nu	Nusselt number
p	gas pressure inside a bubble
P	total pressure in fabricated pore
Pe	Peclet number

P_g	pressure in fuel-clad gap
P_o	coolant pressure
P_v	pressure in central void
q	linear power
Q	activation energy for equiaxed-grain growth
Q_I, Q_{II}, Q_{III}	volumetric heat source in region I, II, and III
Q_s^*	activation energy for surface diffusion
r_1	radius at outer surface of columnar-grain region
r_2	radius at outer surface of equiaxed-grain region
r_i, r_o	radii of clad at inner and outer surfaces
r_s	radius at fuel rod surface
r_v	radius of central void
R	universal gas constant
s	average normal stress or hydrostatic stress
s_r, s_θ, s_z	radial, tangential and axial stress deviators
S_b	Stefan-Boltzmann constant
t	irradiation time
t_{cb}	time when bubble attains its critical size for moving away from grain boundary
t_{cg}	time when bubble attains its critical size for movement in grain
T_a	absolute temperature
T_c	bulk coolant temperature
T_g	average temperature in fuel-clad gap
T_i, T_o	temperature of clad at inner and outer surfaces

T_s	temperature at fuel rod surface
u	radial displacement
v	coolant average velocity
V_b	velocity of bubble leaving grain boundary
V_{cb}	critical velocity for bubble leaving grain boundary
V_{cg}	critical velocity for bubble moving in grain
V_g	velocity of bubble moving in grain

Primary Greek Letter Symbol

α	linear coefficient of thermal expansion
γ	surface tension of fuel material
γ_{gb}	grain boundary surface tension
ε_I	irradiation dilatation strain
ε_{pe}	equivalent plastic strain
ε_{pr}, $\varepsilon_{p\theta}$, ε_{pz}	radial, tangential and axial plastic strains
ε_r, ε_θ, ε_z	radial, tangential and axial total strains
ε_{te}	equivalent total strain
ε_R	thermal-irradiation dilatation strain
ε_i	tangential strain of clad at r_i
ε_s	tangential strain of fuel at r_s
ε_v	tangential strain of fuel at r_v
ΔH_v	molar heat of vaporization
$(\frac{\Delta v}{v})_{gas}$	total swelling due to bubbles
$(\frac{\Delta v}{v})_{sgb}$	swelling due to bubbles on grain boundaries
$(\frac{\Delta v}{v})_{sgg}$	swelling due to anchored bubbles in grains

$(\frac{\Delta V}{V})_{sgg'}$	swelling due to new bubbles anchored on original bubble sites in grains
$(\frac{\Delta V}{V})_{sgm}$	swelling due to bubbles moving in grains before reaching a grain boundary
$(\frac{\Delta V}{V})_{sld}$	swelling due to solid fission products
Δt	time interval for bubble movement in grains
λ	non-negative constant
μ	Poisson's ratio
ν	number of diffusion molecules per unit surface area
σ	cross-sectional radius for collision between matrix and vapor molecules
σ'	intrinsic stress of fuel
σ_e	equivalent stress
σ_H	hydrostatic stress
σ_p	proportional limit
σ_r, σ_θ, σ_z	radial, tangential and axial stresses
σ_y	yield strength of 0.2% offset
ρ_c	coolant density
ρ_I, ρ_{II}, ρ_{III}	fraction of theoretical density in region I, II, and III
Ω	molecular volume of fuel

I. INTRODUCTION

There is a widespread interest in the oxides of plutonium, uranium, and thorium, especially, in the system of $(U_{>0.8}Pu_{<0.2})$ as nuclear fuel materials in fast reactors. Notable advantages of their applications are high melting points, freedom from harmful phase transformation, high neutron utilization, stability in intensive radiation and high-temperature coolant media, and high burn-up potentiality. A breeder fuel in either the system ThO_2-UO_2, UO_2-PuO_2 or ThO_2-UO_2-PuO_2 would be feasible because these oxides are isomorphic in structure, and difference in lattice constants of the three oxides is such that the formation of solid solutions would be indicated (1). Many of the physical properties of these oxides have been evaluated, and currently, these oxides are being investigated as candidate fuels for fast reactors.

Solid cylindrical fuel elements used in fast reactors have the advantages of low fabrication cost, compact core, and high capacity of fission-gas retention.

Recently, the radiation and creep solutions for solid and tubular cylindrical fuel elements at steady state (2-4), the radiation growth and swelling analysis for solid cylindrical fuel elements at unsteady state (5,6), the computer program CYGRO-2 for stress analysis of the growth of concentric cylinders with gas bubbles (7), the computer program KER-4 for

thermal analysis of cylindrical fuel rods (8), the computer program NUKER for thermal and mechanical analysis of fuel rods (9), and the computer program CRASH for the evaluation of the creep and plastic behavior of fuel pin sheaths (10) have been given.

The objective of this work is to analyze and calculate stresses and strains due to thermal, radiation and mechanical effects for cylindrical oxide fuel elements of fast reactors in unsteady state during a constant linear power operation. The variables and parameters dealt with in this work will have significant and important effects on the fuel element performance, reactor safety, reliability, and economic operation of oxide fast breeders.

In order to achieve a long operating life of the fuel element, low density oxide fuels are normally used in a fast reactor. The configuration of the low-density cylindrical oxide fuel element with high temperatures and large temperature gradients is usually changed to form a central void in the axial direction in the early operating life (11-13). This phenomenon is generally believed to be the results of the migration of fabricated pores up the temperature gradients by a vapor transport mechanism to the centerline of the fuel element, and the sintering of equiaxed-grain growth. Thus, from inside to outside, except the central void, the cross-sectional area of the fuel exhibits three regions (or zones):

the columnar grain region, the equiaxed grain region and the unaffected grain region. The densities for the regions are different and so are the heat power generations and the thermal conductivities. The formation of the three regions is time-dependent. In this unsteady condition the temperature distribution, a primary factor to produce stresses in fuel elements, has not been formulated in existing literatures. This temperature distribution will be obtained in Chapter II.

As a result of neutron bombardments of fissionable materials, fission products are produced in a nuclear fuel element. Some of the products are solid atoms and others are gas atoms (most are inert gases). Both can cause swelling in the fuel. This is another factor to produce stresses in the fuel elements. The swelling of fission solids is due to the increase of total atomic volumes. The swelling of fission gases is due to the easy nucleation and formation of gas bubbles and due to the collisions of bubbles with one another to form new bubbles which result in larger volumes. The behavior of fission-gas bubbles in oxide fuel is very complicated and no simple model is available to give the resulted swelling on a quantitative base. Barnes and Nelson have discussed the basic ideas of the nucleation, trapping, and migration of the bubbles (14). They have also given models on a qualitative base (15). Nichols has analyzed

the problem with a great effort and has formulated a semi-quantitative model (16, 17). A model to analyze and calculate the swelling and the gas release will be given in Chapter III of this work. This model will satisfy most of their analytical results and is suitable for the computations by a digital computer.

When the thermal and radiation analyses are obtained, the analysis and calculation of stresses and strains can be carried out.

The method to be used for the calculation of stresses and strains is an iteration method of successive approximations. The steps in the procedure are:

(1) assuming three plastic strains in the three principal directions,

(2) calculating stresses and strains from equations of equilibrium and compatibility with the known values of thermal and swelling strains and the assumed plastic strains to change the nonlinear problem tc a linear solution,

(3) finding the equivalent stress or strain with the calculated stresses and strains and a suitable yielding criterion,

(4) fitting the obtained equivalent stress or strain in the experimental stress-strain curves to obtain three new plastic strains which can be used in the

next iteration, and

(5) iterating successively to obtain the converged values of stresses and strains desired.

This method has been used a great deal by Mendelson (18) and by Manson (19). In its application here, the principles are the same as theirs but different techniques will be developed as can be seen in Chapter IV.

The whole problem is a compound and complex iteration. The stresses and strains in the clad and in the fuel are, of course, iterated values; the temperature of the fuel rod surface and the gap thickness between the fuel and clad are also iterated results. The pressures in the gap and in the central void are treated corresponding to the stress-strain iterations. The sizes of gas bubbles in fuel, which can be influenced by the hydrostatic stress surrounding them due to external load or thermal stresses, is also iterated in the stress-strain calculations of the fuel (20). The whole system may be seen in the general flow charts for the computer program as shown in Figures 5.1 and 5.2.

The convergence of the method of successive approximation has been tested and discussed in details by Mendelson (18) and by Manson (19). A rigorous proof of the convergence problem of the complicated situation is beyond the scope of this thesis. Experience and observations are therefore the guide.

The computer code is called ISUNE 1 (Iowa State University Nuclear Engineering) and the program in FORTRAN IV language is given in Appendix A.

The general physical conditions may be described as follows:

The fuel element is a long thin cylinder with a metal cladding and a low density oxide fuel. The thermal bond material is an inert gas like helium which is preferred to sodium (21). The coolant material is a liquid metal like sodium or NaK.

The fuel element has been operated in a fast reactor for a short, early period of time passing through a preliminary state of cracking.

The gap between the clad and the fuel will not be closed during the analysis since this is a normal provision to avoid distortion of the cladding in fast reactors.

There is little neutron flux depression in the cross section of the fuel element and the volumetric heat rate is proportional to the mass and enrichment of the fuel present.

A plane strain state and an axial symmetry are assumed so that all variables vary only with radius and time.

The coolant temperature, coolant pressure and power level are input values. At a given time, the temperature distribution, irradiation swelling, gas release, fuel-clad gap thickness, gap pressure, radius of the central void, central void

pressure, strains and stresses are calculated or iterated for the analysis of the fuel element.

II. THERMAL ANALYSIS

The purpose of the thermal analysis is to find the temperature distribution in the cross section of the fuel element during a constant linear power operation. The analysis is started from the surface of the clad through the cladding material, the gap and the fuel to the central void.

A. Temperature Distribution in Cladding

For a fast reactor cooled with liquid metal sodium or NaK, the heat transfer coefficient between the metallic coolant and the cladding material can be found with the following experimental relation for turbulent flow in a long tube (22):

$$Nu = 7 + 0.025\ Pe^{0.8}, \qquad (2\text{-}1)$$

where

$Nu = hD_e/K$, the Nusselt number

$Pe = D_e v \rho_c c/K$, the Peclet number

D_e = equivalent diameter of the coolant channel

v = coolant average velocity

ρ_c = coolant density

K = coolant thermal conductivity

c = coolant specific heat

h = heat transfer coefficient between coolant and clad.

Then

$$h = \frac{K}{D_e}\ (7 + 0.025\ Pe^{0.8}). \qquad (2\text{-}2)$$

Mean values of K, ρ_c, and c in the temperature range may be used for the calculation.

For a given bulk coolant temperature T_c the surface temperature T_o, the temperature distribution T(r) and the inner surface temperature T_i of the cladding can be calculated from the basic heat transfer equations:

$$T_o = T_c + \frac{q}{2\pi r_o h} \tag{2-3}$$

$$T(r) = T_o + \frac{q}{2\pi K_c} \ln\left(\frac{r_o}{r}\right) \tag{2-4}$$

$$T_i = T_o + \frac{q}{2\pi K_c} \ln\left(\frac{r_o}{r_i}\right) , \tag{2-5}$$

where q is the linear power, K_c is the thermal conductivity of the cladding material, and r_o and r_i are the outer and inner surface radii of the cladding, respectively.

B. Temperatures Through the Bonding Gap

The inner surface temperature of the clad is given by Equation (2-5). Similarly, the temperature at the surface of the fuel pin, T_s, is given by

$$T_s = T_i + \frac{q}{2\pi K_{gap}} \ln\left\{\frac{r_i(1+\varepsilon_{\theta i})}{r_s(1+\varepsilon_{\theta s})}\right\}, \tag{2-6}$$

where r_s is the surface radius of the fuel rod, K_{gap} the thermal conductivity of the gap, $\varepsilon_{\theta i}$ the tangential strain of clad at r_i and $\varepsilon_{\theta s}$ the tangential strain of fuel at r_s.

The average gap temperature T_g may be written

$$T_g = \frac{T_s + T_i}{2} . \qquad (2\text{-}7)$$

K_{gap} in Equation (2-6) may be written in the form below (23):

$$K_{gap} \simeq K_{gas} + \frac{4 L_g S_b}{(\frac{1}{e_c} + \frac{1}{e_f} - 1)} (T_g)_a^3 . \qquad (2\text{-}8)$$

where K_{gas} is the thermal conductivity of the gaseous medium separating the fuel and the clad, e_c and e_f are the emissivities of the clad and fuel respectively and are functions of temperature, L_g is the gap thickness, S_b is the Stefan-Boltzmann constant, and $(T_g)_a$ is the absolute temperature of T_g.

Additional equations for the calculation of K_{gap} are given by

$$e_f = C_{g1} + C_{g2} T_s \qquad (2\text{-}8a)$$

$$e_c = C_{g3} + C_{g4} T_i \qquad (2\text{-}8b)$$

$$K_{gas} = C_{g5} T_g^{C_{g6}} \qquad (2\text{-}8c)$$

$$L_g = r_i(1 + \varepsilon_{\theta i}) - r_s(1 + \varepsilon_{\theta s}). \qquad (2\text{-}8d)$$

where C_g's are constants.

T_s and K_{gap} are obtained by the combination of equations (2-6) and (2-8) through iteration process since tangential strains are involved.

C. Temperature Distribution in Fuel

In an oxide fuel the temperature is so high that two phenomena, the equiaxed grain growth and the columnar grain growth, (both are temperature and time dependent), should be considered. These structural changes make the problem quite complicated. A detailed stress analysis including time dependent effects has not been reported or published.

The grain growths sinter the fuel and a central void is formed in the axial direction. In an irradiated oxide fuel of low density, a typical cross section starting from the central void to the surface of the fuel exhibits three regions: The first, innermost region is the columnar grain annulus, the second region is the equiaxed-grain annulus, and the last, outermost region is the unaffected grain annulus. Since the densities are different from one another in these regions as are the volumetric heat sources and the thermal conductivities, special techniques should be applied to obtain the temperature distribution. Sayles has formulated the three-region temperature distribution (24) based on Robertson's method (13), but has not considered the time-dependent property. The mechanisms of these phenomena will be examined in order to formulate the temperature distribution.

The mechanism for columnar grain formation in oxide

fuel is not entirely clear. There is evidence, however, that the growth is connected with the presence of porosity-fabricated pores. These pores appear to be moving up the temperature gradients and this migration results in the formation of columnar grains. The migration is usually treated by an evaporation-condensation mechanism that is a mechanism of the evaporation on the hot side followed by the condensation on the cold side of the pore (12,13). Nichols has presented a quantitative analysis for the migration of fabricated pores (12). He derived an equation for the velocity V of the pore with the assumption that the velocity of migration of a non-spherical pore will not differ greatly from that of a spherical pore. The equation is given by

$$V = \frac{9\, C_o\, \Omega\, \Delta H_v\, [N(M_1+M_2)]^{\frac{1}{2}}\, \exp[-\Delta H_v/(RT_a)]}{16\, P\, \sigma^2\, T_a^{3/2}\, (2\pi k\, M_1 M_2)^{1/2}} \cdot \frac{dT}{dr}\,, \quad (2\text{-}9)$$

where

C_o = constant

Ω = molecular volume of fuel

ΔH_v = molar heat of vaporization

N = Avogadro's number

M_1, M_2 = molecular weights of fuel and primary vapor constituent, respectively

R = universal gas constant

P = total pressure in pore

σ = cross-sectional radius for collisions between matrix and vapor molecules

k = Boltzmann constant

T_a = absolute temperature

$\frac{dT}{dr}$ = radial temperature gradient.

It is seen that the velocity is independent of pore size.

With further assumptions that the temperature distribution in fuel is parabolic and the average temperature gradient is that at 1/3 of the fuel rod radius, from Equation (2-9) the centerline temperature required for "significant" motion (defined as 1/3 of fuel rod radius) in the allotted time is calculated. Thus he obtained the "threshold" temperature for columnar grain formation as well as concomitant central void formation as a function of time. The expression can be written as

$$-\frac{r_s}{3t} = \frac{C_1 \exp(-C_2/T_a)}{T_a^{3/2}} \left(\frac{dT}{dr}\right)_{ave}, \qquad (2\text{-}10)$$

where C_1 and C_2 are constants evaluated from the average or constant values of the parameters in Equation (2-9), $\left(\frac{dT}{dr}\right)_{ave}$ is the temperature gradient obtained at the position of 1/3 of r_s, the radius at the fuel rod surface, and t is the time. Thus the threshold centerline temperature in a specific time can be calculated from Equation (2-10). If the centerline

temperature is above the threshold value, the radius of the columnar grain, the temperature at this radius, and radius of the concomitant central void at the specified time can be calculated from the combination of Equation (2-10), the equation of parabolic temperature distribution and the given value of porosity. By this method he obtained results in good agreement with both in-pile and out-of-pile measurements on UO_2 (12).

In the present calculation, Equation (2-10) is coupled with equations for finding the temperature distribution (which is not necessarily parabolic) and the radii of the three regions and the central void as shown later.

Since the porosity in the columnar region has almost moved completely to the central void, a density of about 99% of the theoretical value of fuel may be assumed in this region.

Now the mechanism for the equiaxed grain growth is to be examined.

Burke assumed that the average grain diameter is related to the average radius of curvature of the grain boundaries and that the drag force for the boundary migration during grain growth is the surface tension of the boundary. He deduced the following expression for grain growth (25):

$$D^2 - D_o^2 = k_o t^n \exp(-Q/RT_a) \qquad (2\text{-}11)$$

where

D_o = initial grain size

D = grain size after an annealing of time t

k_o = a constant

Q = activation energy for the process

n = time exponent = 1, theoretically

Grain growth does not normally proceed in exact accordance with Equation (2-11) (11,26,27,28). For oxide fuel UO_2, Lyons et al. analyzed the grain growth data and obtained a cubic equation for the best representation (28) as

$$D^3 - D_o^3 = k_o t \cdot \exp(-\frac{Q}{RT_a}) \quad . \qquad (2\text{-}12)$$

There is a correlation between the porosity and grain size. MacEwan reported that pronounced grain growth does not occur in sintered UO_2 until the porosity decreases to about 3% of the volume of the specimen and then grain growth occurs with no further decrease in porosity (11). From the experimental data a minimum grain size of 15 μm at the outer radius of the equiaxed grain region and a density of about 97% of the theoretical value may be specified to this region for UO_2 (11).

With the specified value of minimum grain size for the extent of equiaxed grain in the fuel and the given value of time and initial grain size, one can calculate the temperature at the outer radius of the equiaxed grain region from Equation

(2-12). This relation will also be coupled with the temperature distribution equations.

Now comes the time to formulate the temperature distribution in the fuel.

The three regions in the cross section of the fuel rod after an irradiation time t at constant linear power q of the reactor operation are designated by I, II, and III as shown in Figure 2.1. The radius of the central void r_v, the outer radius of columnar-grain region r_1, the outer radius of equiaxed-grain region r_2, and the radius at the fuel rod surface r_s are also indicated. The corresponding temperature at these surfaces are designated by T_v, T_1, T_2, and T_s, respectively.

Since fuel pins in fast reactors are very thin, the neutron-flux depression in the pins may be neglected. Therefore, the heat generation is proportional to the density of the fuel when the fuel enrichment is given. For the given linear power q the volumetric heat rates in the three regions are

$$Q_{III} = \frac{q}{\pi r_s^2} \tag{2-13}$$

$$Q_{II} = Q_{III} \frac{\rho_{II}}{\rho_{III}} \tag{2-14}$$

$$Q_{I} = Q_{III} \frac{\rho_{I}}{\rho_{III}} \tag{2-15}$$

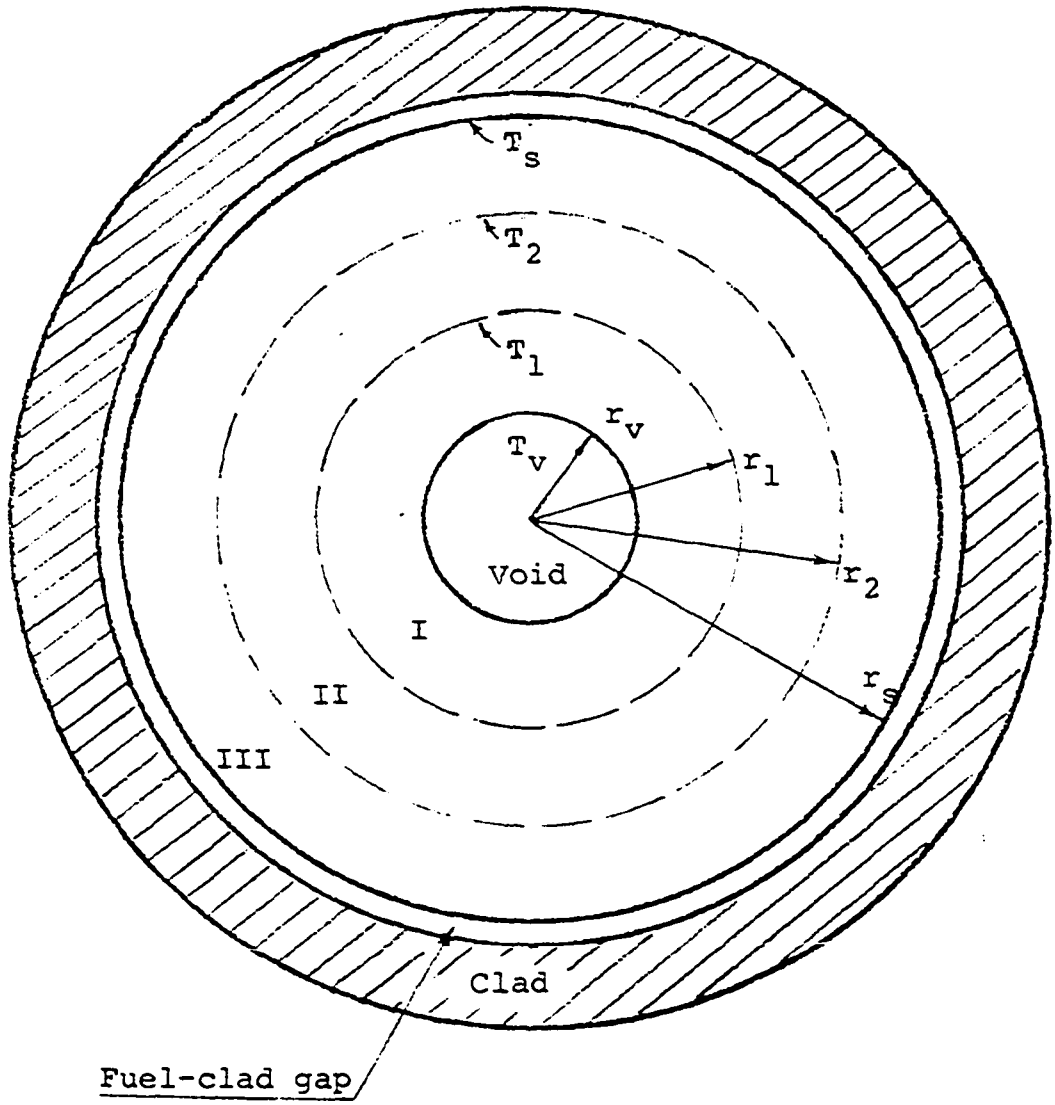

I = columnar grain region
II = equiaxed grain region
III = unaffected grain region

Figure 2.1. Typical cross section of an irradiated, low density, oxide fuel rod

where ρ_I, ρ_{II}, and ρ_{III} are known values of fraction of theoretical density in the three regions, respectively.

To consider the thermal conductivity as a function of temperature and porosity, Robertson employed the concept of $\int K(T)dT$ in heat transfer equations for the fuel, where $K(T)$ is the thermal conductivity at temperature T and the porosity is considered constant in the temperature range of the integration (13). In a recent experimental work, Asamoto et al. give the following expression for the thermal conductivity of UO_2 (29):

$$K_f = 0.0130 + \{T(0.4848 - 0.4465\ \rho)\}^{-1} \frac{w}{cm°C} \qquad (2\text{-}16)$$

where T is temperature in centigrade and ρ is the fraction of theoretical density. A corresponding expression for the general case may be written as

$$K_f(T,\rho) = C_3 + \{T(C_4 - C_5\rho)\}^{-1} \qquad (2\text{-}17)$$

For the long cylindrical fuel rod, the equation of heat conduction is

$$\int Q(r)\ 2\pi r\ dr = -K_f(T,\rho)\ 2\pi r \frac{dT}{dr} \qquad (2\text{-}18)$$

If $Q(r)$, the volumetric heat source, and ρ are constant in the integration range, the above equation becomes

$$Q \frac{r}{2} = -K(T)\frac{dT}{dr} \qquad (2\text{-}19)$$

Therefore, in region III it is

$$Q_{III}\frac{r}{2} = -K_{III}(T)\frac{dT}{dr} \tag{2-20}$$

Integration gives

$$\int_{T_s}^{T} K_{III}(T)dT = \frac{Q_{III}\, r_s^2}{4}\left[1-\left(\frac{r}{r_s}\right)^2\right] \tag{2-21}$$

or

$$C_3(T-T_s) + (C_4-C_5\,\rho_{III})^{-1}\ln\frac{T}{T_s} = \frac{Q_{III}\, r_s^2}{4}\left[1-\left(\frac{r}{r_s}\right)^2\right] \tag{2-22}$$

When $T = T_2$, it gives

$$C_3(T_2-T_s) + (C_4-C_5\,\rho_{III})^{-1}\ln\frac{T_2}{T_s} = \frac{Q_{III}\, r_s^2}{4}\left[1-\left(\frac{r_2}{r_s}\right)^2\right] \tag{2-23}$$

Similarly, in region II the heat conduction equation is

$$\frac{(Q_{III}-Q_{II})r_2^2}{2r} + \frac{Q_{II}r}{2} = -K_{II}(T)\frac{dT}{dr} \tag{2-24}$$

Integration yields

$$\int_{T_2}^{T} K_{II}(T)dT = \frac{Q_{II}r_2^2}{4}\left[1-\left(\frac{r}{r_2}\right)^2 + \left(1-\frac{Q_{III}}{Q_{II}}\right)\ln\left(\frac{r}{r_2}\right)^2\right] \tag{2-25}$$

or

$$C_3(T-T_2) + (C_4-C_5\,\rho_{II})^{-1}\ln\frac{T}{T_2} = \frac{Q_{II}r_2^2}{4}\left[1-\left(\frac{r}{r_2}\right)^2 + \left(1-\frac{Q_{III}}{Q_{II}}\right)\ln\left(\frac{r}{r_2}\right)^2\right] \tag{2-26}$$

When $T=T_1$, the substitution gives

$$C_3(T_1-T_2) + (C_4-C_5\ \rho_{II})^{-1} \ln \frac{T_1}{T_2}$$

$$= \frac{Q_{II}r_2^2}{4} [1-(\frac{r_1}{r_2})^2 + (1- \frac{Q_{III}}{Q_{II}}) \ln(\frac{r_1}{r_2})^2] \qquad (2\text{-}27)$$

In region I these equations are

$$\frac{Q_I}{2} \frac{(r^2-r_v^2)}{r} = -K_I(T)\frac{dT}{dr} \qquad (2\text{-}28)$$

and

$$\int_{T_1}^{T} K_I(T)dT = \frac{Q_I r_1^2}{4} [1-(\frac{r}{r_1})^2 + (\frac{r_v}{r_1})^2 \ln(\frac{r}{r_1})^2] \qquad (2\text{-}29)$$

or

$$C_3(T-T_1)+(C_4-C_5\ \rho_I)^{-1} \ln \frac{T}{T_1}$$

$$= \frac{Q_I r_1^2}{4} [1-(\frac{r}{r_1})^2 + (\frac{r_v}{r_1})^2 \ln (\frac{r}{r_1})^2] \qquad (2\text{-}30)$$

Substitution of T_v for T results

$$C_3(T_v-T_1) + (C_4-C_5\ \rho_I) \ln \frac{T_v}{T_1}$$

$$= \frac{Q_I r_1^2}{4} \{1-(\frac{r_v}{r_1})^2 [1-\ln(\frac{r_v}{r_1})^2]\} \qquad (2\text{-}31)$$

From the equality of power output before and after the formation of regions, an equation can be written as

$$r_v^2 = \frac{r_2^2(Q_{II}-Q_{III})}{Q_I} + \frac{r_1^2(Q_I-Q_{II})}{Q_I} \qquad (2\text{-}32)$$

In the beginning of irradiation the whole fuel cross section is in region III. Equation (2-20) can be used to find

the average temperature gradient, i.e., the temperature gradient at 1/3 of the fuel rod radius. Upon substituting this into Equation (2-10) an expression for solving T_1 at time t can be obtained

$$K_{III}(T_1) = C_1 t \exp[-C_2/(T_1)_a]/[2(T_1)_a^{3/2} Q_{III}] \qquad (2\text{-}33)$$

Also, if there were no central void, a centerline temperature T_{CL} could be found from Equation (2-22). In this case Equation (2-22) becomes

$$C_3(T_{CL}-T_s) + (C_4-C_5\ \rho_{III})^{-1} \ln \frac{T_{CL}}{T_s} = \frac{Q_{III} r_s^2}{4} \qquad (2\text{-}34)$$

At a certain time t, T_1 and T_2 are found from Equations (2-33) and (2-12), respectively. Then r_2 can be calculated from Equation (2-23) and then r_1 from Equation (2-27). Now, r_v and T_v can be found from Equations (2-32) and (2-31).

The temperature distribution can then be obtained from Equations (2-22), (2-26), and (2-30).

If the temperature T_1 calculated from Equation (2-33) is greater than the temperature T_{CL} calculated from Equation (2-34), T_1 is above the 'threshold' value as mentioned before and region I is not formed. T_2 may also be greater than T_{CL} and region II will not occur. Then the problem becomes a two-region or one-region problem. It is easy to write equations for these cases and they will be considered in the

computer program.

The temperature gradients are calculated by Equations (2-20), (2-24), and (2-28).

It should be noted that in solving the nonlinear equations, use has been made of the Muller's iteration method in the computer program (30,31).

III. RADIATION ANALYSIS

A. Introduction

Fission products are new atoms formed during fissioning process in reactor fuels. Some of them are solids which can cause swelling due to the difference in total atomic volumes before and after fissioning. The probable average swelling of fission solids in oxide fuel UO_2 or $(U_{0.80}Pu_{0.20})O_2$ was calculated to be $\Delta V/V = 0.35\%$ per 10^{20} fissions/cm^3 of fuel (32). The other fission products, about 10% of the total, are inert gases xenon and krypton.

The behavior of fission gases in oxide fuels during irradiation is very complex and no simple model is available for describing the complex behavior on a quantitative base. In the early time a simple diffusion model assumed that the fission-gas diffused slowly in the grains of the fuel until it emerged from the surface of the grain and then escaped rapidly through the interconnected channels leading to the specimen surface. This model has been proved incorrect for oxide fuel as discussed by Carroll (33). A widely used model for swelling analysis presented by Greenwood and Speight (34) can not be applied to oxide fuels as discussed by Nichols (16). Still many others (35, 36, 37) are limited by conditions and do not appear to be applicable for the purposes.

Recent results of work (14,38,39) have led to the conclusion that a trapping process during the diffusion of bubbles of fission gases controls the swelling and release of fission gases.

Barnes and Nelson have proposed the basic ideas of fission-gas swelling in oxide fuels and have given a qualitative model for it (14,15). Along the proposed general lines Nichols has also given a semi-quantitative model for the swelling (16).

In the present analysis these models will be referred to from time to time. Hence, the outlines of these models are given as follows:

1. The Barnes and Nelson model

(1) If the solubility of the inert gases during irradiation is small, then bubbles will be formed and will migrate under the influence of the temperature gradient.

(2) The dislocation lines and the grain boundaries will trap the bubbles, and only when their radii are greater than 650 Å and 5500 Å on the respective positions will the temperature gradients drag them off.

(3) Precipitates can also anchor bubbles smaller than about 5500 Å.

(4) The gas in the outer lower temperature region of the fuel rod is not likely to be released until very high

contents are attained. The gas in the inner region, where bubbles can migrate up the temperature gradient, however, will escape from the grains to the grain boundaries or rod center.

2. The Nichols model

(1) Bubbles are trapped by dislocation lines during short exposures and the fission-gas swelling is due to the increase of bubble size at their fixed positions.

(2) As the bubbles grow, it is assumed that they reach a critical size at which the thermal gradient drags them off the dislocations and they migrate with relatively few collisions until they reach a grain boundary. Here the swelling is felt to be primarily due to the capture of incoming bubbles by those already on the grain boundaries.

(3) When the bubbles reach a second critical size, they are dragged from the grain boundaries and migrate up the thermal gradient to the central void and release their gas there.

B. General Descriptions for the Model

General descriptions for the proposed model suitable for the calculation of fission-product swelling and fission gas releasing in a digital computer are given below:

(1) The solubility of inert gases during irradiation

is very small and easily precipitate to form gas bubbles on suitable nuclei - dislocations (14,15,16).

(2) Bubbles are ready to form and to reach their equilibrium pressure as a result of vacancy diffusion since in the fissioning process there are always enough vacancies introduced in accompanying with fission-gas atoms (15,16).

(3) Bubbles are trapped on dislocations and grain boundaries and retarded from motion by the retarding forces of dislocations and grain boundaries (15,16).

(4) When grain growth occurs, all fission gases trapped are assumed to be released to the central void for low density oxide fuels. This assumption is based on the phenomenon that fission gas will escape during any process involving gross reordering of the microstructure (33,39), and the bubble concentration for UO_2 extrapolated from the experimental result of Cornell et al. (40) approaches to zero at about 1600 °C, above which the grain growth is usually considered to occur.

(5) As the bubble size increases with time at dislocations due to the increase of fission-gas atoms, there will be a critical size at which the bubble can be dragged off from the dislocation by the driving force due to thermal gradients, which dominate bubble mobility in an oxide fuel (15,16).

(6) The migration of bubbles up the thermal gradients

is treated by surface diffusion mechanism. Usually, there are three mechanisms for calculation of the migration velocity, i.e., surface diffusion, volume diffusion, and vapor transport mechanisms. Barnes and Nelson showed that the volume diffusion mechanism was not important for oxide fuels (14). Vapor transport is important only at very high temperature at which, however, grain growth occurs in a very short time. Therefore, only the surface diffusion mechanism is considered in this analysis.

(7) The shape of bubbles is assumed to remain spherical during migration. This is normally assumed for swelling analysis.

(8) If the velocity of a bubble calculated from surface diffusion does not enable the bubble to travel one hundredth of the grain diameter in the period after it began to move to the time of analysis, the bubble is assumed still anchored on the dislocation (15).

(9) After bubbles leave the anchored sites, new bubbles will nucleate and grow again on these sites as time preceeds. The moving bubbles will migrate with very few collisions and eventually arrive at the grain boundaries since they leave the sites at approximately the same size and so the same velocity (16). It is assumed that all newly generated gas atoms are absorbed by the new bubbles. In other words, the moving bubbles and the bubbles arriving

at the grain boundaries will not absorb new gas atoms. Although there is some swelling loss for the moving bubbles and those bubbles at the grain boundaries, yet there is some swelling gain for the new bubbles at the original sites.

(10) The swelling at the grain boundaries is primarily due to the capture of incoming bubbles by those already on the grain boundaries (16). There the bubble size increases until reaching another critical size at which the bubble is dragged off the grain boundary by the thermal gradient force and migrates all the way to the central void. This is because the velocity varies exponentially with temperature. But, if the velocity does not enable the bubble to travel one grain diameter in the time under consideration, the bubble is assumed still at the grain boundary (15).

(11) Fission products escaped to the gap between the clad and the fuel is neglected since the trapping process is quite effective in the outer low temperature region (33).

(12) The total fission-product swelling is the sum of the swellings due to solid fission products, gas bubbles anchored in the grains, gas bubbles moving in the grains, and gas bubbles anchored at the grain boundaries. The solid-product swelling is proportional to the fission rate and time as mentioned early in the introduction.

(13) The total gas atoms released to the central void

is the sum of the gas atoms from fabricated pores and gas bubbles as a result of the grain growths, and the gas atoms in bubbles leaving grain boundaries from the outer region.

C. Fission-product Swelling

Fission-product swelling consists of fission-solid swelling and fission-gas swelling. The appropriate formulas will be given in this section.

1. Fission-solid swelling

With a fission rate $\dot{F}$, fissions per unit volume per unit time, in an irradiation time t, the total number of fissions per unit volume is $\dot{F}t$. If the average volumetric contribution of the solid fission products is known, the solid volume swelling is given by

$$(\Delta V/V)_{sld} = C_6 \dot{F} t \qquad (3\text{-}1)$$

where

$(\Delta V/V)_{sld}$ = fission-solid swelling

C_6 = the average volumetric contribution per fission per unit volume.

The fission rate can be related to the volumetric heat rate by

$$\dot{F} = Q/C_1' \qquad (3\text{-}1a)$$

where C_1' is a conversion constant.

2. Anchored gas-bubble swelling in grain

Fission-gas atoms of xenon and krypton are known to be extremely insoluble and easily precipitate to form gas bubbles on suitable nuclei like dislocations as assumed. The bubbles will be anchored there by the retarding force exerted by the tension of the dislocation lines. In calculating the swelling due to these anchored bubbles, one should know the size and number of the bubbles. If there are N_o bubbles with diameter d in a unit volume, then the swelling is given by

$$(\Delta V/V)_{sgg} = \frac{1}{6} \pi d^3 N_o \qquad (3\text{-}2)$$

where $(\Delta V/V)_{sgg}$ = swelling of anchored gas bubbles in grain.

In this equation N_o can be obtained from experimental data and then the problem is to find the diameter of the bubble. There are two relations involving another unknown, the pressure inside the bubble, for evaluating the diameter. One is the pressure equilibrium condition and the other is the state equation of gas.

The pressure equilibrium condition can be written as (14)

$$p + \sigma_H + \sigma' = 4\gamma/d \qquad (3\text{-}3)$$

where

p = gas pressure inside the bubble

γ = surface tension of fuel material

σ_H = hydrostatic stress in the material around the bubble due to externally applied forces or thermal and radiation effects (positive value for tension)

σ' = intrinsic stress of the fuel.

The hydrostatic stress σ_H is the average value of the three principal stresses in the fuel. It should be noted that the swelling of gas bubbles contributes the stress and the stress, in turn, affects bubble size. Therefore, both σ_H and d are values obtained through iteration process (20). The intrinsic stress σ' can generally be neglected for oxide fuel due to high temperature (14). Then Equation (3-3) becomes

$$p + \sigma_H = 4\gamma/d \tag{3-4}$$

The state equation of an ideal gas is

$$p(\frac{1}{6}\pi d^3) = mkT_a \tag{3-5}$$

where

m = number of the fission-gas atoms in the bubble

k = Boltzmann constant.

The total number of fission-produced atoms per unit volume is about $2\dot{F}t$ of which about 10% are the inert gases, xenon and krypton. Therefore, in Equation (3-5) the number of fission-gas atoms in one bubble is

$$m = 0.2\ \dot{F}t/N_o \tag{3-6}$$

Eliminating p from Equations (3-4) and (3-5), it gives

$$d^3 - \frac{4\gamma}{\sigma_H} d^2 - \frac{6mk\ T_a}{\pi\ \sigma_H} = 0 \qquad (3\text{-}7)$$

For bubbles with diameters less than about 10^{-5} cm, the inert gases may not behave ideally and Van der Waals correction should be applied (35). Then the gas equation of state becomes

$$p(\frac{1}{6}\ \pi d^3 - mb) = mk\ T_a \qquad (3\text{-}8)$$

where b is the Van der Waals correction term (a value of 8.3×10^{-23} cm^3 may be used in the computations (20,41)). Again, eliminating p results

$$d^4 - \frac{4\gamma}{\sigma_H} d^3 + \frac{6m}{\pi\ \sigma_H} (k\ T_a - \sigma_H b)d + \frac{24\ mb}{\pi\ \sigma_H} = 0 \qquad (3\text{-}9)$$

This equation is more general than Equation (3-7) and is to be used to compute the diameter of a bubble for the swelling of bubbles at fixed positions. If the value of σ_H in equation is negative, i.e., compressive stress, the solution of the diameter required is the unique positive root. If σ_H is positive, namely tensile stress, there are two positive real roots. It is clear that the smaller one is the desired solution.

If σ_H is very small in comparison with $4\gamma/d$, it may be neglected and Equation (3-9) reduces to

$$d^3 - \frac{3mk\ T_a}{2\pi\gamma}\, d - \frac{6mb}{\pi} = 0 \qquad (3\text{-}10)$$

Here the only positive real root is the solution.

3. Fission-gas swelling after movement of bubbles

The driving force due to thermal gradient has been obtained from thermal diffusion theory (42,43). For surface diffusion mechanism this force can be written as

$$F_s = \frac{\pi\ Q_s^*\ d^3}{6\Omega\ T_a} \frac{dT}{dr} \qquad (3\text{-}11)$$

where Q_s^* is the activation energy for surface diffusion, Ω is the molecular volume of the fuel, and F_s is the driving force.

The maximum retarding force exerted by a dislocation in an oxide fuel is approximately 10^{-4} dyne (14). When the driving force is equal to this value, a critical diameter of bubble for movement can be written as

$$d_{cg} = \left(\frac{6\Omega\ T_a\ 10^{-4}}{\pi\ Q_s^*\ dT/dr}\right)^{\frac{1}{3}} \qquad (3\text{-}12)$$

When the bubble begins to move, its velocity derived from surface diffusion mechanism is given by (43)

$$V_g = \frac{6\ D_s\ \nu\ \Omega\ Q_s^*}{k\ T_a^2\ d} \frac{dT}{dr} \qquad (3\text{-}13)$$

where

D_s = the surface diffusion coefficient

ν = number of diffusion molecules per unit surface area.

The surface diffusion coefficient may be written as (16)

$$D_s = D_o \exp(-\frac{Q_s}{kT_a}) \qquad (3\text{-}13a)$$

where

D_o = coefficient

Q_s = activation energy.

Also, there is a critical velocity as mentioned in the general description. It can be expressed as

$$V_{cg} = \frac{D}{100(t-t_{cg})} \qquad (3\text{-}14)$$

where D is the diameter of grain and t_{cg} is the time when the bubble attains its critical size. This critical time can be evaluated approximately by the combination of Equations (3-4), (3-5), and (3-6).
The result is

$$t_{cg} = \pi N_o (\frac{4\gamma}{d_{cg}} - \sigma_H) d_{cg}^3 / (1.2 \dot{F} k T_a) \qquad (3\text{-}15)$$

The value of the hydrostatic stress, σ_H in the above equation, is obtained by iteration without considering the movement of bubbles. This is why Equation (3-15) is approximate. Since σ_H varies little with time during the constant linear power operation as can be seen from the calculations, thus the approximation is reasonable.

When the velocity is smaller than the critical velocity, it is considered that the bubble will still remain in the grain; otherwise, without this consideration, there will be 1% of the bubbles arriving at the grain boundaries, and the total swelling will not be much different for these two cases.

When the velocity is greater than the critical velocity, bubbles are now moving up the thermal gradient to reach the grain boundaries. The swelling at the grain boundaries is primarily due to the collisions of the incoming bubbles with those already on the grain boundaries. This kind of swelling is the result of volume increase in the formation of a new bubble due to collision and coalescence of two bubbles. The diameter of the new bubble can be obtained from the condition of pressure equilibrium and the conservation of gas atoms.

If one bubble with diameter d_o and number of gas atoms m_o and another with d_i and m_i collide with each other and form the new bubble with diameter d, the equation of state for the new bubble is

$$p(\frac{1}{6}\pi d^3) = (m_o + m_i)k\,T_a \qquad (3\text{-}16)$$

or

$$Pd^3 = P_o d_o^{\,3} + p_i d_i^3 \,. \qquad (3\text{-}17)$$

By substitution of p's from Equation (3-4), the equation

for solving d is found to be

$$d^3 - \frac{4\gamma}{\sigma_H} d^2 - (d_o^3 + d_i^3) + \frac{4\gamma}{\sigma_H} (d_o^2 + d_i^2) = 0. \qquad (3\text{-}18)$$

If σ_H is negative, there is always a solution that is the only positive root. If σ_H is positive, the solution is then the smaller one of the two positive roots and σ_H must be

$$\sigma_H \leq \frac{8\gamma}{3d} . \qquad (3\text{-}19)$$

Otherwise, there will be no equilibrium value of d, i.e., Equation (3-18) gives no solution. Actually, this is not likely to happen in the analysis since the hydrostatic tension stress is produced only in the outer, lower temperature region of the fuel rod where the bubble diameters are small in the period of interest. This may also occur to Equation (3-9) and the discussion has been omitted for the same reason.

If σ_H is small, the diameter is then

$$d = (d_o^2 + d_i^2)^{\frac{1}{2}} \qquad (3\text{-}20)$$

Now for the swelling of bubbles at grain boundaries, consider a small parallelpiped across the grain in the direction of the temperature gradient with cross-section area ΔA and an average length L given by

$$L = \frac{\pi}{4} D \qquad (3\text{-}21)$$

where D is the diameter of the grain.

Since the bubbles are evenly distributed with N_o bubbles per unit volume as assumed, the number of bubbles per unit length is then $N_o^{1/3}$. The time required for a bubble to travel across the parallelpiped is

$$t_g = L/V_g \tag{3-22}$$

where V_g is given by Equation (3-13).

If t_g is divided into n_g intervals where n_g is the number of bubbles on the length L, the time interval Δt can be written as

$$\Delta t = t_g/n_g \tag{3-23}$$

where $n_g = LN_o^{1/3}$. (3-24)

Then,

$$\Delta t = 1/(V_g N_o^{1/3}). \tag{3-25}$$

It is seen that the time interval is just the time for a bubble to travel one bubble spacing. Thus an approximation may be made that the moving bubbles within each time interval will not collide with one another as they arrive at the grain boundary.

The critical time t_{cg} for the movement of bubbles from dislocations was given by Equation (3-15). At any time t before the last bubble arriving the grain boundary, the time-interval number is

$$n = \frac{t-t_{cg}}{\Delta t}, \qquad t_{cg}<t<(t_{cg}+t_g) \tag{3-26}$$

When n=1, the number of bubbles per unit area at the small boundary area ΔA is

$$N_{0,1} = N_0 V_g \Delta t \Delta A/\Delta A = N_o^{2/3} \tag{3-27}$$

The first subscript of $N_{0,1}$ represents the number of collisions for the bubbles at the grain boundary having been collided with incoming bubbles and the second subscript is the number of time intervals passing by after the critical time t_{cg}.

It is clear that in each time interval there will be $N_{0,1}$ bubbles per unit area arriving at ΔA.

The probability for each of the bubbles with diameter d_i on the grain boundary to be collided is $\frac{\pi}{4}(d_o+d_i)^2 N_{0,1}$ where the subscript of the diameter is the number of collisions having been collided and d_o or d_{cg} is the critical diameter given by Equation (3-12). The diameter of a bubble after collision can be calculated from Equation (3-18) or (3-20).

When n=2, the number of bubbles per unit area at ΔA having been collided once is

$$N_{1,2} = \frac{\pi}{4}(d_o+d_o)^2 N_{0,1}\ N_{0,1} \tag{3=28}$$

and the number of uncollided bubbles per unit area at ΔA is

$$N_{0,2} = 2N_{0,1} - 2N_{1,2} \tag{3-28a}$$

When n=3

$$N_{2,3} = \frac{\pi}{4}(d_o+d_1)^2 N_{0,1}N_{1,2}$$

$$N_{1,3} = \frac{\pi}{4}(d_o+d_o)^2 N_{0,1}N_{0,2}+N_{1,2}-N_{2,3} \qquad (3\text{-}29)$$

$$N_{0,3} = N_{0,1}+N_{0,2}-N_{2,3}-2\left(\frac{\pi}{4}(d_o+d_o)^2 N_{0,1}N_{0,2}\right)$$

When n=4

$$N_{3,4} = \frac{\pi}{4}(d_o+d_2)^2 N_{0,1}N_{2,3}$$

$$N_{2,4} = \frac{\pi}{4}(d_o+d_1)^2 N_{0,1}N_{1,3}+N_{2,3}-N_{3,4} \qquad (3\text{-}30)$$

$$N_{1,4} = \frac{\pi}{4}(d_o+d_o)^2 N_{0,1}N_{0,3}+N_{1,3}-\frac{\pi}{4}(d_o+d_1)^2 N_{0,1}N_{1,3}$$

$$N_{0.4} = N_{0.1}+N_{0.3}-\frac{\pi}{4}(d_o+d_2)^2 N_{0,1}N_{2,3}-\frac{\pi}{4}(d_o+d_1)^2 N_{0,1}N_{1,3}$$

$$-2\left(\frac{\pi}{4}(d_o+d_o)^2 N_{0,1}N_{0,3}\right)$$

When n=5

$$N_{4,5} = \frac{\pi}{4}(d_o+d_3)^2 N_{0,1}N_{3,4}$$

$$N_{3,5} = \frac{\pi}{4}(d_o+d_2)^2 N_{0,1}N_{2,4}+N_{3,4}-N_{4,5} \qquad (3\text{-}31)$$

$$N_{2,5} = \frac{\pi}{4}(d_o+d_1)^2 N_{0,1}N_{1,4}+N_{2,4}-\frac{\pi}{4}(d_o+d_2)^2 N_{0,1}N_{2,4}$$

$$N_{1,5} = \frac{\pi}{4}(d_o+d_o)^2 N_{0,1}N_{0,4}+N_{1,4}-\frac{\pi}{4}(d_o+d_1)^2 N_{0,1}N_{1,4}$$

$$N_{0,5} = N_{0,1}+N_{0,4}-\frac{\pi}{4}(d_o+d_3)^2 N_{0,1}N_{3,4}-\frac{\pi}{4}(d_o+d_2)^2 N_{0,1}N_{2,4}$$

$$-\frac{\pi}{4}(d_o+d_1)^2 N_{0,1}N_{1,4}-2\left(\frac{\pi}{4}(d_o+d_o)^2 N_{0,1}N_{0,4}\right)$$

With definitions:

$$C_{i,n} = \frac{\pi}{4}(d_o+d_i)^2 N_{0,1} N_{i,n} \qquad \text{when } -1<i<n$$

$$C_{i,n} = N_{i,n} = 0 \qquad \text{when } i=n \qquad (3\text{-}32)$$

$$C_{i,n} = N_{0,1} - \sum_{k=0}^{n} C_{k,n} \qquad \text{when } i= -1,$$

a general recurrence relation can be expressed as

$$N_{i,n} = C_{i-1,n-1} + N_{i,n-1} - C_{i,n-1} \qquad (3\text{-}33)$$

where i is the number of collisions for a bubble on the grain boundary and n is the number of time intervals having passed. Then, the swelling due to bubbles on grain boundaries is

$$\left(\frac{\Delta V}{V}\right)_{sgb} = \frac{1}{L} \sum_{i=0}^{n-1} \{N_{i,n} (\frac{1}{6} \pi d_i^3)\} \qquad (3\text{-}34)$$

The swelling due to new bubbles nucleated and anchored on the bubble sites is

$$\left(\frac{\Delta V}{V}\right)_{sgg'} = \frac{1}{6} \pi d'^3 N_o \qquad (3\text{-}35)$$

where d' is the diameter of the new bubbles obtained from Equation (3-9) or (3-10) in which m is given by

$$m = 0.2 \dot{F}(t-t_{cg})/N_o \qquad (3\text{-}36)$$

The swelling due to bubbles still moving in the grains is

$$\left(\frac{\Delta V}{V}\right)_{sgm} = \frac{t-t_{cg}}{t_g} \left(\frac{\pi}{6} d_{cg}^3 N_o\right) \qquad (3\text{-}37)$$

The total gas-bubble swelling after the movement of bubbles in the grains is given by the sum of the swellings due to new bubbles nucleated on the bubble sites, bubble collisions at grain boundaries, and bubbles still moving in the grains. That is

$$\left(\frac{\Delta V}{V}\right)_{gas} = \left(\frac{\Delta V}{V}\right)_{sgb} + \left(\frac{\Delta V}{V}\right)_{sgg'} + \left(\frac{\Delta V}{V}\right)_{sgm} \qquad (3\text{-}38)$$

where

$\left(\frac{\Delta V}{V}\right)_{gas}$ = the total gas-bubble swelling

$\left(\frac{\Delta V}{V}\right)_{sgb}$ = the swelling due to bubbles on grain boundaries

$\left(\frac{\Delta V}{V}\right)_{sgg'}$ = the swelling due to new bubbles anchored on the bubble sites

$\left(\frac{\Delta V}{V}\right)_{sgm}$ = the swelling due to bubbles still moving in the grains.

It should be noted that all hydrostatic stresses involved in the calculations of bubble diameters after the movement of bubbles in grains are obtained by iteration processes without considering the movement of bubbles.

If bubbles at grain boundaries attain the critical conditions for migrating away from the grain boundaries at xth collision, then all bubbles after the xth collision will migrate away. The swelling due to bubbles on the grain boundaries given in Equation (3-34) becomes

$$\left(\frac{\Delta V}{V}\right)_{sgb} = \frac{1}{L} \sum_{i=0}^{x-1} \{N_{i,n}(\frac{1}{6} \pi d_i^3)\} \qquad (3\text{-}39)$$

If $n \geq n_g$ or $t \geq (t_{cg}+t_g)$, the swelling due to moving bubbles in Equation (3-37) is then equal to zero.

The calculations of bubble number and diameters are given in the computer program.

The operating time t in the analysis may not exceed $2t_{cg}$, a period of time more than 8 months estimated from the calculations of a numerical example in this work.

D. Gas Release

The fission-gas release consists of two parts: (1) due to grain growth and (2) due to bubbles moving away from grain boundaries. These can be formulated in the following:

1. The region of grain growth in the fuel rod is the circular area with radius r_2 indicated in Figure 2.1. At a time t, the total number of fission-gas atoms released to the central void due to this part can be written as

$$m_{gg} = 0.2 \dot{F} t(\pi r_2^2) \qquad (3\text{-}40)$$

2. Bubbles on grain boundaries will migrate away under two conditions as assumed in the model:

(a) They must attain a critical size at which the force due to temperature gradients equals the retarding

force exerted by grain boundaries. The latter is given by (16)

$$F_{gb} = \frac{\pi}{2} \gamma_{gb} \, d \tag{3-41}$$

where F_{gb} = the maximum retarding force of grain boundary

γ_{gb} = grain boundary surface tension.

The former is given by Equation (3-11). From the equality of these two forces, a critical diameter for bubbles at grain boundaries being able to move away is given by

$$d_{cb} = \sqrt{\frac{3\Omega \, \gamma_{gb} \, T_a}{Q_s^* (dT/dr)}} \tag{3-42}$$

where

d_{cb} = the critical diameter for bubbles at grain boundaries being able to move away.

If the bubbles start movement at xth collision at which the diameter of a collided bubble obtained from Equation (3-18) equals or exceeds d_{cb} for the first time, then the corresponding critical time is

$$t_{cb} = t_{cg} + x \cdot \Delta t \tag{3-43}$$

where t_{cg} and Δt are obtained from Equations (3-15) and (3-25), respectively.

(b) The moving bubbles must move quickly enough so that the higher and higher temperatures can accelerate them all the way to the central void. This critical velocity

based on the concept of Barnes and Nelson (15) can be written as

$$V_{cb} = D/(t-t_{cb}) \tag{3-44}$$

The velocity of the moving bubbles is given by Equation (3-13) for the surface diffusion mechanism, i.e.,

$$V_b = \frac{6\ D_s\ \nu\ \Omega\ Q_s^*}{k\ T_a\ d}\ \frac{dT}{dr} \tag{3-45}$$

where V_b is the velocity of the moving bubbles leaving grain boundaries.

If $V_b < V_{cb}$, the bubbles are assumed to be still anchored on the grain boundaries.

If $V_b \geq V_{cb}$, the total number of moving bubbles per unit volume migrating away is

$$N_t = \frac{1}{L} \sum_{k=x+1}^{n} N_{x,k} \tag{3-46}$$

where $N_{x,k}$ is the number of bubbles per unit area moving away from the grain boundary after k time-intervals and having been collided x times with incoming bubbles. The combination of Equations (3-4) and (3-5) gives the total number of gas atoms released to the central void from bubbles at station j of the fuel rod, i.e.,

$$m_b = N_t\left(\frac{4\gamma}{d_{cb}} - \sigma_H\right)\left(\frac{\pi\ d_{cb}^3}{6\ k\ T_a}\right)\pi\left(r_j^2 - r_{j-1}^2\right) \tag{3-47}$$

The calculations for gas release under the conditions are shown in the computer program.

IV. THERMAL, RADIATION AND STRESS ANALYSIS

A. Introduction

After the temperature distribution, the thermal expansion and the irradiation swelling are determined, the next task is to formulate the problem of stress analysis.

Because of the high thermal stress, the yield points of both clad and fuel of an oxide fuel element in a fast reactor may be exceeded. The equations of equilibrium and compatibility for stress analysis must be combined with nonlinear stress-strain relations instead of the linear Hooke's law. To solve the nonlinear equations a method of successive approximations is used in this analysis. This method is an extension of Picard's method (44) of successive approximations to nonlinear equations and was first used by Ilyushin (45) in his treatment of a thin shell.

In the earlier days this method may be used only for relatively simple problems because of the cumbersome calculations. Recently, the high-speed computing machinery came into existence, and it becomes a powerful method in the stress calculations involving the strain-hardening exhibited in experimental stress-strain curves and has been used in various problems by Manson (19) and Mendelson (18). Usually, problems of stress analysis solved in the elastoplastic range are simplified by assumptions such as the elastic strains to be neglected and the material

to be perfectly plastic in the plastic range. The method of successive approximations makes these assumptions unnecessary.

In the stress analysis of nuclear reactor fuel elements the special phenomenon of radiation effects and the variable thermal conductivity in the fuel make the analysis different from ordinary problems.

B. Basic Assumptions

In this analysis the following basic assumptions are made:

1. Both fuel and cladding materials under irradiation are approximately isotropic.
2. The fuel element is in a plane strain state.
3. It is also in an axial symmetry.
4. The Prandtl-Reuss equations are applicable (46,47).
5. The von Mises yield criterion is to improve the assumptions (48).
6. The Bauschinger effect is ignored.

The first assumption implies that the material properties are functions of radius but not of direction during the irradiation.

Since the cylindrical fuel element in a fast reactor is long and thin and the axial displacement could be ignored, the basic assumption 2 is sound.

The third basic assumption implies that all variables vary only with radius and time.

The Prandtl-Reuss relation is a more general case for elastoplastic stress-strain expressions, and has been confirmed experimentally by Lode (49).

Two criteria for the yielding, the von Mises and the Tresca yield conditions, have received appreciable acceptance in engineering applications. The Mises yield criterion, however, has been indicated the more general validity and it becomes the choice in this analysis.

The last basic assumption means that both the fuel and clading materials have the strength equally in tension and in compression. This is a most frequently used assumption in stress analysis.

C. Equations and Solutions of Stress Analysis

Since the cylindrical-type fuel element is in axial symmetry, the three principal axes are coincided with the cylindrical coordinates. The stresses are designated by σ_r, σ_θ and σ_z and the corresponding strains by ε_r, ε_θ and ε_z in the cylindrical coordinates. The body force is neglected and the plane strain as assumed. At a given time the equilibrium equation is then

$$\frac{d\sigma_r}{dr} + \frac{\sigma_r - \sigma_\theta}{r} = 0 \qquad (4\text{-}1)$$

The strain-displacement relations are

$$\varepsilon_r = \frac{du}{dr} \tag{4-2}$$

$$\varepsilon_\theta = \frac{u}{r} \tag{4-3}$$

where u is the radial displacement at r, and the corresponding compatibility equation is

$$\frac{d\varepsilon_\theta}{dr} + \frac{\varepsilon_\theta - \varepsilon_r}{r} = 0 \ . \tag{4-4}$$

The strain consists of four parts: the elastic strain, the thermal expansion strain, the irradiation dilatation strain and the plastic strain. The equations are

$$\begin{aligned}
\varepsilon_r &= \frac{1}{E}[\sigma_r - \mu(\sigma_\theta + \sigma_z)] + \alpha T + \varepsilon_I + \varepsilon_{pr} \\
\varepsilon_\theta &= \frac{1}{E}[\sigma_\theta - \mu(\sigma_z + \sigma_r)] + \alpha T + \varepsilon_I + \varepsilon_{p\theta} \\
\varepsilon_z &= \frac{1}{E}[\sigma_z - \mu(\sigma_r + \sigma_\theta)] + \alpha T + \varepsilon_I + \varepsilon_{pz}
\end{aligned} \tag{4-5}$$

where α is the linear coefficient of thermal expansion, T is the temperature rise with respect to a reference temperature, E is the modulus of elasticity, μ is Poisson's ratio, ε_I is the irradiation dilatation strain and ε_{pr}, $\varepsilon_{p\theta}$ and ε_{pz} are the plastic strains.

For plane strain state the axial total strain ε_z may be neglected

$$\varepsilon_z = 0 \tag{4-6}$$

The thermal and irradiation dilatation strains may be combined in a single term, ε_R (2). Equations (4-5) become

$$\varepsilon_r = \frac{1}{E}[\sigma_r - \mu(\sigma_\theta + \sigma_z)] + \varepsilon_R + \varepsilon_{pr}$$

$$\varepsilon_\theta = \frac{1}{E}[\sigma_\theta - \mu(\sigma_z + \sigma_r)] + \varepsilon_R + \varepsilon_{p\theta} \qquad (4\text{-}7)$$

$$\varepsilon_z = \frac{1}{E}[\sigma_z - \mu(\sigma_r + \sigma_\theta)] + \varepsilon_R = \varepsilon_{pz}$$

where

$$\varepsilon_R = \alpha T + \varepsilon_I. \qquad (4\text{-}7a)$$

The basic assumption 4 implies the material to be incompressible in the pastic range, i.e.

$$\varepsilon_{pr} + \varepsilon_{p\theta} + \varepsilon_{pz} = 0 \qquad (4\text{-}8)$$

Then, the mean strain e is

$$e \equiv \frac{1}{3}(\varepsilon_r + \varepsilon_\theta - 3\varepsilon_R). \qquad (4\text{-}9)$$

The average normal stress is

$$s = \frac{1}{3}(\sigma_r + \sigma_\theta + \sigma_z). \qquad (4\text{-}10)$$

The combination of Equations (4-7), (4-8), (4-9) and (4-10) results

$$s = \frac{E}{1-2\mu} e \qquad (4\text{-}11)$$

The elastic strain deviators are

$$e_r = (\varepsilon_r - \varepsilon_R - \varepsilon_{pr}) - e$$

$$e_\theta = (\varepsilon_\theta - \varepsilon_R - \varepsilon_{p\theta}) - e \qquad (4\text{-}12)$$

$$e_z = (-\varepsilon_R - \varepsilon_{pz}) - e$$

and the stress deviators are

$$s_r = \sigma_r - s = \frac{E}{1+\mu} e_r$$

$$s_\theta = \sigma_\theta - s = \frac{E}{1+\mu} e_\theta \qquad (4\text{-}13)$$

$$s_z = \sigma_z - s = \frac{E}{1+\mu} e_z \ .$$

If another function g is defined as

$$g \equiv \frac{1}{3}(\varepsilon_r - \varepsilon_\theta - 3\varepsilon_R), \qquad (4\text{-}14)$$

and if ε_R and plastic strains are known, all other variables of interest may be expressed in terms of e and g as follows:

Combination of Equations (4-2), (4-3), (4-9) and (4-14) gives

$$u = \frac{3}{2}(e-g)r \qquad (4\text{-}15)$$

and then

$$\varepsilon_r = \frac{du}{dr} = \frac{3}{2}(e+g+2\ \varepsilon_R) \qquad (4\text{-}16)$$

$$\varepsilon_\theta = \frac{u}{r} = \frac{3}{2}(e-g) \qquad (4\text{-}17)$$

The elastic strain deviators become

$$e_r = \frac{1}{2}(e+3g+4\ \varepsilon_R-2\ \varepsilon_{pr})$$

$$e_\theta = \frac{1}{2}(e-3g-2\ \varepsilon_R-2\ \varepsilon_{p\theta}) \qquad (4\text{-}18)$$

$$e_z = -\varepsilon_R-\varepsilon_{pz}-e$$

The average normal stress has already been in the right form given by Equation (4-11). The stress deviators in Equation (4-13) are then

$$s_r = \frac{E}{2(1+\mu)}\ (e+3g+4\ \varepsilon_R-2\ \varepsilon_{pr})$$

$$s_\theta = \frac{E}{2(1+\mu)}\ (e-3g-2\ \varepsilon_R-2\ \varepsilon_{p\theta}) \qquad (4\text{-}19)$$

$$s_z = \frac{E}{1+\mu}\ (-\varepsilon_R-\varepsilon_{pz}-e).$$

The three components of stress can now be written as

$$\sigma_r = \frac{3E}{2(1+\mu)(1-2\mu)}\ e + \frac{3E}{2(1+\mu)}\ g + \frac{E}{1+\mu}\ (2\ \varepsilon_R-\varepsilon_{pr}) \qquad (4\text{-}20)$$

$$\sigma_\theta = \frac{3E}{2(1+\mu)(1-2\mu)}\ e - \frac{3E}{2(1+\mu)}\ g - \frac{E}{1+\mu}\ (\varepsilon_R+\varepsilon_{p\theta}) \qquad (4\text{-}20a)$$

$$\sigma_z = \frac{3\mu E}{(1+\mu)(1-2\mu)}\ e - \frac{E}{1+\mu}\ (\varepsilon_R+\varepsilon_{pz}). \qquad (4\text{-}20b)$$

By substitution of the stresses and strains from Equations (4-16), (4-17), (4-20) and (4-20a) into the equilibrium Equation (4-1) and the compatibility Equation (4-4), new equilibrium and compatibility equations with the defined variables e and g as dependent variables can be obtained. With suitable boundary conditions, e and g can be solved easily from these equations.

If the modulus of elasticity and Poisson's ratio vary moderately along the radius, their average values in the temperature range may be used. Then the coefficients of the equations are constants and a closed-form solution can be obtained. This fact will be applied to the thin cladding material in the analysis. As for the oxide fuel region, the temperature gradient and the density changes due to irradiation are so large that the coefficients can not be assumed constant any more. In this case a method of finite difference will be used to solve the differential equations.

1. Closed-form solution for clad

Consider the clad a hollow cylinder with inner radius r_i and outer radius r_o, subjected to an internal pressure p_g which is the pressure in the gap between the fuel and the clad, an external pressure P_o due to coolant, and a radial temperature distribution T(r). All the stresses and strains are functions of radius r at a given time. The modulus of elasticity E and the Poisson ratio μ are assumed to be constant.

Upon substitution of σ_r, σ_θ, ε_r and ε_θ from Equations (4-20), (4-20a), (4-16) and (4-17) into (4-1) and (4-4), the equilibrium Equation (4-1) becomes

$$\frac{d}{dr}\left[\frac{3E}{2(1+\mu)(1-2\mu)}\, e + \frac{3E}{2(1+\mu)}\, g + \frac{E}{1+\mu}\,(2\,\varepsilon_R - \varepsilon_{pr})\right]$$

$$+ \frac{3E}{1+\mu}\,\frac{g}{r} + \frac{E}{(1+\mu)r}\,(3\varepsilon_R - \varepsilon_{pr} + \varepsilon_{p\theta}) = 0 \qquad (4\text{-}21)$$

or

$$\frac{1}{1-2\mu}\frac{de}{dr} + \frac{dg}{dr} = -\frac{2(g+\varepsilon_R)}{r} - \frac{4}{3}\frac{d\varepsilon_R}{dr} + \frac{2}{3}\frac{d\,\varepsilon_{pr}}{dr} + \frac{2(\varepsilon_{pr}-\varepsilon_{p\theta})}{3r} \qquad (4\text{-}21a)$$

and the compatibility Equation (4-4) changes to

$$\frac{de}{dr} - \frac{dg}{dr} = \frac{2(g+\varepsilon_R)}{r} \qquad (4\text{-}22)$$

Solving for e and g from the combination of Equations (4-21a) and (4-22), one obtains

$$e = \frac{1-2\mu}{3(1-\mu)}\left[\varepsilon_{pr} - 2\,\varepsilon_R + \int_{r_i}^{r}\frac{\varepsilon_{pr}-\varepsilon_{p\theta}}{r}\,dr\right] + C_1 \qquad (4\text{-}23)$$

$$g = -\frac{2(1+\mu)}{3(1-\mu)}\frac{1}{r^2}\int_{r_i}^{r} r\,\varepsilon_R\,dr + \frac{1-2\mu}{3(1-\mu)}\left[\varepsilon_{pr} - 2\,\varepsilon_R - \frac{1}{r^2}\int_{r_i}^{r} r(\varepsilon_{pr}+\varepsilon_{p\theta})dr\right] + \frac{C_2}{r^2} \qquad (4\text{-}24)$$

where C_1 and C_2 are integral constants to be determined.

The boundary conditions for the clad are

$$\begin{aligned} r &= r_i, & \sigma_r &= -P_g \\ r &= r_o, & \sigma_r &= -P_o \end{aligned} \qquad (4\text{-}25)$$

where the coolant pressure P_o is a given value and the gap pressure P_g will be formulated in the next section.

With these, C_1 and C_2 are determined

$$C_1 = \frac{2(1+\mu)(1-2\mu)}{3E(r_o^2-r_i^2)}\left[r_i^2\,P_g - r_o^2(P_o+G)\right] \qquad (4\text{-}26)$$

$$C_2 = \frac{2r_i^2 r_o^2(1+\mu)}{3E(r_o^2-r_i^2)} [-P_g + P_o + G] \qquad (4\text{-}27)$$

where

$$G = \frac{E}{1-\mu} \left[\frac{1}{2(1+\mu)} \int_{r_i}^{r_o} \frac{\varepsilon_{pr}-\varepsilon_{p\theta}}{r} dr - \frac{1}{r_o^2} \int_{r_i}^{r_o} r\, \varepsilon_R\, dr \right.$$

$$\left. - \frac{1-2\mu}{2(1+\mu)r_o^2} \int_{r_i}^{r_o} r(\varepsilon_{pr}+\varepsilon_{p\theta})dr\right] . \qquad (4\text{=}28)$$

The integrals can be evaluated by numerical methods if the values of the integrands at each station are known.

2. Finite-difference method for fuel zone

The fuel has an outer surface radius r_s and may have an inner void along the axial axis with a radius r_v as a result of irradiation. There are also internal and external pressures P_v and P_g. The fuel is divided into N intervals (not necessarily equal) along the radius and so there are N+1 stations. The first station is at the center for a solid fuel rod, or at the inner radius r_v for the fuel with a central void. In an application of central difference between station i and i-1 (50), the compatibility Equation (4-22) can be written as

$$\frac{e_i-e_{i-1}}{r_i-r_{i-1}} - \frac{g_i-g_{i-1}}{r_i-r_{i-1}} = \frac{1}{2}\left[\frac{2(g_i+\varepsilon_{Ri})}{r_i} + \frac{2(g_{i-1}+\varepsilon_{R,i-1})}{r_{i-1}}\right. \qquad (4\text{-}29)$$

or

$$e_i - A_i\, g_i = e_{i-1} - B_i\, g_i + C_i \qquad (4\text{-}29a)$$

where

$$A_i = 1 + a_i$$

$$B_i = 1 - b_i$$

$$C_i = a_i \varepsilon_{R,i} + b_i \varepsilon_{R,i-1} \tag{4-30}$$

$$a_i = \frac{r_i - r_{i-1}}{r_i}$$

$$b_i = \frac{r_i - r_{i-1}}{r_{i-1}}$$

In the same manner the equilibrium Equation (4-21) can be written as

$$D_i e_i + F_i g_i = U_i e_{i-1} + V_i g_{i-1} - W_i \tag{4-31}$$

where

$$D_i = \frac{c_i}{1-2\mu_i}$$

$$F_i = c_i(1+a_i)$$

$$U_i = D_{i-1}$$

$$V_i = c_{i-1}(1-b_i) \tag{4-32}$$

$$W_i = \frac{1}{3}(f_i - f_{i-1} + a_i h_i + b_i h_{i-1})$$

$$c_i = \frac{3E_i}{2(1+\mu_i)}$$

$$f_i = 2c_i(2 \varepsilon_{R,i} - \varepsilon_{pr,i})$$

$$h_i = c_i(-\varepsilon_{pr,i} + \varepsilon_{p\theta,i} + 3 \varepsilon_{R,i})$$

Combination of Equation (4-29a) and (4-31) gives e and g at ith station in terms of those at the (i-1)st station, i.e.,

$$e_i = K_i e_{i-1} + L_i g_{i-1} + M_i \tag{4-33}$$

$$g_i = K_i' e_{i-1} + L_i' g_{i-1} + M_i' \tag{4-34}$$

where

$$K_i = \frac{F_i + A_i U_i}{F_i + A_i D_i} \qquad K_i' = \frac{U_i - D_i}{F_i + A_i D_i}$$

$$L_i = \frac{A_i V_i - F_i B_i}{F_i + A_i D_i} \qquad L_i' = \frac{V_i + D_i B_i}{F_i + A_i D_i} \tag{4-35}$$

$$M_i = \frac{F_i C_i - A_i W_i}{F_i + A_i D_i} \qquad M_i' = \frac{-W_i - C_i D_i}{F_i + A_i D_i} \quad .$$

By successive application of Equations (4-33) and (4-34), the values of e and g at the ith station can be correlated to the values of e and g at the first station. Let this linear relation be written as

$$e_i = \alpha_i e_1 + \beta_i g_1 + \gamma_i \tag{4-36}$$

$$g_i = \alpha_i' e_1 + \beta_i' g_1 + \gamma_i' . \tag{4-37}$$

Also

$$e_{i-1} = \alpha_{i-1} e_1 + \beta_{i-1} g_1 + \gamma_{i-1} \tag{4-38}$$

$$g_{i-1} = \alpha_{i-1}' e_1 + \beta_{i-1}' g_1 + \gamma_{i-1}' \tag{4-39}$$

where the coefficients α_i, β_i, γ_i,... are to be determined.

Substituting Equations (4-36), (4-37), (4-38) and (4-39) into Equations (4-33) and (4-34), and rearranging, one obtains

$$(\alpha_i - K_i\alpha_{i-1} - L_i\alpha'_{i-1})e_1 + (\beta_i - K_i\beta_{i-1} - L_i\beta'_{i-1})g_1 + (\gamma_i - K_i\gamma_{i-1} - L_i\gamma'_{i-1} - M_i) = 0 \qquad (4\text{-}40)$$

$$(\alpha'_i - K'_i\alpha_{i-1} - L'_i\alpha'_{i-1})e_1 + (\beta'_i - K'_i\beta_{i-1} - L'_i\beta'_{i-1})g_1 + (\gamma'_i - K'_i\gamma_{i-1} - L'_i\gamma'_{i-1} - M'_i) = 0 \qquad (4\text{-}41)$$

Because e_1 and g_1 depend on boundary conditions and can be completely arbitrary; Equations (4-40) and (4-41) are therefore valid for all values of e_1 and g_1. It follows that the coefficients in these equations must be zero, or

$$\begin{aligned}
\alpha_i &= K_i\alpha_{i-1} + L_i\alpha'_{i-1} \\
\beta_i &= K_i\beta_{i-1} + L_i\beta'_{i-1} \\
\gamma_i &= K_i\gamma_{i-1} + L_i\gamma'_{i-1} + M_i \qquad (4\text{-}42) \\
\alpha'_i &= K'_i\alpha_{i-1} + L'_i\alpha'_{i-1} \\
\beta'_i &= K'_i\beta_{i-1} + L'_i\beta'_{i-1} \\
\gamma'_i &= K'_i\gamma_{i-1} + L'_i\gamma'_{i-1} + M_i \ .
\end{aligned}$$

If the kinds of Equations (4-33), (4-34), (4-36) and (4-37) are written for the second station, one gets

$$e_2 = K_2 e_1 + L_2 g_1 + M_2$$

$$g_2 = K_2' e_1 + L_2' g_1 + M_2' \qquad (4\text{-}43)$$

and

$$e_2 = \alpha_2 e_1 + \beta_2 g_1 + \gamma_2$$

$$g_2 = \alpha_2' e_1 + \beta_2' g_1 + \gamma_2' \qquad (4\text{-}44)$$

comparison of Equations (4-43) and (4-44) gives

$$\alpha_2 = K_2 \qquad \beta_2 = L_2 \qquad \gamma_2 = M_2$$

$$\alpha_2' = K_2' \qquad \beta_2' = L_2' \qquad \gamma_2' = M_2' \qquad (4\text{-}45)$$

Subsequently all the other α's, β's,... can be computed successively by the recurrence Equations (4-42). If e_1 and g_1 are obtained, all the other values of e and g can then be found by Equations (4-36) and (4-37). To evaluate e_1 and g_1, use is made of the boundary conditions. At the (N+1)st station the radial stress is equal to the gap pressure, i.e.

$$\sigma_{r,N+1} = -P_g = \frac{-P_o(r_i^2 - r_s^2)(T_g)_a}{[r_i^2(1+\varepsilon_{\theta i})^2 - r_s^2(1+\varepsilon_{\theta s})^2](T_o)_a} \qquad (4\text{-}46)$$

where

P_o = initial pressure

$(T_o)_a$ = initial absolute temperature

$(T_g)_a$ = absolute temperature of gap

$\varepsilon_{\theta i}$ = tangential strain of clad at r_i

$\varepsilon_{\theta s}$ = tangential strain of fuel at r_s

and from Equation (4-20)

$$\sigma_{r,N+1} = \frac{3E_{N+1}}{2(1+\mu_{N+1})(1-2\mu_{N+1})} e_{N+1} + \frac{3E_{N+1}}{2(1+\mu_{N+1})} g_{N+1}$$

$$+ \frac{E_{N+1}}{1+\mu_{N+1}} (2\ \varepsilon_{R,N+1} - \varepsilon_{pr,N+1}) \qquad (4\text{-}47)$$

or

$$-P_g = D_{N+1} e_{N+1} + C_{N+1} g_{N+1} + \frac{2}{3} C_{N+1} (2\ \varepsilon_{R,N+1} - \varepsilon_{pr,N+1}) \qquad (4\text{-}48)$$

Equations (4-36) and (4-37) can be written for the last station as

$$e_{N+1} = \alpha_{N+1} e_1 + \beta_{N+1} g_1 + \gamma_{N+1}$$

$$g_{N+1} = \alpha'_{N+1} e_1 + \beta'_{N+1} g_1 + \gamma'_{N+1} \ . \qquad (4\text{-}49)$$

Substituting in Equation (4-47) and solving for e_1 result

$$e_1 = P_{N+1} g_1 + Q_{N+1} \qquad (4\text{-}50)$$

where

$$P_{N+1} = \frac{-(D_{N+1}\beta_{N+1} + C_{N+1}\beta'_{N+1})}{D_{N+1}\alpha_{N+1} + C_{N+1}\alpha'_{N+1}}$$

$$Q_{N+1} = \frac{-(P_g + D_{N+1}\gamma_{N+1} + C_{N+1}\gamma'_{N+1} + \frac{1}{3} f_{N+1})}{D_{N+1}\alpha_{N+1} + C_{N+1}\alpha'_{N+1}} \qquad (4\text{-}51)$$

For a solid fuel rod the boundary condition at the first station is

$$\sigma_{r,1} = \sigma_{\theta,1} \cdot \tag{4-52}$$

$\sigma_{r,1}$ and $\sigma_{\theta,1}$ can be obtained from Equations (4-20) and (4-20a), i.e.,

$$\sigma_{r,1} = D_1 e_1 + c_1 g_1 + \frac{2}{3} c_1 (2\ \varepsilon_{R,1} - \varepsilon_{pr,1}) \tag{4-53}$$

$$\sigma_{\theta,1} = D_1 e_1 - c_1 g_1 - \frac{2}{3} c_1 (\varepsilon_{R,1} + \varepsilon_{p\theta,1}) \tag{4-54}$$

Thus the value of g_1 for the boundary condition is obtained:

$$g_1 = \frac{1}{3}(\varepsilon_{pr,1} - \varepsilon_{p\theta,1} - 3\ \varepsilon_{R,1}) \tag{4-55}$$

For a fuel rod with a central void, the boundary condition at the first station is

$$\sigma_{r,1} = -P_v = -\{\frac{P_o (T_v)_a}{(T_o)_a (1+\varepsilon_{\theta v})^2} + \frac{(0.2\ \pi\ r_2^2\ \dot{F}t + M_b) k (T_v)_a}{\pi\ r_v^2 (1+\varepsilon_{\theta v})^2}\} \tag{4-56}$$

where

$(T_v)_a$ = absolute temperature in central void at time t.

$\varepsilon_{\theta v}$ = tangential strain at r_v

The value of g_1 can then be found from the combination of Equations (4-50), (4-53) and (4-56)

$$g_1 = \frac{-P_v - D_1\ Q_{N+1} - \frac{1}{3} f_1}{c_1 + D_1 P_{N+1}} \tag{4-57}$$

After g_1 is determined by Equation (4-55) or (4-57) for

the different boundary conditions, e_1 can then be computed from Equation (4-50).

For the case of solid fuel rod, the value of r at the first station is zero and some of the coefficients become infinite. Therefore, a relatively small value may be assigned to r_1 in order to avoid the situation in the computation for this case.

As soon as e and g are solved from the equilibrium and the compatibility equations in either the closed form solution or the finite-difference method described above, all stresses and strains can then be determined.

In solving e and g, plastic strains are assumed to be known. In the method of successive approximations, values of plastic strains at stations will be assumed at first and then solutions of stresses and strains are obtained. Hereafter the problem is to find new plastic strains to continue the successive calculations till convergence is satisfied.

When plastic strains occur, a yield criterion and a flow rule will bring the triaxial problem to be associated with uniaxial problem. The equivalent quantities will be compared to actual experimental results thus to obtain new plastic strains. These will be developed as follows:

The flow rule of Prandtl-Reuss relations describes that the plastic strain increment at any instant of loading is proportional to the instantaneous stress deviator. That is

$$\frac{d\,\varepsilon_{pr}}{s_r} = \frac{d\,\varepsilon_{p\theta}}{s_\theta} = \frac{d\,\varepsilon_{pz}}{s_z} = d\lambda \tag{4-58}$$

or

$$\frac{\varepsilon_{pr}}{s_r} = \frac{\varepsilon_{p\theta}}{s_\theta} = \frac{\varepsilon_{pz}}{s_z} = \lambda \tag{4-59}$$

where λ is a non-negative constant.

According to Mises' yield criterion, the distortion energy stored in a unit volume of the material at yielding is a constant quantity. The result may be expressed as

$$\sqrt{s_r^2 + s_\theta^2 + s_z^2} = K \tag{4-60}$$

where K is the constant. For the case of simple tension,

$$K = \frac{2}{3}\sigma_e \tag{4-61}$$

where σ_e, the equivalent stress, is the axial stress in the simple tension case. Then the triaxial stresses can be related to the equivalent stress by

$$\sigma_e = \frac{3}{2}\sqrt{s_r^2 + s_\theta^2 + s_z^2} \tag{4-62}$$

The equivalent stress deviator corresponding to the equivalent stress is

$$s_e = \frac{2}{3}\sigma_e \tag{4-63}$$

Hence the equivalent plastic strain is

$$\varepsilon_{pe} = \lambda\ s_e = \frac{2}{3}\lambda\sigma_e \tag{4-64}$$

The combination of Equations (4-59), (4-62) and (4-64) gives

$$\varepsilon_{pe} = \sqrt{\frac{2}{3}(\varepsilon_{pr}^2 + \varepsilon_{p\theta}^2 + \varepsilon_{pz}^2)} \tag{4-65}$$

The total strain deviators are

$$\begin{aligned} e_{tr} &= \varepsilon_r - e = e_r + \varepsilon_R + \varepsilon_{pr} \\ e_{t\theta} &= \varepsilon_\theta - e = e_\theta + \varepsilon_R + \varepsilon_{p\theta} \\ e_{tz} &= \varepsilon_z - e = e_z + \varepsilon_R + \varepsilon_{pz} \end{aligned} \tag{4-66}$$

If three modified total strain deviators are defined as

$$\begin{aligned} e'_{tr} &= e_{tr} - \varepsilon_R = e_r + \varepsilon_{pr} \\ e'_{t\theta} &= e_{t\theta} - \varepsilon_R = e_\theta + \varepsilon_{p\theta} \\ e'_{tz} &= e_{tz} - \varepsilon_R = e_z + \varepsilon_{pz}, \end{aligned} \tag{4-67}$$

or

$$\begin{aligned} e'_{tr} &= \frac{1}{2}(e + 3g + 4\ \varepsilon_R) \\ e'_{t\theta} &= \frac{1}{2}(e - 3g - 2\ \varepsilon_R) \\ e'_{tz} &= -e - \varepsilon_R\ , \end{aligned} \tag{4-67a}$$

the following expressions can be obtained by substituting e_r, e_θ and e_z from Equation (4-13) into (4-67) and using the rela-

tions from Equation (4-59):

$$e'_{tr} = \left(\frac{1+\mu}{E\lambda} + 1\right)\varepsilon_{pr}$$

$$e'_{t\theta} = \left(\frac{1+\mu}{E\lambda} + 1\right)\varepsilon_{p\theta} \qquad (4\text{-}68)$$

$$e'_{tz} = \left(\frac{1+\mu}{E\lambda} + 1\right)\varepsilon_{pz}$$

Squaring both sides of the above three equations, adding together, multiplying with a value of 2/3 on either side and then taking square root, one obtains

$$e'_{te} = \left(\frac{1+\mu}{E\lambda} + 1\right)\varepsilon_{pe} \qquad (4\text{-}69)$$

where

$$e'_{te} = \sqrt{\frac{2}{3}\left(e'^{2}_{tr} + e'^{2}_{t\theta} + e'^{2}_{tz}\right)} \qquad (4\text{-}70)$$

$$\varepsilon_{pe} = \sqrt{\frac{2}{3}\left(\varepsilon^{2}_{pr} + \varepsilon^{2}_{p\theta} + \varepsilon^{2}_{pz}\right)} \qquad (4\text{-}65)$$

Here e'_{te} is the corresponding modified total equivalent strain defined.

Combination of Equations (4-68) and (4-69) results

$$\varepsilon_{pr} = \frac{\varepsilon_{pe}}{e'_{te}}\, e'_{tr}$$

$$\varepsilon_{p\theta} = \frac{\varepsilon_{pe}}{e'_{te}}\, e'_{t\theta} \qquad (4\text{-}71)$$

$$\varepsilon_{pz} = \frac{\varepsilon_{pe}}{e'_{te}}\, e'_{tz} \quad .$$

If λ obtained from Equation (4-64) is substituted into (4-69), the result is

$$e'_{te} = \varepsilon_{pe} + \frac{2(1+\mu)\sigma_e}{3E} \tag{4-72}$$

Here, σ_e and ε_{pe} can be related to the actual stress-strain curves obtained in simple tension or compression test. The equation representing these curves may be written in a general form as

$$\varepsilon_{te} = \varepsilon_{pe} + \frac{\sigma_e}{E} = f(\sigma_e, T) \tag{4-73}$$

where ε_{te} is the total equivalent strain which can be expressed as a function of equivalent stress and temperature.

To represent the stress-strain curve for the cladding material, an empirical equation due to Ramberg and Osgood (51) may be used, i.e.,

$$\varepsilon_{te} = \frac{\sigma_e}{E_c} + K_c\left(\frac{\sigma_e}{E_c}\right)^{n_c} \tag{4-74}$$

or

$$\varepsilon_{pe} = K_c\left(\frac{\sigma_e}{E_c}\right)^{n_c} \tag{4-75}$$

where n_c, a function of temperature, may be written as

$$n_c = C_{c1} + C_{c2}T_c^{C_{c3}} \tag{4-76}$$

where C_{c1}, C_{c2}, and C_{c3} are constant, T_c is the temperature in clad, E_c is the modulus of elasticity of clad, and K_c can be written as (52)

$$K_c = \frac{3}{7}\left(\frac{E_c}{\sigma_y}\right)^{n_c-1} \tag{4-77}$$

where σ_y is the assumed yield strength of 0.2% offset and is a function of temperature, i.e.,

$$\sigma_y = C_{c4} - C_{c5} T_c \tag{4-78}$$

in which C_{c4} and C_{c5} are constant.

For the oxide fuel material the stress-strain curve beyond the proportional limits may be represented by

$$\varepsilon_{te} = K_f \left(\frac{\sigma_e}{\sigma_p}\right)^{n_f} \tag{4-79}$$

where

$$K_f = \frac{\sigma_p}{E_f} \tag{4-80}$$

$$E_f = (C_{14} - C_{15} T_f)(1 - C_{16} P - C_{17} P^2) \tag{4-81}$$

$$\sigma_p = C_{18}/(T_f - C_{19}) \tag{4-82}$$

$$n_f = C_{20}(T_f - C_{21})^2 + C_{22} \tag{4-83}$$

the C's are constant, σ_p is the proportional limit, E_f is the modulus of elasticity and T_f is the temperature in the fuel, and P is the porosity given for each zone in the fuel.

It should be noted that the oxide fuel material at high temperature in a fast reactor during normal operation is assumed to be plastic. The ductile-brittle transition occurs in the temperature range of 600°C to 800°C for UO_2 (54).

From the combination of Equations (4-72) and (4-73), an equivalent plastic strain associated with experimental stress-

strain curves can be obtained. Inserting this value of ε_{pe} into Equations (4-71), one can obtain the new plastic strains required for the iteration process.

D. The Method of Successive Approximation

The principle of the successive-approximation method is to solve the elastoplastic problem through iterations in which each time involves essentially the solution of a linear problem, when the plastic strains are presumed.

The steps in the procedure to carry out the successive approximations are:

(a) Assuming three plastic strains ε_{pr}, $\varepsilon_{p\theta}$, and ε_{pz} for each station along the radius.

(b) With the known values of plastic strains, thermal expansion strains and irradiation dilatation strains, solving the variables e and g from the combination of the equilibrium Equation (4-21) and the compatibility Equation (4-22) in closed-form solution for clad or in finite-difference solution for fuel.

(c) Calculating the modified total strain deviators e'_{tr}, $e'_{t\theta}$ and e'_{tz} from Equation (4-67a)

(d) Calculating the corresponding modified total equivalent strain e'_{te} from Equation (4-70) (a result of the application of Prandtl-Reuss relations and the von Mises yield criterion).

(e) Solving equivalent plastic strain ε_{pe} from the combination of Equations (4-72) and (4-73) (stress-strain curves being associated).

(f) Calculating new plastic strains from Equation (4-71) with obtained values in steps (c), (d) and (e). These new plastic strains are to be used in the next iteration.

(g) Repeat steps (b), (c), (d), (e) and (f). The iteration proceeds till desired convergence is obtained.

Experience shows that the iterated results are converged rapidly.

V. COMPUTER PROGRAM AND NUMERICAL EXAMPLE

A. Introduction to Computer Program

A computer code, ISUNE 1, written in Fortran IV language and adapted for the IBM 360 computer at the Iowa State University Computer Center was developed to perform the thermal, radiation and stress analysis for oxide cylindrical fuel pins or fuel elements of fast reactors in unsteady state.

The coolant is a liquid metal. The clad is a metal tube. The bonding material is an inert gas. For the fuel, pure UO_2 or a mixture of $PuO_2 \cdot UO_2$ (or $PuO_2 \cdot ThO_2 \cdot UO_2$) is applicable.

The function of the Code is to analyze and calculate several important variables as the functions of radial space and irradiation time of the fuel elements:

1. The irradiation swelling, fission-gas release and fuel burnup,
2. The temperature distributions and thermal gradients in the cladding and in the fuel zone,
3. The changes of fission-gas pressure in the fuel elements,
4. The fuel-clad gap thickness and the radii of the central void, the columnar-grain region and equi-axed-grain region,
5. The stresses and strains produced in the fuel elements.

The complete computer program is presented in Appendix A.

Schematic flowcharts of the code are shown in Figures 5.1 and 5.2. Important notations in the program are given in Tables 5.1 and 10.1.

The input data which must be given to the computer including geometric parameters, thermal parameters, radiation parameters, elastic and plastic parameters and all constants involved. These parameters, constants and their values for the numerical example are tabulated with names arranged in alphabetical order in Table 5.1.

B. Results

In the numerical example, the fuel rod is UO_2 of 90% smeared density with an outer diameter of 0.215 inch, the clad tube is Type 316 stainless steel with an outer diameter of 0.250 inch and an inner diameter of 0.220 inch, and the fuel element is cooled with sodium, bonded with helium and irradiated at 15 kw/ft of constant linear power. All other values of parameters and constants for performing the calculation are listed in Table 5.1.

Some important results of the numerical example are presented in Figures 5.3 through 5.13, and also tabulated in Tables 11.1 through 11.21, Appendix B.

Figures 5.3 and 5.4 show the time variation with the temperature and radii at the surfaces of the columnar-grain and equiaxed-grain regions in the fuel zone respectively. The

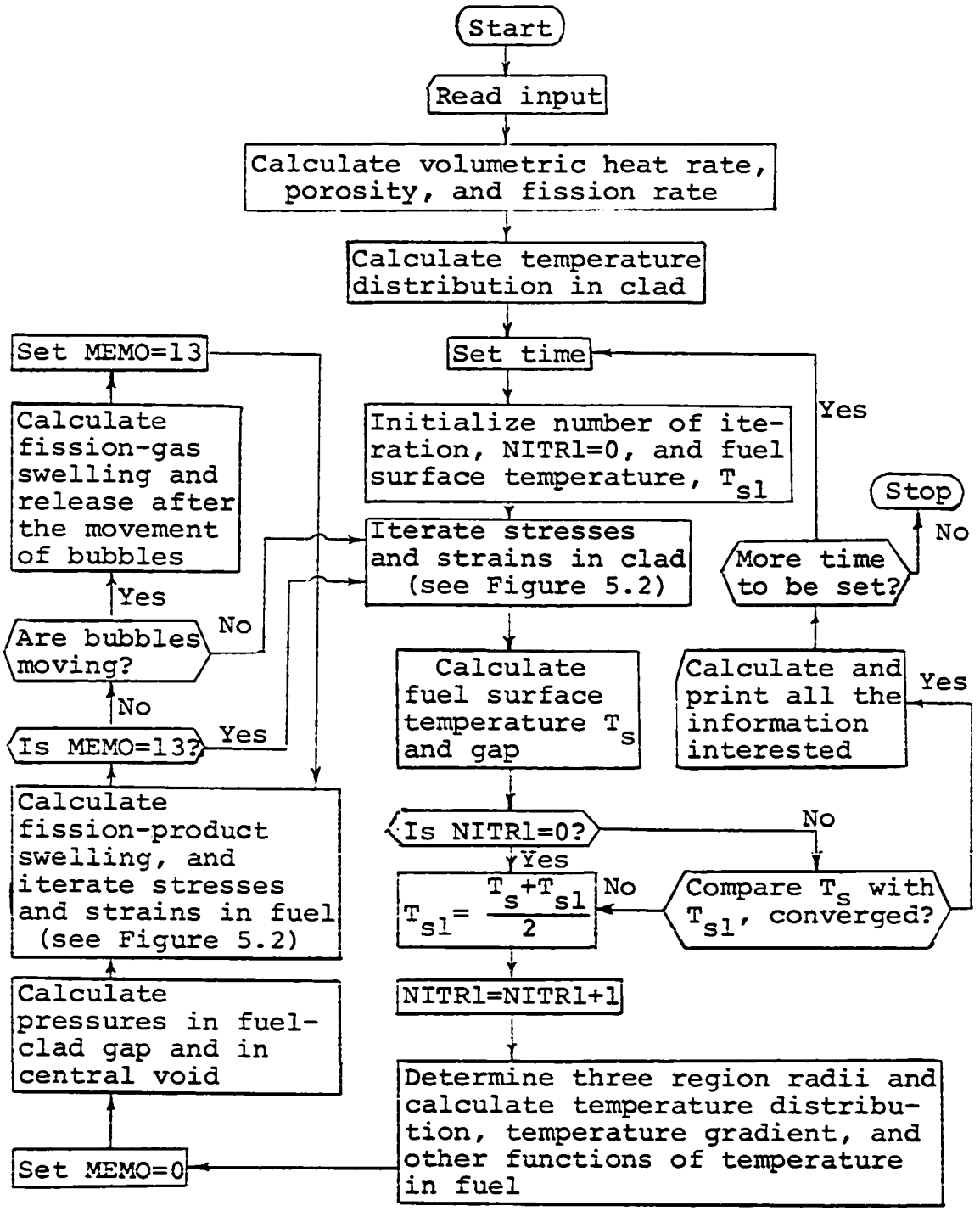

Figure 5.1. General flowchart for the code

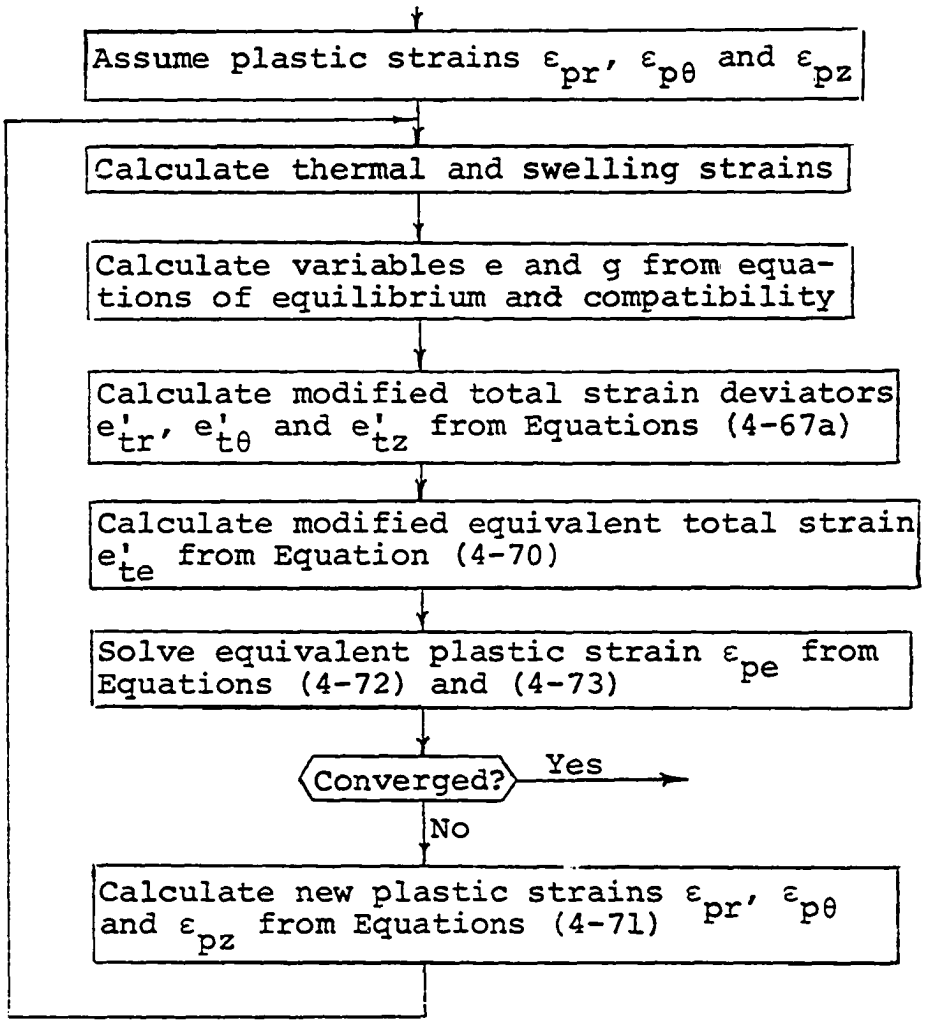

Figure 5.2. Flowchart for computing stresses and strains by the method of successive approximations

Table 5.1. Input data

Name	Description	Data	Units
ABST	Absolute temperature conversion constant	273.	°C
ACTEGD	Activation energy for grain growth[a]	8.38×10^{-12}	erg/mol.
AMIG	Molecular volume of the matrix[b]	4.09×10^{-23}	cm^3
AVCV	Coolant average velocity[c]	793.0	cm/sec
AVGDN	Avogadro number	6.025×10^{23}	mol./mole
BOLZ	Boltzmann constant	1.380×10^{-16}	erg/°K/mol.
CDEN	Coolant density[c]	0.867	gm/cm^3
CELSMD	Clad elastic modulus	$24. \times 10^3$	1000psi
CEXCL	Thermal linear expansion coefficient of clad	19.26×10^{-6}	cm/cm-°C
CLDK	Clad thermal conductivity	0.16748	w/cm-°C
CNAVST	Minimum significant hydrostatis stress	1000.	$dynes/cm^2$
CNER	Control error	0.001	-
CNT1	Conversion constant for fission rate	3.206×10^{-11}	w-sec
CNT2	Constant for calculation of thermal conductivity of fuel[d]	0.0130	-

[a] Calculated from experimental data (27).

[b] Data given by Nichols (12).

[c] Data provided by Ma (5).

[d] Empirical constants (29).

Table 5.1 (Continued)

Name	Description	Data	Units
CNT3	Constant for calculation of thermal conductivity of fuel[d]	0.4848	-
CNT4	"	0.4465	-
CNT5	Constant for calculation of grain size[a]	0.2306	-
CNT6	Constant for calculation of solid fission-product swelling[e]	0.35×10^{-22}	-
CNT7	Constant for calculation of linear expansion coefficient of fuel[f]	6.0×10^{-6}	-
CNT8	"	2.0×10^{-9}	-
CNT9	"	1.7×10^{-12}	-
CNT10	Fraction of fission gas atoms	0.2	-
CNT11	Constant for determining bubble number per unit volume[g]	3.83×10^{17}	-
CNT12	"	0.66×10^{14}	-
CNT14	Constant for calculation of elastic modulus of fuel[h]	26.	-
CNT15	"	0.0025	-
CNT16	"	1.9	-

[e]Experimental result (32).

[f]Empirical constants (23).

[g]Obtained from experimental data (40).

[h]Constants in the empirical equation in reference (53).

Table 5.1 (Continued)

Name	Description	Data	Units
CNT17	Constant for calculation of elastic modulus of fuel[h]	0.9	-
CNT18	Constant for fitting stress-strain curves of fuel[i]	10^4	-
CNT19	"	375.	-
CNT20	"	6.17×10^{-6}	-
CNT21	"	400.	-
CNT22	"	4.	-
CNTC1	Constant for fitting stress-strain curves of clad[j]	5.5	-
CNTC2	"	7.11×10^{-20}	-
CNTC3	"	7.03	-
CNTC4	"	40.60	-
CNTC5	"	0.01785	-
CNTG1	Constant for calculating fuel emmissivity[f]	0.986	-
CNTG2	"	1.625×10^{-4}	-
CNTG3	Constant for calculating clad emmissivity[k]	0.544	-
CNTG4	"	3.540×10^{-4}	-

[i] From experimental results (54).

[j] From experimental results (55,56).

[k] From reference (57).

Table 5.1 (Continued)

Name	Description	Data	Units
CNTG5	Constant for calculating thermal conductivity of gas in fuel-clad gap[f]	6.875×10^{-4}	
CNTG6	"	0.25	-
CPR	Total vapor pressure in fabricated pores[b]	10^{6}	dynes/cm^2
CPSNRT	Poisson's ratio of clad	0.3	-
CSPH	Cooland specific heat[c]	1.377	w-sec/gm-°C
CSRC	Cross-sectional radius for collisions between matrix and vapor molecule[b]	3×10^{-8}	cm
CTHK	Thermal conductivity of coolant[c]	0.817	w/cm-°C
DENFR(1)	Fraction of fuel theoretical density in columnar grain region	0.99	-
DENFR(2)	Fraction of fuel theoretical density in equiaxed grain region	0.97	-
DENFR(3)	Fraction of fuel theoretical density in unaffected grain region	0.90	-
DGG2	Diameter of grain at equiaxed-grain region surface	15×10^{-4}	cm
DGGI	Initial diameter of grain	5×10^{-4}	cm
DSLF	Dislocation retarding force	10^{-4}	dyne
EQDIA	Equivalent diameter of coolant channel[c]	3.20	cm

Table 5.1 (Continued)

Name	Description	Data	Units
GBTF	Grain boundary retarding force	300.	dyne/cm
HTVP	Heat of vaporization[b]	9.91×10^{-12}	erg/mol.
MMAX	A maximum number for setting time	10	-
MNITR	Maximum number of iteration	50	-
NINTC	Number of interval in clad	10	-
NINTT	Number of interval in fuel	20	-
PRESF	Coolant pressure	0.0147	1000psi
PSNRT	Poisson's ratio of fuel	0.3	-
PWRL	Linear heat power	492.	w/cm
RMT	Room temperature	25.	°C
RRIN	Internal surface radius of clad tube	0.2790	cm
RROU	Outer surface radius of clad tube	0.3175	cm
RRS	Surface radius of fuel	0.2730	cm
SACTE	Surface diffusion activation energy[1]	6.606×10^{-12}	erg/mol.
SCACTE	Activation energy for surface diffusion coefficient[1]	6.606×10^{-12}	erg/mol.

[1] From reference (16).

Table 5.1 (Continued)

Name	Description	Data	Units
SPR	Constant[b]	1.64×10^{14}	dynes/cm^2
SRDFCO	Coefficient of surface diffusion coefficient[1]	10^4	cm^2/sec
STBO	Stefan-Boltzmann constant	5.71×10^{-12}	w/cm^2-°K
SURT	Surface tension of fuel matrix[1]	10^3	dyne/cm
TCLMAX	Maximum allowable centerline temperature	2800	°C
TFLU	Coolant temperature	550.	°C
UNIVGC	Universal gas constant	1.3804×10^{-16}	erg/°K/mol.
VNDWC	Van der Waals correction term	8.3×10^{-23}	cm^3
WTML1	Molecular weight of fuel matrix	270	gm/mole
WTML2	Molecular weight of vapor constituent	4	gm/mole

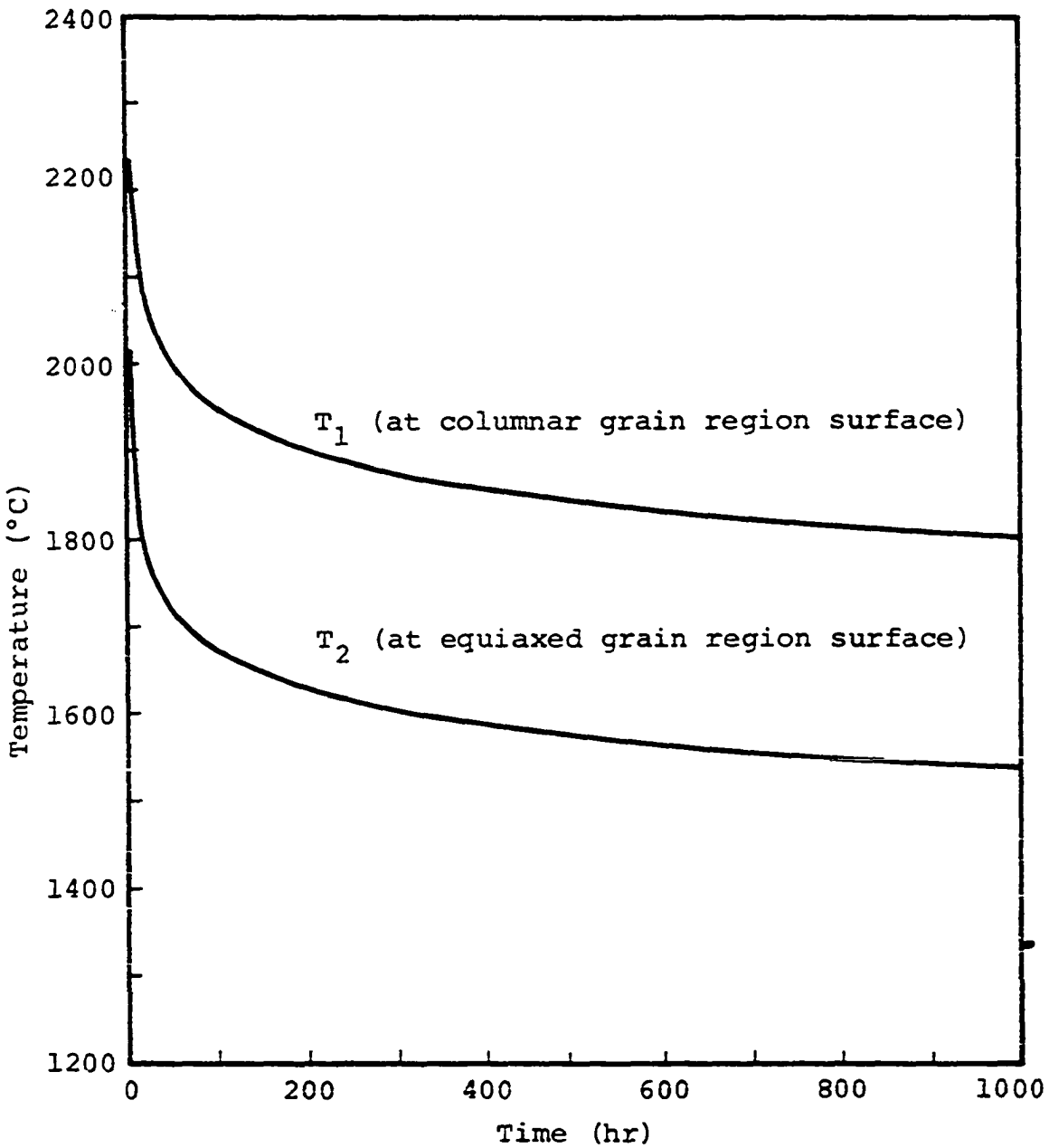

Figure 5.3. Temperature varies with time at surfaces of columnar and equiaxed grain regions

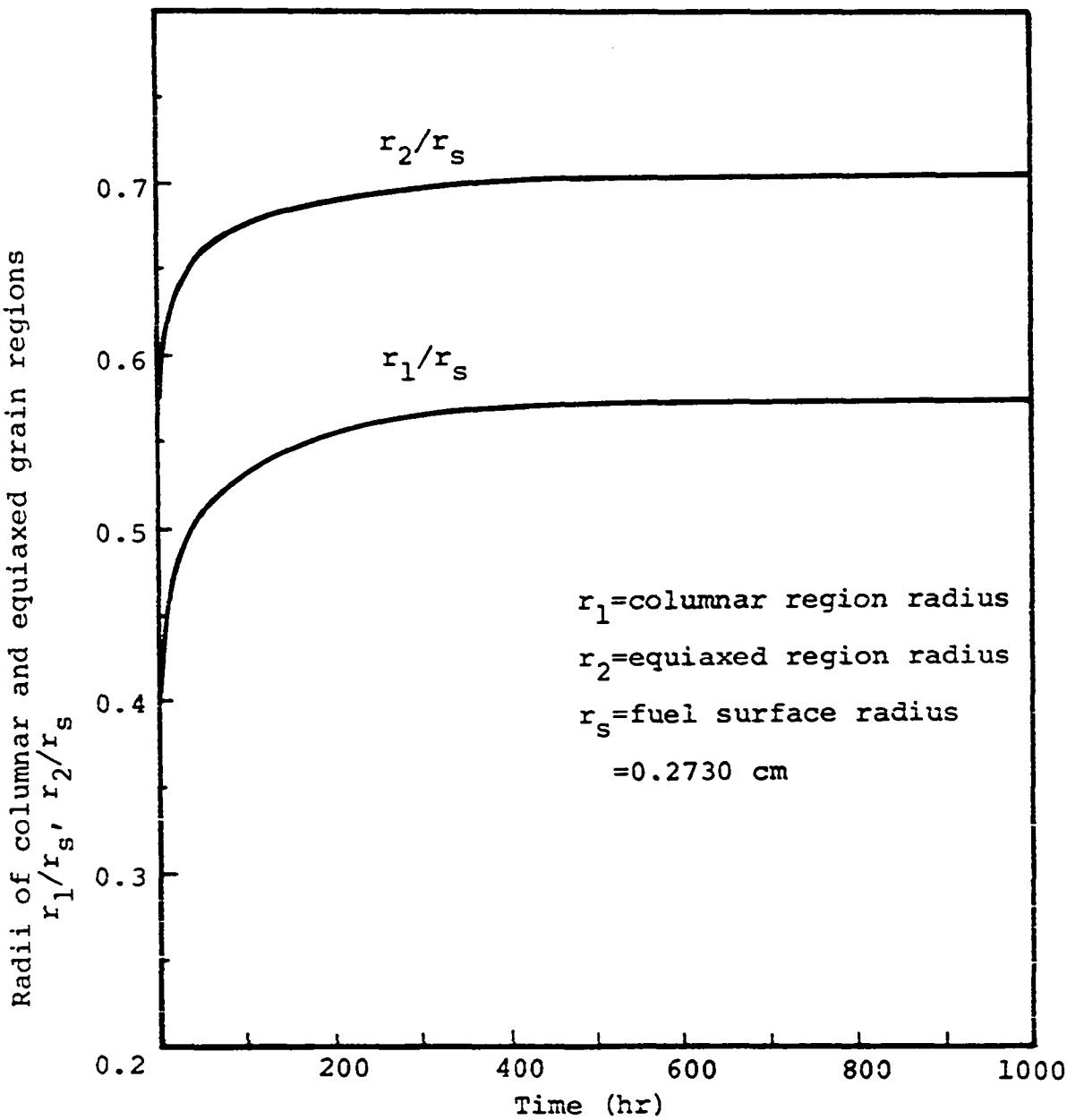

Figure 5.4. Time variations of radii of columnar and equiaxed grain regions

variations are rapid during the first hundred hours, and reach almost constant values after about 500 hours of the normal operation at the given linear power.

Figure 5.5 shows the temperature distributions in the cross section of the fuel element at different times. The clad outer surface temperature is 588.6°C and its inner surface temperature is 649.1°C. The temperature drop of 60.5°C across the clad corresponds to the linear power of 15 kw/ft. Temperatures in the outer region (about 1/3) of the fuel rod change very little with time. Those in the inner region decrease significantly in the early stage of the operation due primarily to the grain growths in the fuel. Thus, the effect of change of fuel rod surface temperature upon the time-dependent property of the temperature distribution in fuel may be neglected in the analysis.

In Figure 5.6, the fuel-clad gap increases with time during the first hundred hours and decreases hereafter. The increase in the early stage is due to the temperature decrease in the fuel as a result of grain growths, while the decrease is due to the effects of the fission-product swelling and the increase of pressure in the central void as soon as the grain growths are not significant. Also, Figure 5.6 shows the time variation of the radius of central void, increasing continuously and approaching almost constant after about 500 hours of the operation.

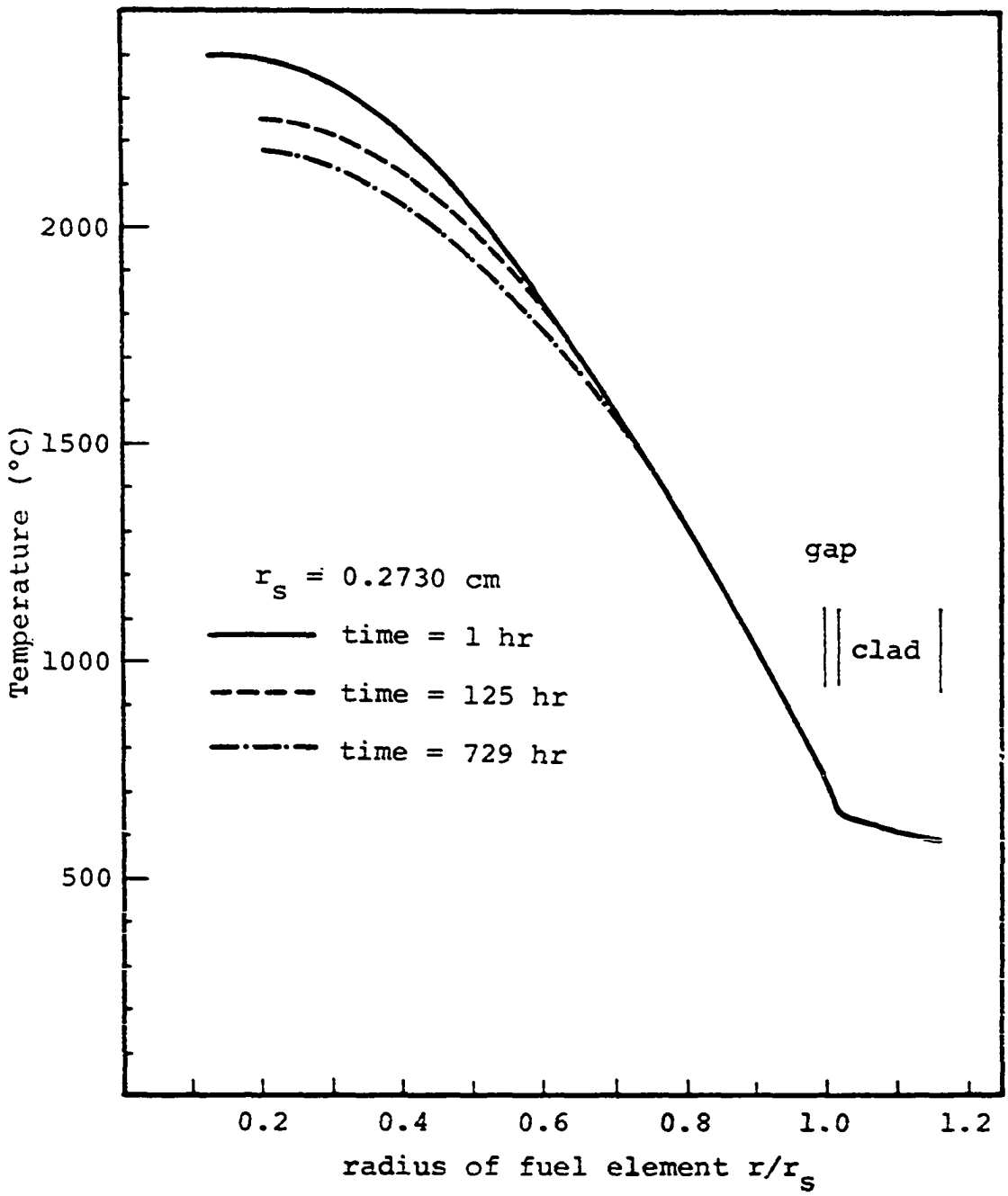

Figure 5.5. Temperature distribution in the fuel element

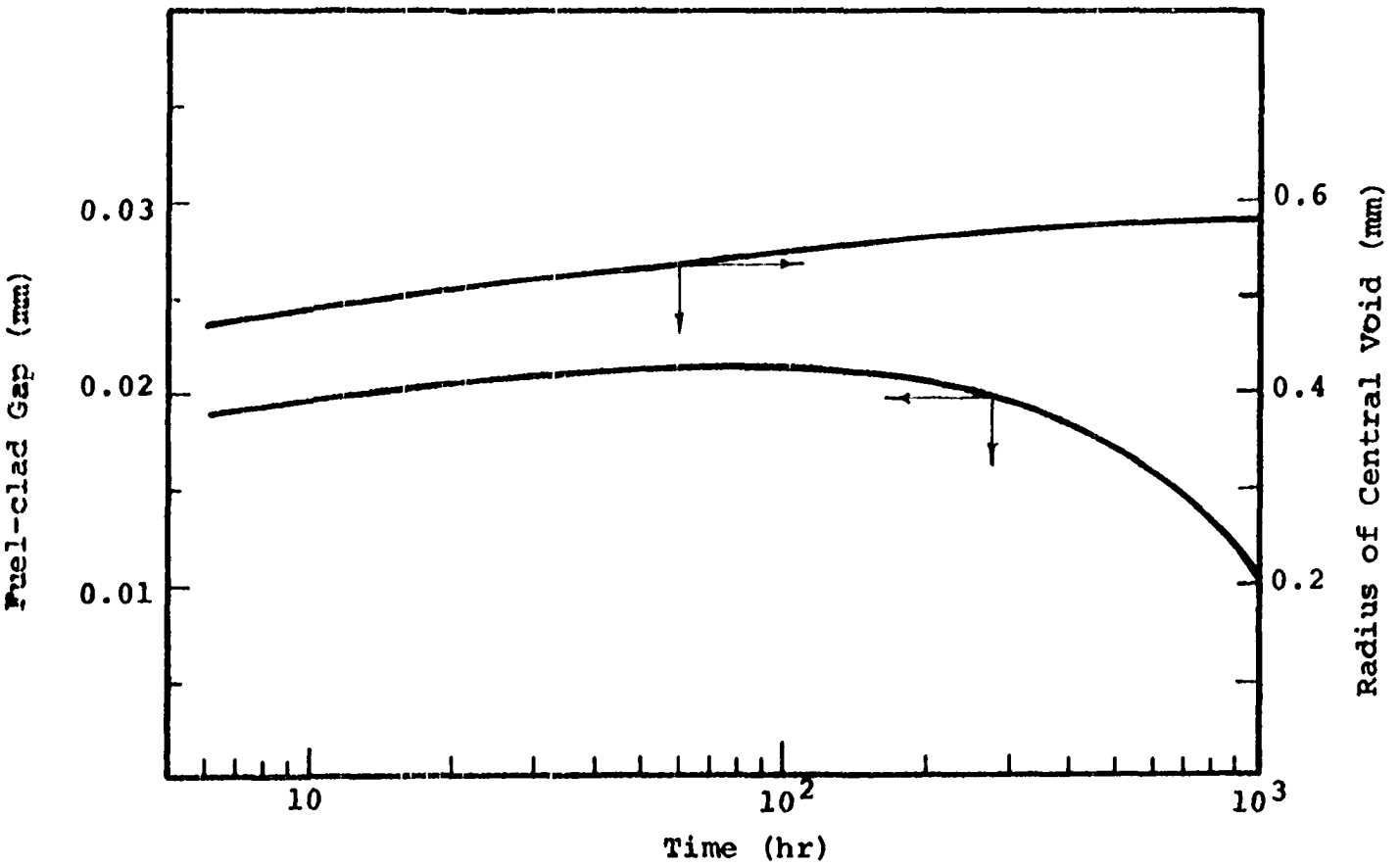

Figure 5.6. Time variations of fuel-clad gap and radius of central void

Figure 5.7 shows the time variation of pressures in the fuel-clad gap and in the central void. The pressure in the central void increases with time due to the increase of fission gas atoms escaped to it. The pressure in the fuel-clad gap decreases during the first hundred hours and then increases with time because of the variation on the gap thickness.

Figures 5.8 and 5.9 show the stress and strain distributions in the clad. The distributions remain little changed after 1000 hours of the operation. The radial stresses are so small that they may be neglected in the analysis. The tangential stresses vary from compression at the inner surface to tension at the outer surface.

Figure 5.10 gives the plastic strain and thermal strain distributions in the clad at 1000 hours of the operation.

The stress and strain distributions in the fuel zone at different times are shown in Figures 5.11 and 5.12. During the operation the changes in the distributions are relatively insensitive. The tangential stresses change from compression to tension with zero stress at about 0.7 of the fuel rod radius. The radial stresses at the outer and inner surfaces are very small. This implies that the pressures in the central void and in the fuel-clad gap may be neglected in comparison with the thermal stresses in the analysis. The radial strains decrease with radius for a given time and increase

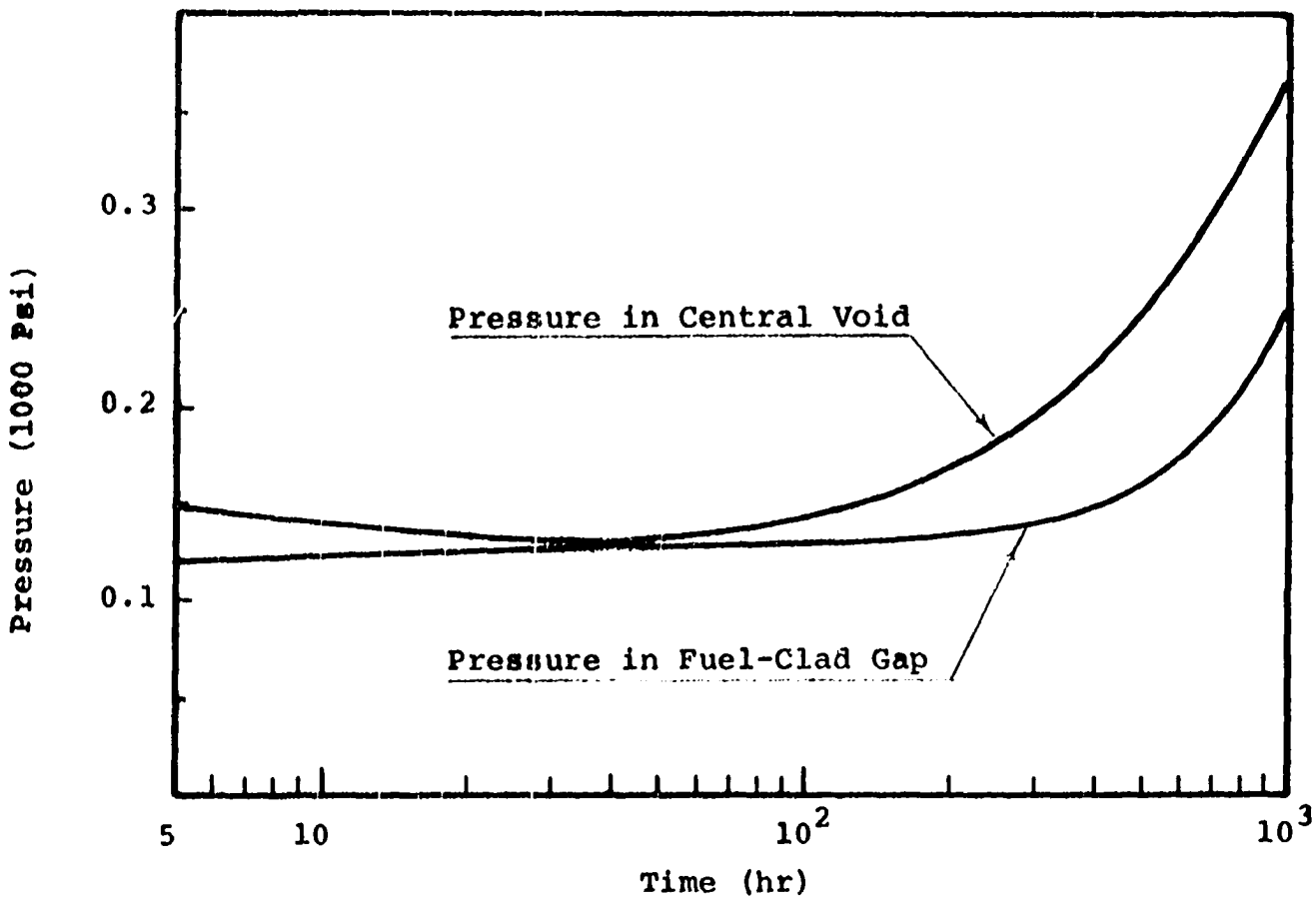

Figure 5.7. Time variations of pressure in central void and fuel-clad gap

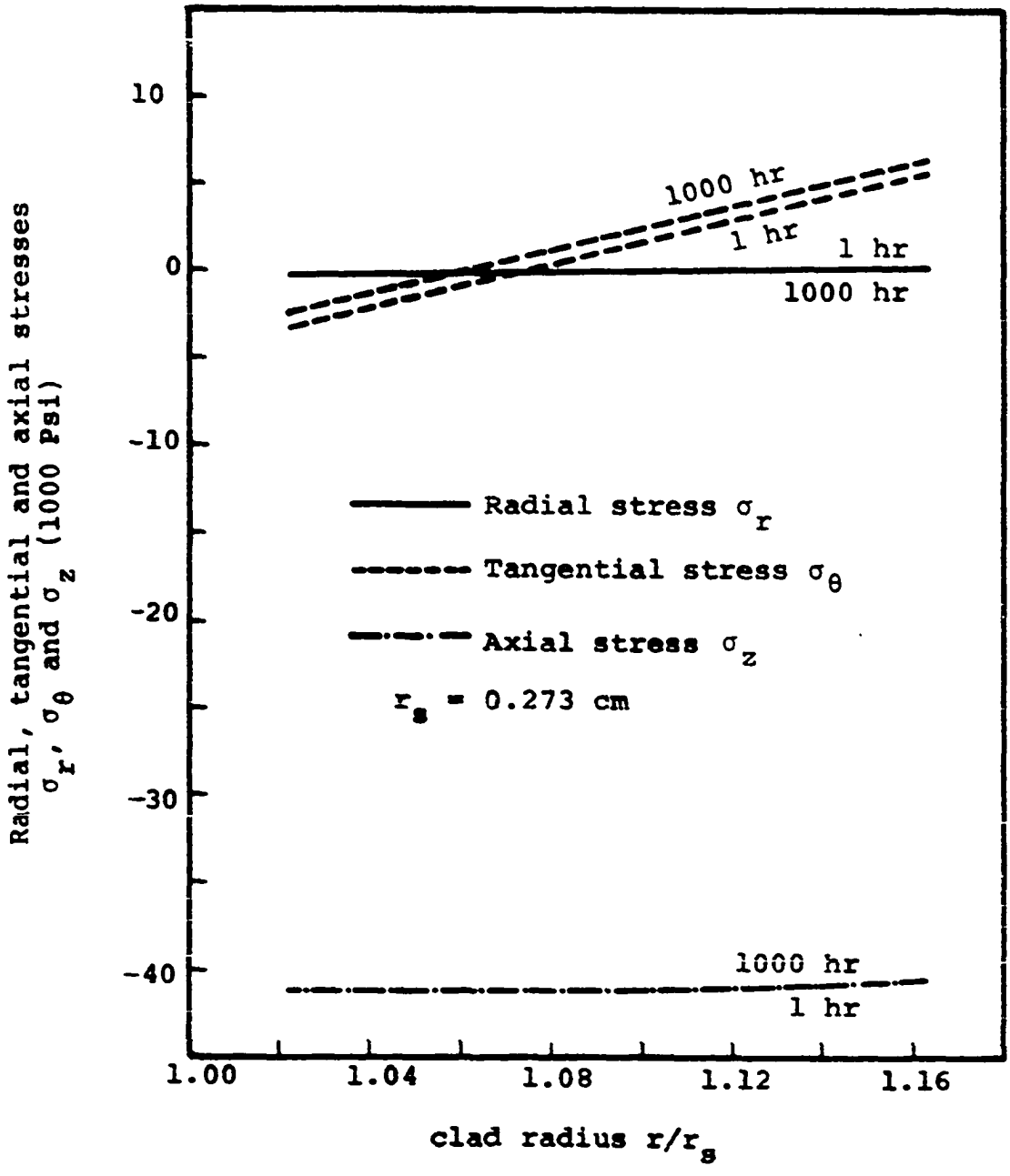

Figure 5.8. Radial, tangential and axial stress distributions in clad at irradiation times of 1 and 1000 hrs

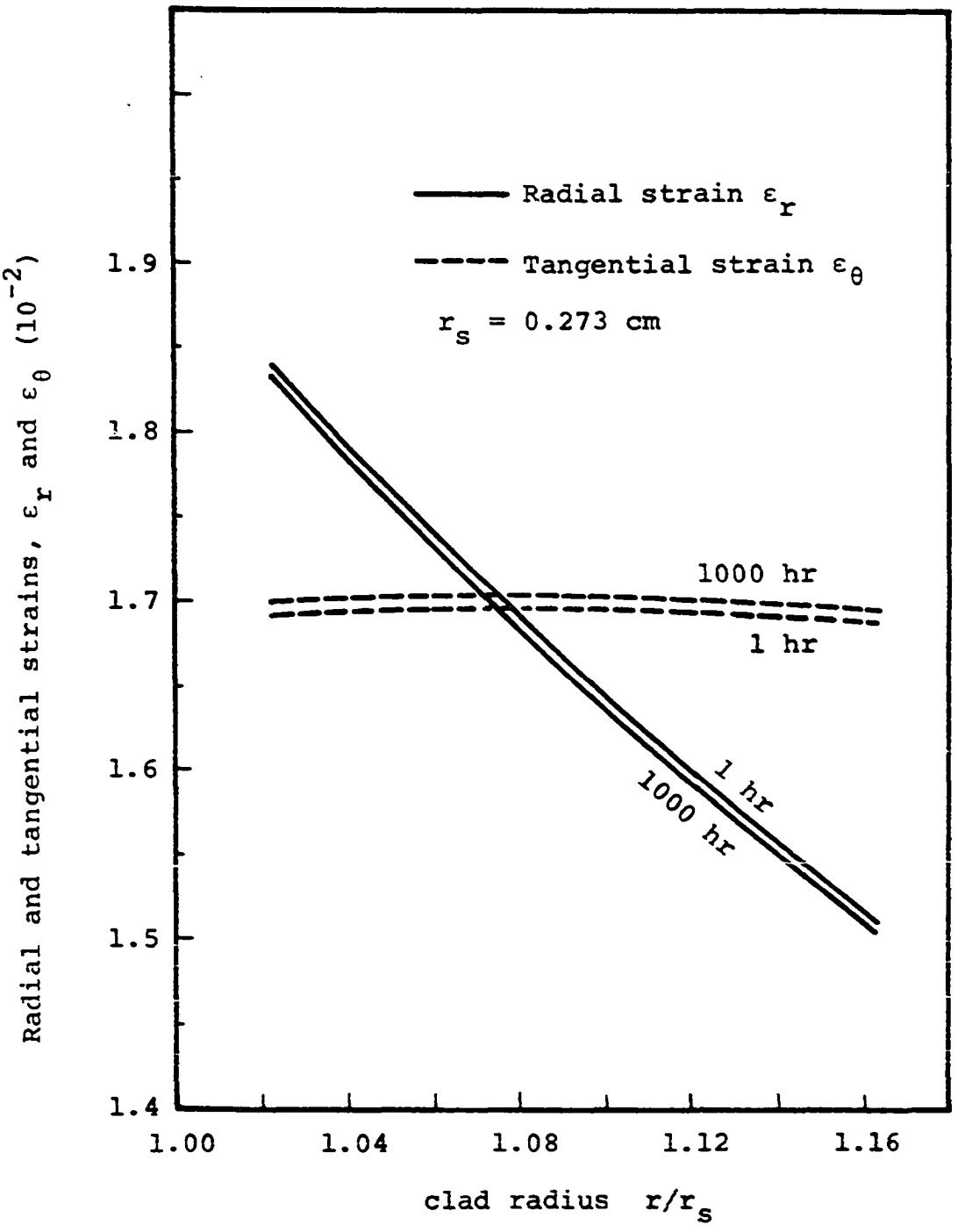

Figure 5.9. Radial and tangential strain distributions in clad at irradiation times of 1 and 1000 hrs

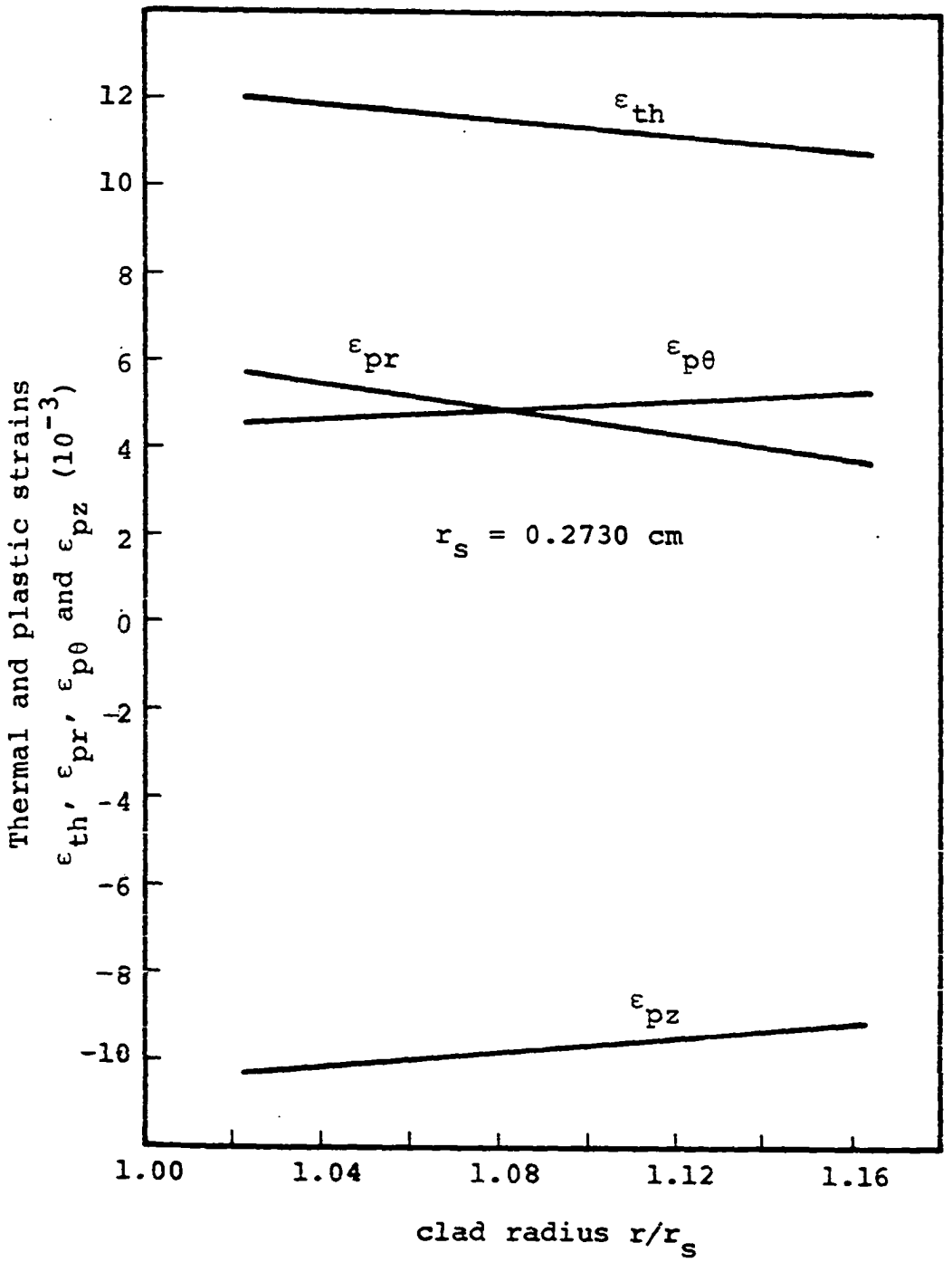

Figure 5.10. Thermal and plastic strain distributions in clad at irradiation time of 1000 hrs

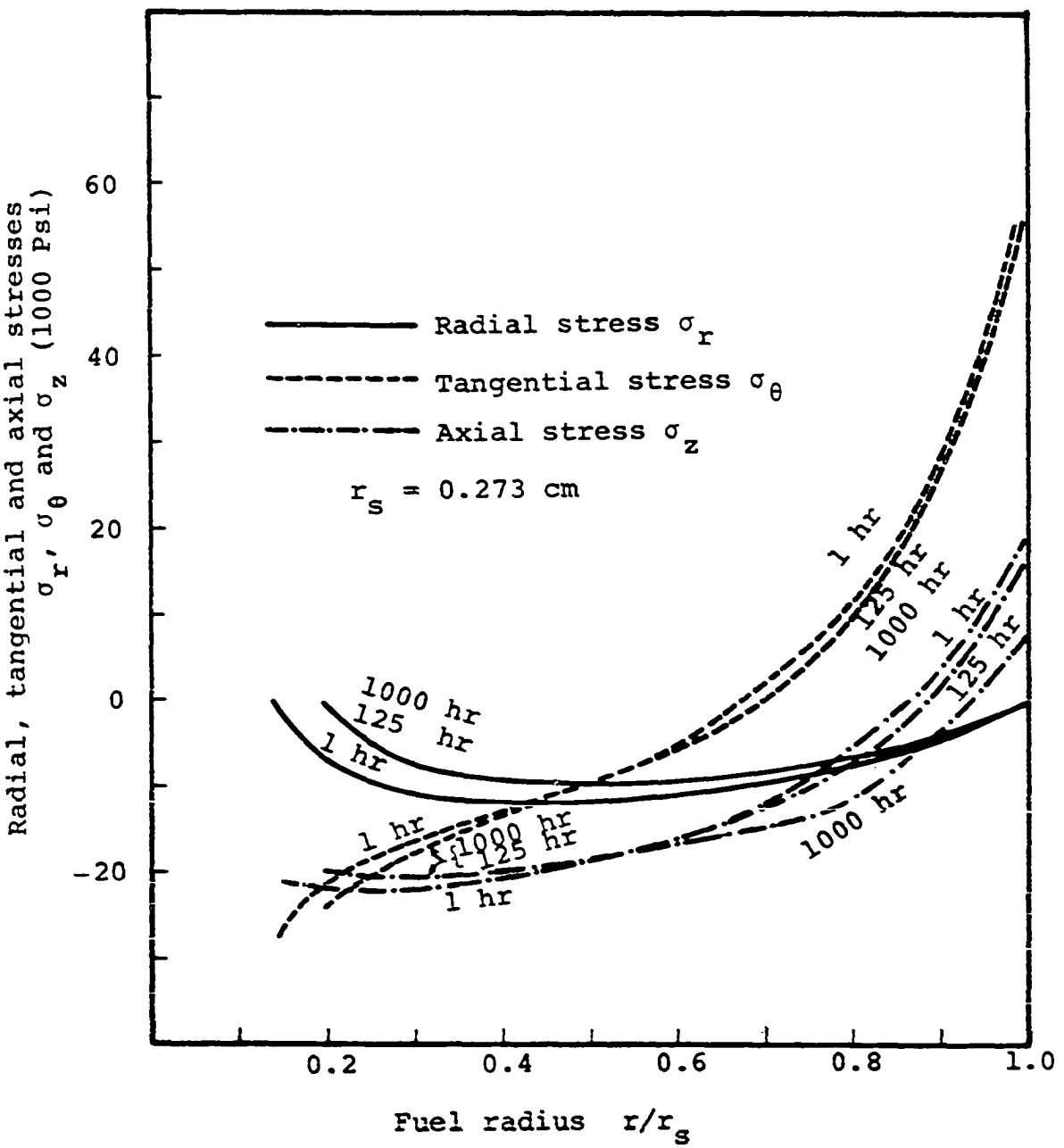

Figure 5.11. Radial, tangential and axial stress distributions in fuel zone vary with time

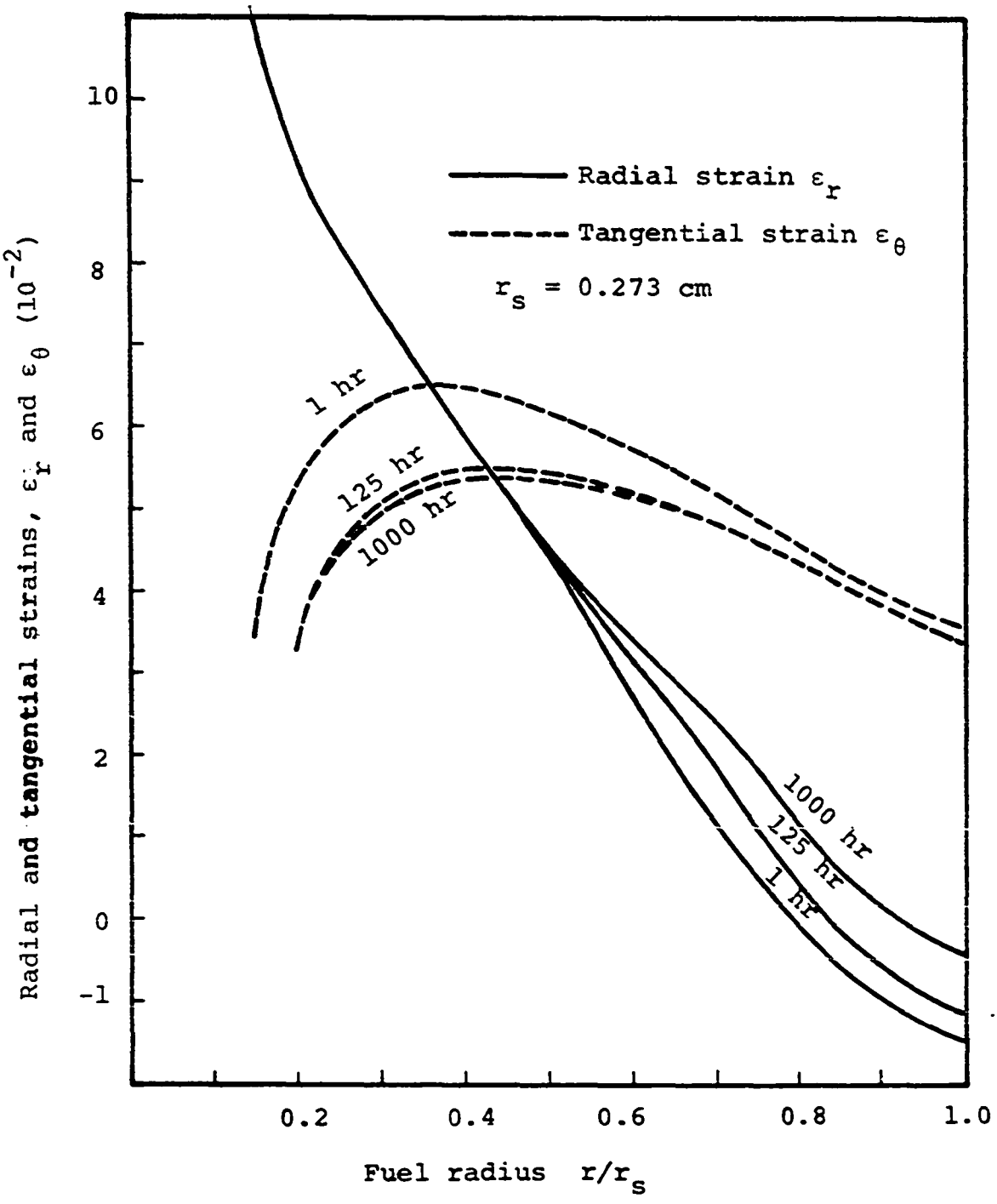

Figure 5.12. Radial and tangential strain distributions in fuel zone vary with time

with time in the outer region. The tangential strains increase to a maximum and then decrease with radius as shown in Figure 5.12.

Figure 5.13 shows the swelling, thermal and plastic strain distributions in the fuel rod at 729 hours of the operation. The plastic strains are comparative to the thermal strains. The swelling strains are small at this time in comparison with the plastic and thermal strains. The gas-bubble swelling in the unaffected region and the change of density passing through the surface of the equiaxed-grain region have marked effect on the swelling and plastic strains as shown in Figure 5.13.

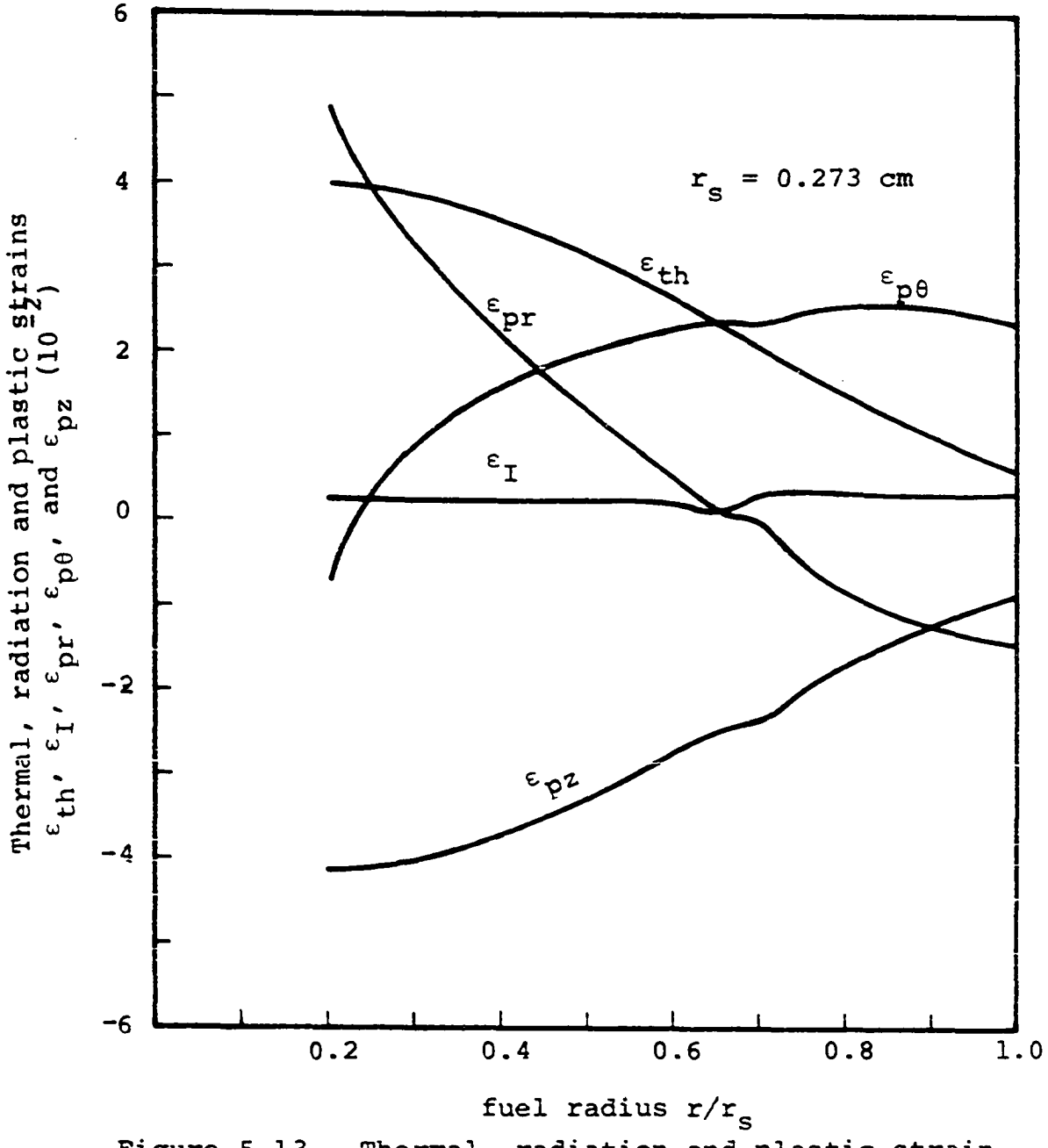

Figure 5.13. Thermal, radiation and plastic strain distributions in fuel zone at radiation time of 729 hours

VI. DISCUSSION

Equation (2-9) gives the migration rate of fabricated pores. Nichols used this equation to find the extent of the columnar grains (12). The trouble for him was the unknown temperature profile in the oxide fuel. Hence he had to assume a parabolic temperature distribution and found the results are not very sensitive to the choice of fuel surface temperature. Thus he set this temperature at 800°K and calculated the extent of the columnar grains as a function of time. In this analysis Equation (2-9) has also been used to couple with the heat transfer equations for oxide fuels. Here the fuel surface temperature is an iterated value. The temperature distribution is not necessary to be parabolic. The computed radius of the columnar-grain region is in good agreement with that obtained from Nichols. For example, at 1000 hours of irradiation the radius of columnar-grain region is 0.5719 of the fuel surface radius in this analysis, while in Nichols' analysis, the fictitious centerline temperature (a centerline temperature without considering grain growths) is 2829°K and so the radius is about 0.58 of the fuel surface radius. The agreement confirms that variation of the temperature distribution with irradiation time is primarily due to the grain growths. Nichols reported recently that the observations of cross section of a $ThO_2 \cdot UO_2$ fuel rod after irradiation (supplied by J. E. McCauly) were in good agreement

with his theoretical predictions (17). In the prediction of the radius of the central void, he did not consider the sintering of equiaxed grain growth, yet his assumption of a 100% of theoretical density in the columnar-grain region, which may not be so high, made a compensation. In the present analysis the sintering of equiaxed grain growth has been considered and the fraction of theoretical density in the columnar-grain zone has been assumed in the general accepted range, 98% to 99%. This analysis is shown to be applicable.

In the radiation analysis, fission gases in the regions where grain growth took place were assumed releasing to the central void. This assumption was made neither in the Barnes and Nelson model nor in the Nichols model. However, it has a sound basis due to the recent experimental work by Carroll et al. (39). Their result is quoted as below: "Equiaxed grain growth in UO_2 occurs at 1650°C and fission gas, normally trapped in a grain boundary, can then migrate along the mobile grain boundary. The fission-gas release rate is thus greatly increased during the time of grain growth, but the increase in grain size has little influence on the subsequent gas release at lower temperatures." Because of this assumption, the analysis of fission-gas swelling after movement of bubbles from their anchored sites, dislocations, can seldom be applied except at very high

burnups since anchored bubbles can exist only in the unaffected zone or the outerperiphery of the fuel rod in which the movement of bubbles is very unlikely as shown by Barnes and Nelson (15) and in the illustrative calculations of this analysis.

Oxide cracking may take place in an early period of irradiation time when the reactor was brought up to the normal operation, and not occur again until high burnups (58). Numerous experiments have shown that at temperatures where oxide material shows plastic or viscous flow, thermal stress failure occurred in fuel elements is negligible. In this work, it is assumed that the fuel element has been operated in a fast reactor for a short period of early time passing through a preliminary state of cracking and the fuel has been in a ductile state. Therefore, the effect of oxide cracking has not been taken into account in this analysis.

In the method of successive approximations for the stress analysis, there are several ways to relate the experimental stress-strain curves with plastic strains. These ways have thoroughly been discussed from the views of convergence by Mendelson (18). The way given in this analysis has avoided the situations of slow convergence or divergence. In applying the method of successive approximations, the major unusual techniques used are (a) The equilibrium and the compatibility

equations are solved in terms of the defined variables e and g. (b) In the fuel, the bubble size, which can be influenced by the hydrostatic stress (or average stress), is iterated in connection with the stress iterations. The number of iterations for convergence accurate to 10^{-3} is no more than 5 for clad and 6 for fuel in the illustrative calculations. These are very good results.

In iterating the fuel surface temperature, the average value of the preceding and the present calculated surface temperature is used for the next iteration. This simple device accelerated the convergence a great deal. By doing this, an accuracy of 10^{-2} can be obtained in two iterations for most the cases; otherwise, it may need more than eight iterations.

In addition to the present analysis the computer program is versatile for the design of oxide fuel elements. One can vary the fuel rod radius, the fuel-clad gap, the clad thickness, the fuel porosity, the power level and the coolant temperature and pressure to investigate problems concerning safety, economics and optimum parameters. The computing time is sufficiently short for carrying out the studies.

Discussions about results in this analysis have been given in Chapter V.

VII. CONCLUSIONS

The thermal, radiation and mechanical analysis for oxide cylindrical fuel pins or fuel elements of fast reactors in unsteady state has been developed. The computer program ISUNE 1 designed for performing the analysis has been proved useful to analyze and calculate several important variables as the functions of radial space and irradiation time of the fuel elements:

1. The irradiation swelling, fission-gas release and fuel burnup,
2. The temperature distributions and thermal gradients in the cladding and in the fuel zone,
3. The changes of fission-gas pressure in the fuel elements,
4. The fuel-clad gap thickness and the radii of the central void, the columnar-grain region and equiaxed-grain region,
5. The stresses and strains produced in the fuel elements.

These variables are significantly related to the fuel element performance as well as the reactor safety and operation economics.

The calculation as a whole is a compound and complex iteration. Experience shows that all the iteration results are converged rapidly.

Based on the results calculated from the numerical example using the computer code, the following main conclusions are drawn:

1. The radii of the central void, columnar-grain region and equiaxed-grain region near the mid-plane of the fuel element increase very rapidly during the first hundred hours of irradiation time; then gradually slow down, and reach almost constant values of radii after about 500 hours of normal operation at the given linear power.
2. The change of temperature distribution in the fuel depends greatly on the grain growths and not much on the surface temperature of the fuel rod during an early period of the constant linear power operation.
3. The thickness of fuel-clad gap increases with time during the first hundred hours and decreases hereafter.
4. The pressure in the central void increases with time, while the pressure in the fuel-clad gap decreases during the first hundred hours and then increases with time.
5. The plastic strains are comparable to the thermal strains in the fuel element.
6. The gas-bubble swelling in the unaffected region and the change of density passing through the surface of

the equiaxed-grain region have marked effects on the swelling and plastic strains.

7. After a sufficiently long period of constant linear power operation (about 1000 hours) the changes in stress and strain distributions in the fuel element are relatively insensitive.

VIII. LITERATURE CITED

1. Handwerk, J. H. Ceramic fuel elements in the ThO_2-UO_2 and UO_2-PuO_2 systems. U.S. Atomic Energy Commission Report TID-7546 [Technical Information Service Extension, Oak Ridge, Tenn.]. 1957.

2. Ma, B. M. and Murphy, G. Radiation and creep analysis for strain and stress distributions in tubular fuel elements. Nucl. Sci. and Eng. 20: 536-546. 1964.

3. Ma, B. M. Mechanical analysis for cylindrical fuel elements of a fast reactor for use in lunar power plant. ASME-SAE Air Transport and Space Meeting, New York, N.Y., Paper 861B. 1964.

4. Ma, B. M. and Murphy, G. Radiation and creep analysis of strains and stresses in annular fuel elements. Nucl. Structur. Eng. 1: 141-154. 1965.

5. Ma. B. M. The radiation growth and swelling analysis for cylindrical fuel elements during a positive reactor period. Nucl. Sci. and Eng. 26: 99-109. 1966.

6. Ma, B. M. Radiation growth and swelling analysis of solid cylindrical fuel rods during a complete reactor period. Nucl. Eng. Design 7: 181-193. 1968.

7. Friedrich, C. M. and Guilinger, W. H. CYGRO-2 stress analysis of the growth of concentric cylinders with gas bubbles. U.S. Atomic Energy Commission Report WAPD-TM-547 [Bettis Atomic Power Laboratory, Pittsburgh, Pa.]. 1966.

8. Anderson, W. K. and Mueller, G. O. KER-4, the thermal analysis of cylindrical fuel rods. U.S. Atomic Energy Commission Report KAPL-M-6475 [Knolls Atomic Power Lab., Schenectady, N.Y.]. 1965.

9. Moyar, G. L., Koenig, E. F., Lechliter, G. L. and Anderson, W. K. NUKER: A program for thermal and mechanical analysis of fuel rods. Amer. Nucl. Soc. Trans. 9: 379-380. 1966.

10. Guyette, M. CRASH: A computer program for the evaluation of the creep or plastic behavior of fuel pin sheaths. Amer. Nucl. Soc. Trans. 12: 524-525. 1969.

11. MacEwan, J. R. Grain growth in sintered uranium dioxide: I. Equiaxed grain growth. J. Amer. Ceram. Soc. 45: 37-41. 1962.

12. Nichols, F. A. Theory of columnar grain growth and central void formation in oxide fuel rods. J. Nucl. Mater. 22: 214-222. 1967.

13. Robertson, A. L., Ross, A. M., Notley, M. J. F. and MacEwan, J. R. Temperature distribution in UO_2 fuel elements. J. Nucl. Mater. 7: 225-262. 1962.

14. Barnes, R. S. and Nelson, R. S. Theories of swelling and gas retention in reactor materials. AIME Conf. on Radiation Effects, Ashville, N.C., Proc. 1965: 225-267. 1966.

15. Barnes, R. S. and Nelson, R. S. The behavior of inert gases in ceramic fuels. British Ceram. Soc. Proc. 7: 343-353. 1967.

16. Nichols, F. A. Behavior of gaseous fission products in oxide fuel elements. U.S. Atomic Energy Commission Report WAPD-TM-570 [Bettis Atomic Power Laboratory, Pittsburgh, Pa.]. 1966.

17. Nichols, F. A. Movement of pores in solids. J. Metals 21: 19-27. 1969.

18. Mendelson, A. Plasticity: theory and application. New York, N.Y., The Macmillan Co. 1968.

19. Manson, S. S. Thermal stress and low-cycle fatigue. New York, N.Y., McGraw-Hill Book Co., Inc. 1966.

20. Eyre, B. L. and Bullough, R. The formation and behavior of gas bubbles in a non-uniform temperature environment. J. Nucl. Mater. 26: 294-366. 1968.

21. Sofer, G. A., Kazi, A. H., Teer, B. R. and Cherry, B. H. Selected optimization studies in the use of carbide fuel in large fast breeder reactors. U.S. Atomic Energy Commission Report ANL-7120 [Argonne National Laboratory, Lemont, Ill.]. 1965.

22. Zudans, Z., Yen, T. C. and Steigelmann, W. H. Thermal stress techniques in the nuclear industry. New York, N.Y., American Elsevier Publishing Co., Inc. 1965.

23. Belle, J. Uranium dioxide: Properties and nuclear applications. Washington, D.C., U.S. Govt. Print. Off. 1961.

24. Sayles, C. W. A three-region analytical model for the description of the thermal behavior of low density oxide fuel rods in a fast reactor environment. Amer. Nucl. Soc. Trans. 10: 458. 1967.

25. Burk, J. E. Some factors affecting rate of grain growth in metals. Amer. Inst. Minig. Met. Engrs. Trans. 180: 73-91. 1949.

26. MacEwan, J. R. and Hayashi, J. Grain growth in UO_2, III. Some factors influencing equiaxed grain growth. British Ceram. Soc. Proc. 7: 245-272. 1967.

27. Nichols, F. A. Theory of grain growth in porous compacts. J. Appl. Phys. 37: 4599-4602. 1966.

28. Lyons, M. F., Coplin, D. H. and Weidenbaum, B. Analysis of UO_2 grain growth data from 'out of pile' experiments. U.S. Atomic Energy Commission Report GEAP-4411 [General Electric Co., Vallecitos Atomic Lab., San Jose, Calif.]. 1963.

29. Asamoto, R. R., Anselin, F. L. and Conti, A. E. The effect of density on the thermal conductivity of uranium dioxide. J. Nucl. Mater. 29: 67-81. 1969.

30. IBM Application Program H20-0205-3. System/360 Scientific Subroutine Package, (360A-CM-03X) Version III. RTMI-determine root within range by Muller's iteration. IBM, Technical Publication Dept., White Plains, N.Y. c1968.

31. Kristiansen, G. K. Zero of arbitrary function. BIT 3: 205-206. 1963.

32. Anselin, F. and Baily, W. E. The role of fission products in the swelling of irradiated UO_2 and $(U,Pu)O_2$ fuels. Amer. Nucl. Soc. Trans. 11: 103-104. 1968.

33. Carroll, R. M. The behavior of fission-gas in fuel. AIME Conf. on Radiation Effects, Ashville, N.C., Proc. 1965: 535-557. 1966.

34. Greenwood, G. W. and Speight, M. V. An analysis of the diffusion of fission gas bubbles and its effect on the behavior of reactor fuels. J. Nucl. Mater. 10: 140-144. 1963.

35. Barnes, R. S. A theory of swelling and gas release for reactor materials. J. Nucl. Mater. 11: 135-148. 1964.

36. Speight, M. V. Bubble diffusion and coalescence during the heat treatment of materials containing irradiation-induced gases. J. Nucl. Mater. 12: 216-220. 1964.

37. Gruber, E. E. On the theory of migration and coalescence of bubbles in solids. U.S. Atomic Energy Commission Report ANL-7079 [Argonne National Laboratory, Lemont, Ill.]. 1965.

38. Carroll, R. M. Fission-product release from UO_2. J. Nucl. Safety 5: 356-360. 1964.

39. Carroll, R. M., Morgan, J. G., Perez, R. B. and Sisman, O. Fission density, burnup, and temperature effects on fission-gas release from UO_2. Nucl. Sci. and Eng. 38: 143-155. 1969.

40. Cornell, R. M., Speight, M. V. and Masters, B. C. The role of bubbles in fission gas release from uranium dioxide. J. Nucl. Mater. 30: 170-178. 1969.

41. Barnes, R. S. Fundamentals of inert-gas agglomeration and swelling in metals. AIME, Nuclear Metallurgy 6: 21-24. 1959.

42. Shewmon, P. G. The movement of small inclusions in solid by a temperature gradient. Met. Soc. Trans. 230: 1134-1137. 1964.

43. Nichols, F. A. Kinetics of diffusional motion of pores in solids. J. Nucl. Mater. 30: 143-156. 1969.

44. Ince, E. L. Ordinary differential equations. New York, N.Y., Dover Co. 1944.

45. Ilyushin, A. A. Some problems in the theory of plastic deformation. Translation from Prikl. Math. Mech. 7: 245-272. 1943. U.S. Atomic Energy Commission Report RMB-12 [Grad. Div. Appl. Math., Brown Univ., Providence]. 1946.

46. Prandtl, L. Spannungsverteilung in plastischen Koerpern. International Congress on Applied Mechanics, 1st, Delft, Technishe Boekhandel en Druckerij, J. Waltman, Jr., 1925: 43-54. 1925.

47. Reuss, E. Beruecksichtigung der elastischen Formaenderungen in der plastizitaetstheorie. Z. Angew. Math. Mech. 10: 266-274. 1930.

48. von Mises, R. Mechanik der fersten Koeper im plastisch deformierbaren Zustan. Nachr. Ges. Wiss. Goettinger Math. Phys. Klasse 582-592. 1931.

49. Lode, W. Versuche ueger den Einfluss der mittleren Hauptspannung auf das Fliessen der Metalle Eisen Kupfer und Nickel. Z. Phys. 36: 913-939. 1962.

50. Fox, L. Numerical solution of ordinary and partial differential equations. London, Pergamon press. 1962.

51. Ramberg, W. and Osgood, W. R. Description of stress-strain curves by three parameters. NACA Technical Note No. 902. 1943.

52. Watter, M. and Lincoln, R. A. Strength of stainless steel structural members as function of design. Pittsburgh, Pa., The Republic Press. 1950.

53. Lechliter, G. L. and Anderson, W. K. Some input functions for computer description of fuel properties, Part 2-Mechanical properties. Amer. Nucl. Soc. Trans. 9: 376. 1966.

54. Byron, J. F. Yield and flow of polycrystalline uranium dioxide. J. Nucl. Mater. 27: 48-53. 1968.

55. Newell, H. D. Some creep properties of 16 chromium-13 nichel-3% molybdenum steel. Metals and Alloys 14: 173-181. 1941.

56. Simmons, W. F. and Van Echo, J. A. Report on the elevated-temperature properties of stainless steels. ASTM Data Series Publication DS 5-S1 [ASTM, Philadelphia, Pa.]. c1965.

57. McAdams, W. H. Heat transmission. New York, N.Y., McGraw-Hill Book Co., Inc. 1942.

58. Eichenberg, J. D., Frank, P. W., Kisiel, T. J., Lustman, B. and Vogel, K. H. Effects of irradiation on bulk UO_2. U.S. Atomic Energy Commission Report WAPD-183 [Bettis Plant, Pittsburgh, Pa.]. 1957.

IX. ACKNOWLEDGMENTS

The author wishes to express his sincere gratitude to his major professor, Dr. Benjamin M. Ma for the guidance, encouragement, and criticism which made this study possible.

His thanks are also due the other members of his graduate work committee, Dr. Glenn Murphy, Distinguished Professor and Head of the Department of Nuclear Engineering, Dr. Alfred F. Rohach, Dr. Donald F. Young, and Dr. Frederick M. Graham, for their review of this work and their helpful comments.

X. APPENDIX A: COMPUTER PROGRAM ISUNE-1

```
C
C
C
C
C     ISUNE-1 IS A FORTRAN IV COMPUTER PROGRAM FOR MECHANICAL, RADIATION
C     AND THERMAL ANALYSIS OF CYLINDRICAL OXIDE FUEL ELEMENTS OF FAST
C     REACTOR IN UNSTEADY STATE AT CONSTANT LINEAR POWER.
C
      EXTERNAL FCT1,FCT2,FCT3,FCT4,FCT5,FCT6,FCT7,FCTD
      EXTERNAL FCTG1
      EXTERNAL FCTC4
      DIMENSION PORST(3),         RDR(3),T(21),FSNRT(3),EQSTS3(21)
      DIMENSION CPLSTR(11),CPLSTT(11),CPLSTA(11),CTHSTN(11),FCTC1(11),
     1FCTC2(11),FCTC3(11),ZINVL1(11),ZINVL2(11),ZINVL3(11),SEC(11),
     2SGC(11),CTTNDR(11),CTTNDT(11),CTTNDA(11),CAVSTS(11),CESTS1(11),
     3CESTS2(11),CEPLS1(11),CEPLS2(11),CETSTN(11),CRAT1(11),CRAT2(11),
     4CERR1(11),CERR2(11),TC(11),RC(11),CSTSR(11),CSTST(11),CSTSA(11),
     5CSTNR(11),CSTNT(11)
      DIMENSION STSR(21),STST(21),STSA(21),STNR(21)
      DIMENSION PLSTR(21),PLSTT(21),PLSTA(21),ELSMD(21),ALPH(21),
     1BETA(21),GAMA(21),ALPHP(21),BETAP(21),GAMAP(21),SG(21),SE(21),
     2TSTNDR(21),TSTNDT(21),TSTNDA(21),EQTSTN(21),EQPLS1(21),EQPLS2(21),
     3RATIO2(21),ERR2(21), STNT(21),VELG(21), VELCG(21),TIMEG(21),
     4SWESTN(21),PPTLMT(21),FEXPN(21),FCOEFK(21),DTEMP(21),EQSTS1(21),
     5          STSDVR(21),STSDVT(21),STSDVA(21),EQSTS2(21)
      COMMON /FCTC4X/      CCOEFK,CEXPN,CPSNRT, ALSE,CELSMD
      COMMON /FCTG1X/RC,TC,CSTNT,STNT,             PWRL,STBO,CNTG1,CNTG2,
     1CNTG3,CNTG4,CNTG5,CNTG6
      COMMON CNT2,CNT3,CNT4,DENFR(3), PWRV(3)/FCT123/I,R(21)
     1/FCT15/RRV,RR1,TEMP1/FCT24/TEMP2,RR2/FCT34/RRS/FCT3X/TEMPS
      COMMON /FCT4X/ EQTSTN,PPTLMT,ELSMD,FCOEFK,FEXPN,PSNRT ,J
      COMMON /FCT6X/TIME,CNTC,HTVP,      ABST
      COMMON /FCTDX/COEF(5),MNITR
      COMMON /HAPPY1/  NUTIME,GASNM(21),DTIME(21),TIMECG(21),DG(21),
     1      DBCG(21),CNTE,CNTF,TGDN(21),SCACTE
     2/HAPPY2/AVSTS(21),ATEMP(21),BNU(21),SURT,CNAVST,SGB(21)
     3/HAPPY3/THSWST(21),GATMN(21),BATMN(21),THSTN(21),NSTNT,NINT(3),
```

```
     4SGG(21),SGGM(21),VNDWC,SWSLD(21),DB(21)/HAPPY4/BOLZ
      FPRESA(AT,STNT1,RR2,FSNRT3,TIME,GATMNM,RRV)=(CPR*AT/(RMT+ABST)/((
     11.+STNT1)**2)+(RR2**2*FSNRT3*TIME*CNT10*PI+GATMNM)/((PI*RRV*(1.+
     2STNT1))**2)*BOLZ*AT)/(6.91E+07)
      PRESG(AT,STNC,STNF)=CPR*(RRIN**2-RRS**2)/(RMT+ABST)*AT/((RRIN*(1.+
     1STNC))**2-(RRS*(1.+STNF))**2)/(6.91E+07)
      FK(TEM,DENF)=CNT2+1./(TEM*(CNT3-CNT4*DENF))
      READ (1,1011) EQDIA,AVCV,CDEN,CSPH,CTHK,TFLU,RROU,RRIN,
     1CLDK,CPSNRT,PRESF,CNTC1,CNTC3,CNTC5,CNER,NINTC,
     2CEXCL,CELSMD,CNTC2,CNTC4
      READ (1,1012) STBO,CNTG1,CNTG2,CNTG3,CNTG4,CNTG5,CNTG6
      READ (1,1001)  RMT,DENFR(1),DENFR(2),DENFR(3),RRS,CNT2,CNT3,
     1CNT4,CNT5,ACTEGD,ABST,PWRL,TCLMAX,
     2CNT1,UNIVGC,DGG2,DGGI,MMAX , NINTT,MNITR
      READ (1,1002) SPR,AMIG,HTVP,AVGDN,CPR,CSRC
      READ (1,1003) BOLZ,WTML1,WTML2
      READ (1,1004) CNT7,CNT6,CNT8,CNT9,CNT10,CNT11,CNT12
      READ (1,1005) CNT13,CNT14,CNT15,CNT16,CNT17,CNT18,CNT19
      READ (1,1006) CNT20,CNT21,CNT22
      READ (1,1008) SURT,VNDWC,SRDFCO,DFMLN,SCACTE,DSLF,
     1SACTE,GBTF,PSNRT, CNAVST
1011 FORMAT (8F10.4/7F10.5,I5/4E12.5)
1012 FORMAT (E12.5,F10.4,E12.5,F10.4,2E12.5,F10.4)
1001 FORMAT (7F10.5/2F10.5,4F10.2/4E12.5,3I5)
1002 FORMAT (6E12.4)
1003 FORMAT (E12.4,2F10.3)
1004 FORMAT (E12.5,E10.3,2E12.5,F10.4,E12.4,E12.4)
1005 FORMAT (5F10.4,E12.4,F10.4)
1006 FORMAT (E12.4,2F10.4)
1008 FORMAT (6E12.5/E12.5,3F10.4)
      PI=3.14159
      CNTCA=PWRL/(2.*PI*CLDK)
      CNTCB=(1.-2.*CPSNRT)/3./(1.-CPSNRT)
      CNTCC=-2.*(1.+CPSNRT)/3./(1.-CPSNRT)
      CNTCE=CELSMD/(1.-2.*CPSNRT)
      CNTCH=CELSMD/2./(1.+CPSNRT)
      CNTC=1./2.*9.*SPR*AMIG*HTVP*SQRT(AVGDN*(WTML1+WTML2))/(16.*CPR*
```

```
     1CSRC**2*SQRT(2.*PI*BOLZ*WTML1*WTML2))
C
C         CALCULATION OF VOLUMETRIC HEAT SOURCE
C
      PWRV(3)=PWRL/PI/RRS**2
      PWRV(2)=PWRV(3)*DENFR(2)/DENFR(3)
      PWRV(1)=PWRV(3)*DENFR(1)/DENFR(3)
C
C         CALCULATION OF FISSION RATE AND POROSITY
C
      DO 2 J=1,3
      PORST(J)=1.-DENFR(J)
    2 FSNRT(J)=PWRV(J)/CNT1
C
C         CALCULATION OF HEAT TRANSFER COEFFICIENT
C
      PECLET=EQDIA*AVCV*CDEN*CSPH/CTHK
      HCOEF=CTHK/EQDIA*(7.+0.025*PECLET**0.8)
      TOU=TFLU+PWRL/(2.*PI*RROU*HCOEF)
      TIN=TOU+ALOG(RROU/RRIN)/CLDK*PWRL/(2.*PI)
C
C         SET TIME
C
      M=2
    1 TIME=3600.*FLOAT(M)**3
      MT=M**3
C
C         INITIALIZE NUMBER OF ITERATION  OF FUEL SURFACE TEMPERATURE
C
      NITR1=0
C
C         CALCULATION OF TEMPERATURE DISTRIBUTION IN CLAD
C         CALCULATION OF THERMAL STRAINS IN CLAD
C
      NSTNC=NINTC+1
      RDC=(RROU-RRIN)/FLOAT(NINTC)
      RC(1)=RRIN
```

```
      DO 10 I=2,NSTNC
      RC(I)=RC(I-1)+RDC
   10 CONTINUE
      TC(NSTNC)=TOU
      TC(1)=TIN
      DO 15 I=1,NSTNC
      TC(I)=TOU+ALOG(RROU/RC(I))*CNTCA
      CTHSTN(I)=CEXCL*(TC(I)-RMT)
   15 CONTINUE
C
C        MECHANICAL ANALYSIS FOR CLAD
C
      CSTNT(1)=0.
      NSTNT=NINTT+1
      STNT(1)=0.
      STNT(NSTNT)=0.
      ATGAP=(TIN+700.)/2.+ABST
      PRESGP=PRESG(ATGAP,CSTNT(1),STNT(NSTNT))
C
C        INITIALIZE NUMBER OF ITERATION FOR CLAD STRESS AND STRAINS
C
   21 NITR3=0
      DO 20 J=1,NSTNC
      CPLSTR(J)=0.
      CPLSTT(J)=0.
      CPLSTA(J)=0.
      CEPLS1(J)=0.
      CESTS1(J)=0.
   20 CONTINUE
   22 DO 30 I=1,NSTNC
      FCTC1(I)=(CPLSTR(I)-CPLSTT(I))/RC(I)
      FCTC2(I)=RC(I)*CTHSTN(I)
      FCTC3(I)=RC(I)*(CPLSTR(I)+CPLSTT(I))
      CALL QTFE (RDC,FCTC1,ZINVL1,I)
      CALL QTFE (RDC,FCTC2,ZINVL2,I)
      CALL QTFE (RDC,FCTC3,ZINVL3,I)
   30 CONTINUE
```

```
C
C          CALCULATION OF INTEGRATION CONSTANTS
C
      BNCG=CELSMD/(1.-CPSNRT)*(ZINVL1(NSTNC)/2./(1.+CPSNRT)-
     1ZINVL2(NSTNC)/RC(NSTNC)**2-(1.-2.*CPSNRT)*ZINVL3(NSTNC)/(2.*(1.+
     2CPSNRT)*RC(NSTNC)**2))
      BNCC1=2.*(1.+CPSNRT)*(1.-2.*CPSNRT)/(3.*CELSMD*(RC(NSTNC)**2-RC(1)
     1**2))*(RC(1)**2*PRESGP-RC(NSTNC)**2*(PRESF+BNCG))
      BNCC2=2.*RC(1)**2*RC(NSTNC)**2*(1.+CPSNRT)/(3.*CELSMD*(RC(NSTNC)**
     12-RC(1)**2))*(-PRESGP+PRESF+ BNCG)
      CER=0.
      DO 40 I=1,NSTNC
      SEC(I)=CNTCB*(CPLSTR(I)-2.*CTHSTN(I)+ZINVL1(I))+BNCC1
      SGC(I)=CNTCC*ZINVL2(I)/RC(I)**2+CNTCB*(CPLSTR(I)-2.*CTHSTN(I)-
     1ZINVL3(I)/RC(I)**2)+BNCC2/RC(I)**2
C
C          CALCULATION OF MODIFIED EQUIVALENT TOTAL STRAIN
C
      CTTNDR(I)=1./2.*(SEC(I)+3.*SGC(I)+4.*CTHSTN(I))
      CTTNDT(I)=1./2.*(SEC(I)-3.*SGC(I)-2.*CTHSTN(I))
      CTTNDA(I)=           -SEC(I)-CTHSTN(I)
      CETSTN(I)=SQRT(2./3.*(CTTNDR(I)**2+CTTNDT(I)**2+CTTNDA(I)**2))
      CAVSTS(I)=CNTCE*SEC(I)
      CEXPN=CNTC1+CNTC2*TC(I)**CNTC3
      CCOEFK=3./7.*(CELSMD/(CNTC4-CNTC5*TC(I)))**(CEXPN-1.)
       ALSE=CETSTN(I)
C
C          CALCULATION OF EQUIVALENT STRESS AND STRAIN
C
      CALL RTMI(CESTS,FCTC4V,FCTC4,0.,100.    ,1.E-07 , 50,    IERC4)
      CESTS2(I)=CESTS
      CEPLS2(I)=CETSTN(I)-2.*(1.+CPSNRT)*CESTS2(I)/3./CELSMD
C
C          CALCULATION OF RATIOS AND ERRORS FOR CONVERGENCE
C
      CRAT1(I)=CESTS1(I)/CESTS2(I)
      CERR1(I)=ABS(CRAT1(I)-1.)
```

```
      CER=AMAX1(CER,CERR1(I))
      IF (CEPLS2(I).LT.0.002) GO TO 35
      CRAT2(I)=CEPLS1(I)/CEPLS2(I)
      CERR2(I)=ABS(CRAT2(I)-1.)
      CER=AMAX1(CER,CERR2(I))
   35 CESTS1(I)=CESTS2(I)
      CEPLS1(I)=CEPLS2(I)
   40 CONTINUE
      NITR3=NITR3+1
      IF (NITR3.EQ.MNITR) GO TO 1000
      IF(CER.LT.CNER) GO TO  60
C
C        CALCULATION OF PLASTIC STRAINS
C
      DO 50 J=1,NSTNC
      CPLSTR(J)=       CEPLS2(J)/CETSTN(J)*CTTNDR(J)
      CPLSTT(J)=       CEPLS2(J)/CETSTN(J)*CTTNDT(J)
      CPLSTA(J)=-CPLSTR(J)-CPLSTT(J)
   50 CONTINUE
      GO TO 22
C
C        CALCULATION OF FUEL SURFACE TEMPERATURE
C
   60 R(NSTNT)=RRS
      IF (NITR1.GT.0) GO TO 61
      TEMPS=700.
      GO TO 199
   61 CALL RTMI(TEMPS,FCTG1V,FCTG1,TIN,2600.,0.0001,MNITR,IERG1)
C
C        TEST CONVERGENCE OF FUEL SURFACE TEMPERATURE
C
      GRATIO=TEMPS1/TEMPS
      GER=ABS(GRATIO-1.)
      IF (GER.LE.0.01) GO TO 990
      TEMPS=(TEMPS1+TEMPS)/2.
  199 TEMPS1=TEMPS
C
```

```
C         CALCULATION OF GAP THICKNESS
C
      GAP=          RC(1)*(1.+CSTNT(1))-R(NSTNT) *(1.+STNT(NSTNT))
      ATGAP= (TIN+TEMPS)/2+ABST
      NITR1=NITR1+1
      WRITE (3,1073) TEMPS,ATGAP,GAP,NITR1,NITR3
 1073 FORMAT (//'1TEMPS=',F8.3,5X,'ATGAP=',F8.3,5X,'GAP=',F9.6,5X,'NITR1
     1=',I2,5X,'NITR3=',I2)
      IF (GAP.LE.0.) GO TO 1000
      IF (NITR1.EQ.10   ) GO TO  1000
C
C         CALCULATION OF T2, T1, R1, R2, RV, AND TV
C
      I=1
      R(I)=0.
      CALL RTMI(TEMPC,FCT3V,FCT3,TEMPS,5000.,0.0001,MNITR,IERC)
      WRITE (3,1050) TEMPC,IERC
 1050 FORMAT (///' ',3X,'TEMPC=',F8.2,3X,'IERC=',I2)
      IF (TEMPC.GT.TCLMAX) GO TO 1000
            IF (IERC-1) 200,1000,1000
  200 TEMP2=ACTEGD/UNIVGC/ALOG(CNT5*TIME/(DGG2**3-DGGI**3))-ABST
      RR2=RRS*SQRT(1.-4./(PWRV(3)*RRS**2)*(CNT2*(TEMP2-TEMPS)+ALOG(TEMP2
     1/TEMPS)/(CNT3-CNT4*DENFR(3))))
      KO=1
      CALL RTMI(TEMP1,FCT6V,FCT6,TEMP2,TEMPC,0.0001,MNITR,IER6)
      RRX=RR2*SQRT(1.-PWRV(3)/PWRV(2))
      CALL RTMI(RR1,FCT7V,FCT7,RRX,    RR2,0.0001,MNITR,IER7 )
      IF((IER7.EQ.2).AND.(TEMP2.GE.TEMPC)) GO TO 208
      IF (IER7.EQ.2)GO TO 207
      IF (TEMP2.GE.TEMPC) GO TO 205
  206 RRV=SQRT(RR2**2*(PWRV(2)-PWRV(3))/PWRV(1)+RR1**2*(PWRV(1)-PWRV(2))
     1/PWRV(1))
      CALL RTMI(TEMPV,FCT5V,FCT5,TEMP1,2600.,0.0001,MNITR,IER5)
      WRITE (3,1051) TEMPV,TEMP1,TEMP2,RRV,RR1,RR2,IER5,IER6,IER7
 1051 FORMAT ('0THREE REGIONS',3X,'TEMPV=',F8.2,3X,'TEMP1=',F8.2,3X,
     1'TEMP2=',F8.2/' ',16X,'RRV=',F8.6,3X,'RR1=',F8.6,3X,'RR2=',F8.6/
     2' ',16X,'IER5 (FOR TEMPV)=',I1,3X,'IER6(FOR TEMP1) =',I1,3X,
```

```
     3 'IER7(FOR RR1)=',I1)
       IF (IER5-1) 210,100C,1000
C          CONSIDERATION OF TWO REGIONS
  205 RR2=RR1
      TEMP2=TEMP1
      DENFR(2)=DENFR(1)
      PWRV(2)=PWRV(1)
      FSNRT(2)=FSNRT(1)
      PORST(2)=PORST(1)
  207 KO=2
      RRV=SQRT(RR2**2*(PWRV(2)-PWRV(3))/PWRV(2))
      I=1
      R(I)=RRV
      CALL RTMI(TEMPV,FCT2V,FCT2,TEMP2,TEMPC,0.0001,MNITR, IER2)
      RR1=RRV
      TEMP1=TEMPV
      WRITE (3,1052) TEMPV,TEMP2,RRV,RR2,IER7
 1052 FORMAT ('OFOR TWO REGIONS',4X,'TEMPV=',F8.2,3X,'TEMP2=',F8.2,3X,
     1'RRV=',F8.6,3X,'RR2=',F8.6/' ',15X,'IER7=',I1,3X,'IF IER7=2, NO CO
     2LUMNAR GRAIN ZONE')
       GO TO 210
  208 KO=3
      RRV=0.
      RR1=0.000001
      RR2=0.000001
      TEMPV=TEMPC
      TEMP1=TEMPC
      TEMP2=TEMPC
  210 RD=(RRS-RRV)/FLOAT(NINTT)
      NINT(1)=IFIX((RR1-RRV)/RD)+1
      NINT(2)=IFIX((RR2-RR1)/RD)
      RDR(1)=(RR1-RRV)/FLOAT(NINT(1))
      RDR(2)=(RR2-RR1)/FLOAT(NINT(2))
  220 IF (KO.NE.2) GO TO 225
C      IN CASE OF TWO REGION, NINT(1)=0.
      NINT(1)=0
      GO TO 230
```

```
  225 IF(KO.NE.3) GO TO  230
      NINT(1)=0
      NINT(2)=0
  230 NINT(3)=NINTT-NINT(1)-NINT(2)
      RDR(3)=(RRS-RR2)/FLOAT(NINT(3))
      NSTN1=NINT(1)+1
      NSTN2=NSTN1+NINT(2)
      NSTNT=NSTN2+NINT(3)
      WRITE (3,1053) (NINT(I),I=1,3),NSTN1,NSTN2,NSTNT,(RDR(I),I=1,3)
 1053 FORMAT ('ONUMBER OF INTERVALS IN REGION 1 IS ',I2,3X,'IN REGION2 I
     1S ',I2,3X,'IN REGION 3 IS ',I2/' ','STATION NUMBER AT R1 IS ',
     2      I2,3X,'AT R2 IS ',    I2,3X,'AT RS IS ',      I2,3X/' RADIAL
     3 DIFFERENCE IN THE THREE REGIONS ARE (1) ',F8.6,2X'(2) ',F8.6,2X,
     4'(3) 'F8.6)
C
C         CALCULATION OF TEMPERATURE DISTRIBUTION IN FUEL
C
      NSTNA=2
      NSTNB=1
      R(1)=RRV
      T(1)=TEMPV
      RO1=R(1)
      IF (R(1).GT.0.) GO TO 300
      R(1)=0.000001
      RRV=0.000001
  300 DO 390 NR=1,3
      NSTNB=NSTNB+NINT(NR)
      DO 340 I=NSTNA,NSTNB
      R(I)=R(I-1)+RDR(NR)
      GO TO (310,320,330),NR
  310 CALL RTMI(T(I),FCT1V,FCT1,TEMP1,2600.,0.0001,MNITR,IER1)
      GO TO 340
  320 CALL RTMI(T(I),FCT2V,FCT2,TEMP2,TEMP1,0.0001,MNITR,IER2)
      GO TO 340
  330 CALL RTMI(T(I),FCT3V,FCT3,TEMPS,TEMP2,0.0001,MNITR,IER3)
  340 CONTINUE
      NSTNA=NSTNB+1
```

```
  390 CONTINUE
C
C         TEMPERATURE GRADIENTS AND FUNCTIONS OF TEMPERATURE
C
      GATMNM=0.
      NSTNA=1
      NSTNB=1
  400 DO 490 NR=1,3
      NSTNB=NSTNB+NINT(NR)
      DO 480 I=NSTNA,NSTNB
      SGB(I)=0.
      SGGM(I)=0.
      GATMN(I)=CNT10*FSNRT(NR)*TIME
      GO TO (410,420,430),NR
  410 TGDN(I)=PWRV(1)*(R(I)**2-RRV**2)/(2.*FK(T(I),DENFR(1))*R(I))
      BNU(I)=0.
      SGG(I)=0.
      GO TO 440
  420 TGDN(I)=((PWRV(3)-PWRV(2))*RR2**2+PWRV(2)*R(I)**2)/(2.*R(I)*
     1FK(T(I),DENFR(2)))
      SGG(I)=0.
      BNU(I)=0.
      GO TO 440
  430 TGDN(I)=PWRV(3)*R(I)/2./FK(T(I),DENFR(3))
      GASNM(I)=0.
  440 ATEMP(I)=T(I)+ABST
      BNU(I)=CNT11-CNT12*T(I)
      DTEMP(I)=T(I)-RMT
      SWSLD(I)=CNT6*FSNRT(NR)*TIME
      THSTN(I)=(CNT7+CNT8*T(I)+CNT9*T(I)**2)*T(I)
      DG(I)=(DGGI**3+CNT5*TIME*EXP(-ACTEGD/(UNIVGC*ATEMP(I))))**(1./3.)
      ELSMD(I)=(CNT14-CNT15*T(I))*(1.-CNT16*PORST(NR)-CNT17*PORST(NR)**2
     1)*1.0E+03
      PPTLMT(I)=CNT18/(T(I)-CNT19)
      FEXPN(I)=CNT20*(T(I)-CNT21)**2+CNT22
      FCOEFK(I)=PPTLMT(I)/ELSMD(I)
  480 CONTINUE
```

```
      NSTNA=NSTNB+1
  490 CONTINUE
C
C         MECHANICAL ANALYSIS IN FUEL
C
      DO 500 J=1,NSTNT
      PLSTR(J)=0.
      PLSTT(J)=0.
      PLSTA(J)=0.
      EQSTS3(J)=0.
      AVSTS(J)=0.
  500 CONTINUE
  501 NITR2=0
      MEMO=0
C
C         CALCULATION OF PRESSURES IN GAP AND IN CENTRAL VOID
C
      PRESA=FPRESA(ATEMP(1),STNT(1),RR2,FSNRT(3),TIME,GATMNM,RRV)
      PRESGP=PRESG(ATGAP,CSTNT(1),STNT(NSTNT))
  505 CALL THSW
  510 NSTNA=2
      NSTNB=1
      SC1=3./2.*ELSMD(1)/(1.+PSNRT)
      SF1=2.*SC1*(2.*THSWST(1)-PLSTR(1))
      SH1=SC1*(-PLSTR(1)+PLSTT(1)+3.*THSWST(1))
      CD1=SC1/(1.-2.*PSNRT)
      SC11=SC1
      SF11=SF1
      SH11=SH1
      CD11=CD1
      DO 590 NR=1,3
      NSTNB=NSTNB+NINT(NR)
      DO 580 I=NSTNA,NSTNB
      SA=RDR(NR)/R(I)
      SB=RDR(NR)/R(I-1)
      SC2=3.*ELSMD(I)/(2.*(1.+PSNRT))
      SF2=2.*SC2*(2.*THSWST(I)-PLSTR(I))
```

```
      SH2=SC2*(-PLSTR(I)+PLSTT(I)+3.*THSWST(I))
      CA=1.+SA
      CB=1.-SB
      CC=SA*THSWST(I)+SB*THSWST(I-1)
      CD2=SC2/(1.-2.*PSNRT)
      CF=SC2*CA
      CU=CD1
      CV=SC1*CB
      CW=1./3.*(SF2-SF1+SA*SH2+SB*SH1)
      DENOM=CF+CA*CD2
      CK=(CF+CA*CU)/DENOM
      CL=(CA*CV-CF*CB)/DENOM
      CM=(CF*CC-CA*CW)/DENOM
      CKP=(CU-CD2)/DENOM
      CLP=(CV+CD2*CB)/DENOM
      CMP=(-CW-CC*CD2)/DENOM
      IF (I.GT.2) GO TO 560
      ALPH(I)=CK
      BETA(I)=CL
      GAMA(I)=CM
      ALPHP(I)=CKP
      BETAP(I)=CLP
      GAMAP(I)=CMP
      GO TO 570
  560 ALPH(I)=CK*ALPH(I-1)+CL*ALPHP(I-1)
      BETA(I)=CK*BETA(I-1)+CL*BETAP(I-1)
      GAMA(I)=CK*GAMA(I-1)+CL*GAMAP(I-1)+CM
      ALPHP(I)=CKP*ALPH(I-1)+CLP*ALPHP(I-1)
      BETAP(I)=CKP*BETA(I-1)+CLP*BETAP(I-1)
      GAMAP(I)=CKP*GAMA(I-1)+CLP*GAMAP(I-1)+CMP
  570 SC1=SC2
      SF1=SF2
      SH1=SH2
      CD1=CD2
  580 CONTINUE
      NSTNA=NSTNB+1
  590 CONTINUE
```

```
      QNPL1=(-PRESGP-CD2*GAMA(NSTNT)-SC2*GAMAP(NSTNT)-1./3.*SF2)/(CD2*
     1ALPH(NSTNT)+SC2*ALPHP(NSTNT))
      PNPL1=-(CD2*BETA(NSTNT)+SC2*BETAP(NSTNT))/(CD2*ALPH(NSTNT)+SC2*
     1ALPHP(NSTNT))
      IF ( RO1.GT.0.) GO TO 650
      SG(1)=1./3.*(PLSTR(1)-PLSTT(1)-3.*THSWST(1))
      GO TO 660
  650 SG(1)=(-PRESA-CD11*QNPL1-1./3.*SF11)/(SC11+CD11*PNPL1)
  660 SE(1)=PNPL1*SG(1)+QNPL1
      DO 670 I=2,NSTNT
      SE(I)=ALPH(I)*SE(1)+BETA(I)*SG(1)+GAMA(I)
      SG(I)=ALPHP(I)*SE(1)+BETAP(I)*SG(1)+GAMAP(I)
  670 CONTINUE
      ER=0.
      DO 680 J=1,NSTNT
      AVSTS(J)=ELSMD(J)/(1.-2.*PSNRT)*SE(J)*(6.91E+07)
      STSDVR(J)=ELSMD(J)/(2.*(1.+PSNRT))*(SE(J)+3.*SG(J)+4.*THSWST(J)-2.
     1*PLSTR(J))
      STSDVT(J)=ELSMD(J)/(2.*(1.+PSNRT))*(SE(J)-3.*SG(J)-2.*THSWST(J)-2.
     1*PLSTT(J))
      STSDVA(J)=ELSMD(J)/(1.+PSNRT)*(-SE(J)-THSWST(J)+PLSTR(J)+PLSTT(J))
      EQSTS1(J)=SQRT(1.5*(STSDVR(J)**2+STSDVT(J)**2+STSDVA(J)**2))
      IF (EQSTS1(J).LT.PPTLMT(J)) GO TO 680
C
C        CALCULATION OF MODIFIED EQUIVALENT TOTAL STRAIN
C
      TSTNDR(J)=1./2.*(SE(J)+3.*SG(J)+4.*THSWST(J))
      TSTNDT(J)=1./2.*(SE(J)-3.*SG(J)-2.*THSWST(J))
      TSTNDA(J)=-SE(J)-THSWST(J)
      EQTSTN(J)=SQRT(2./3.*(TSTNDR(J)**2+TSTNDT(J)**2+TSTNDA(J)**2))
C
C        CALCULATION OF EQUIVALENT STRESS AND STRAIN
C
  676 PLT1=PPTLMT(J)/1.5
      PLT2=PPTLMT(J)*8.
      CALL RTMI(SIG,FCT4V,FCT4,PLT1,PLT2,1.E-07,MNITR,IER4)
      EQSTS2(J)=SIG
```

```
      EQPLS2(J)= EQTSTN(J)-2./3.*(1.+PSNRT)*EQSTS2(J)/ELSMD(J)
C
C        TEST CONVERGENCE
C
      RATIO2(J)=EQSTS3(J)/EQSTS2(J)
  678 ERR2(J)=ABS(RATIO2(J)-1.)
      ER=AMAX1(ER,ERR2(J))
      EQSTS3(J)=EQSTS2(J)
  680 CONTINUE
      NITR2=NITR2+1
      IF (ER.LT.CNER) GO TO 695
      IF (NITR2.EQ.20   ) GO TO 1000
C
C        CALCULATION OF PLASTIC STRAINS
C
      DO 690 J=1,NSTNT
      PLSTR(J)=EQPLS2(J)/EQTSTN(J)*TSTNDR(J)
      PLSTT(J)=EQPLS2(J)/EQTSTN(J)*TSTNDT(J)
      PLSTA(J)=-PLSTR(J)-PLSTT(J)
  690 CONTINUE
      GO TO 505
  695 IF (MEMO.EQ.13) GO TO 796
C
C        DETERMINE WHETHER BUBBLES ARE IN MOTION
C
  800 NSTNA=NINT(1)+NINT(2)+1
      NSTNB=NSTNT
      N=NSTNA-1
      CNTD=(6.*AMIG*DSLF/(PI*SACTE))**(1./3.)
      CNTE=6.*SRDFCO*DFMLN*AMIG*SACTE/BOLZ
      CNTF=SQRT(3.*AMIG*GBTF/SACTE)
      DO 890 I=NSTNA,NSTNB
      DBCG(I)=CNTD*(ATEMP(I)/TGDN(I))**(1./3.)
      IF (DBCG(I).GT.DB(I)) GO TO  880
      VELG(I)=CNTE*TGDN(I)/(ATEMP(I)**2*DBCG(I))*EXP(-SCACTE/(BOLZ*
     1ATEMP(I)))
      TIMECG(I)=PI*BNU(I)*(4.*SURT/DBCG(I)-AVSTS(I))*DBCG(I)**3/(6.
```

```
     1*CNT10*FSNRT(3)*BOLZ*ATEMP(I))
      VELCG(I)=DG(I)/100./(TIME-TIMECG(I))
      IF (VELCG(I).GT.VELG(I)) GO TO 880
      DTIME(I)=1./(VELG(I)*BNU(I)**(1./3.))
      TIMEG(I)=PI*DG(I)/(4.*VELG(I))
      IF (TIME-TIMECG(I)-TIMEG(I)) 820,830,830
  820 NUTIME=(TIME-TIMECG(I))/DTIME(I)
      SGGM(I)=(TIME-TIMECG(I))/TIMEG(I)*PI/6.*DBCG(I)**3*BNU(I)
      GO TO 840
  830 NUTIME=(TIMEG(I)            )/DTIME(I)
      SGGM(I)=0.
  840 NUT=NUTIME+2
      WRITE (3,1058)I,DBCG(I),VELG(I),TIMECG(I),VELCG(I),NUTIME
 1058 FORMAT (///' STATION',5X,'DBCG',12X,'VELG',10X,'TIMECG',10X,
     1'VELCG',10X, 'NUTIME'//' ',3X,I2,2X,4E15.5, I10)
      CALL SGASB(DBGB,NUT,SGBC,SGBN,I,TIME)
      GATMNM=GATMNM+GASNM(I)*4./PI/DG(I)*(PI*(R(I)**2-R(I-1)**2))
      GATMN(I)=GATMN(I)*(TIME-TIMECG(I))/TIME
  880 N=N+1
  890 CONTINUE
      IF (N.EQ.NSTNB) GO TO 795
      MEMO=13
      GO TO 505
  795 WRITE (3,1059) MT
 1059 FORMAT (///' TILL THE TIME,',I6 ,     '  HOURS, THERE IS NO MOTION
     1 OF BUBBLES')
  796 WRITE (3,1060)  MEMO
 1060 FORMAT (' MEMO=',I2)
      CSTNT(1)=3./2.*(SEC(1)-SGC(1))
       STNT(1)=3./2.*(SE(1)-SG(1))
       STNT(NSTNT)=3./2.*(SE(NSTNT)-SG(NSTNT))
      RRRV=RRV*(1.+STNT(1))
      WRITE (3,1056) NITR2,PRESA,PRESGP,RRRV
 1056 FORMAT (///' NITR2=',I2,5X,'PRESSURE IN THE VOID=',F10.5,5X,'PRESS
     1URE IN THE GAP =',F10.5,5X,'RADIUS OF  VOID=',F10.6)
      IF (NITR1.EQ.1) GO TO  61
      GO TO 21
```

```
 990 FFSNTT=FSNRT(3)*TIME/(1.E+20)
     BURNUP=PWRV(3)*TIME/(8.64E+05)
     WRITE (3,993) FFSNTT,BURNUP,TIME
 993 FORMAT (//'  TOTAL FISSIONS = ',E12.5,2X,'FISSIONS/CM**3/10**20'//
    1' BURNUP = ',E12.5,2X,'MW-DAY/TONNE',5X,'TIME=',E12.2,' SECONDS')
     DO 2000 I=1,NSTNT
2000 SWESTN(I)=1./3.*(SWSLD(I)+SGG(I)+SGB(I)+SGGM(I))
     WRITE (3,1072) (I,RC(I),TC(I),CTHSTN(I),CPLSTR(I),CPLSTT(I),
    1CPLSTA(I),I=1,NSTNC)
1072 FORMAT ('1'//////' ',54X,'TABLE'//' ',
    1                      23X,'    TEMPERATURE DISTRIBUTION, THERMAL
    1STRAIN AND PLASTIC STRAINS IN CLADDING'///' ',23X,'STATION
    2RADIUS  TEMPERATURE   THERMAL     RADIAL    TANGENTIAL    AXIAL',
    3/' ',72X,'PLASTIC     PLASTIC     PLASTIC'/' ',39X,'(CM)', 7X,
    4'(C)',8X,'STRAIN     STRAIN      STRAIN      STRAIN'//(' ',23X,I6,
    54X,F12.5,F10.2,F12.5,F13.6,F11.6,F13.6/))
     WRITE (3,1054) (I,R(I),T(I),TGDN(I),THSTN(I),I=1,NSTNT)
1054 FORMAT ('1'//////' ',48X,'TABLE'//
    1                  ' ',23X,'    TEMPERATURE DISTRIBUTION, TEMPERAT
    1URE GRADIENTS'/' ',36X,'AND THERMAL STRAINS IN FUEL'///' ',23X,
    2'STATION    RADIUS     TEMPERATURE  TEMPERATURE   THERMAL'/' ',
    358X,'GRADIENT      STRAIN'/' ',35X,'(CM)',10X,'(C)',9X,'(C/CM)'//
    4(' ',23X,I4,3X,F12.6,2F12.2,F14.7 /))
     WRITE (3,1103) (I,SWESTN(I),PLSTR(I),PLSTT(I),PLSTA(I),I=1,NSTNT)
1103 FORMAT ('1'//////' ',48X,'TABLE'//
    1                  ' ',30X,'SWELLING STRAIN AND PLASTIC STRAINS IN
    1 FUEL '///' ',23X,'STATION   SWELLING      RADIAL   TANGENTIAL
    2AXIAL '/' ',33X,'STRAIN        PLASTIC   PLASTIC      PLASTIC'/' '
    3, 47X,'STRAIN    STRAIN       STRAIN'//(' ',23X,I4,3X,4F12.7/ ))
     J=NSTNT
     STSR(J)=ELSMD(J)/2./(1.+PSNRT)*(SE(J)+3.*SG(J)+4.*THSWST(J)-2.*
    1PLSTR(J))+AVSTS(J)/(6.91E+07)
     STNR(J)=1.5*(SE(J)+SG(J)+2.*THSWST(J))
     STNT(J)=1.5*(SE(J)-SG(J))
     ERF=STNR(J)
     ETF=STNT(J)
     SRF=STSR(J)
```

```
      CSTSR(1)=    (SEC(1)+3.*SGC(1)+4.*CTHSTN(1)-2.*CPLSTR(1))*CNTCH+
     1CAVSTS(1)
      SRO=CSTSR(1)
      I=NSTNC
      CSTNR(I)=1.5*(SEC(I)+SGC(I)+2*CTHSTN(I))
      CSTNT(I)=1.5*(SEC(I)-SGC(I))
      ETO=CSTNT(I)
      ERO=CSTNR(I)
      WRITE (3,995)
  995 FORMAT (     '1',30X,'STRAINS AND STRESSES IN CLADDING MATERIAL'
     1          ///' ',15X,'STATION' ,6X,'RC',11X,'CSTNR',10X,'CSTNT',
     210X,'CSTSR',10X,'CSTST',10X,'CSTSA'//)
      DO 991 I=1,NSTNC
      CSTNR(I)=1.5*(SEC(I)+SGC(I)+2*CTHSTN(I))
      CSTNT(I)=1.5*(SEC(I)-SGC(I))
      CSTSR(I)=    (SEC(I)+3.*SGC(I)+4.*CTHSTN(I)-2.*CPLSTR(I))*CNTCH+
     1CAVSTS(I)
      CSTST(I)=    (SEC(I)-3.*SGC(I)-2.*CTHSTN(I)-2.*CPLSTT(I))*CNTCH+
     1CAVSTS(I)
      CSTSA(I)=2.*CNTCH*(-SEC(I)-CTHSTN(I)-CPLSTA(I))+CAVSTS(I)
      WRITE (3,996) I,RC(I),CSTNR(I),CSTNT(I),CSTSR(I),CSTST(I),CSTSA(I)
  996 FORMAT (' ',15X,I4, 4X,6E15.5)
      RC(I)=RC(I)/ RRS
      CSTST(I)=CSTST(I)/(ABS(SRO))
      CSTSA(I)=CSTSA(I)/(ABS(SRO))
      CSTSR(I)=CSTSR(I)/(ABS(SRO))
      CSTNR(I)=CSTNR(I)/CSTNR(NSTNC)
      CSTNT(I)=CSTNT(I)/CSTNT(NSTNC)
  991 CONTINUE
      WRITE (3,994)
  994 FORMAT (///' ',30X,'STRAINS AND STRESSES IN FUEL MATERIAL'///' ',
     115X,'STATION',7X,'R',11X,'STNR',11X,'STNT',11X,'STSR',11X,'STST',
     211X,'STSA'//)
      DO 992 J=1,NSTNT
      STNR(J)=1.5*(SE(J)+SG(J)+2.*THSWST(J))
      STNT(J)=1.5*(SE(J)-SG(J))
      STSR(J)=ELSMD(J)/2./(1.+PSNRT)*(SE(J)+3.*SG(J)+4.*THSWST(J)-2.*
```

```
     1PLSTR(J))+AVSTS(J)/(6.91E+07)
      STST(J)=ELSMD(J)/2./(1.+PSNRT)*(SE(J)-3.*SG(J)-2.*THSWST(J)-2.*
     1PLSTT(J))+AVSTS(J)/(6.91E+07)
      STSA(J)=ELSMD(J)/(1.+PSNRT)*(-SE(J)-THSWST(J)-PLSTA(J))+AVSTS(J)/
     1(6.91E+07)
      WRITE (3,998) J,R(J),STNR(J),STNT(J),STSR(J),STST(J),STSA(J)
  998 FORMAT (' ',15X,I4,6E15.5)
      R(J)=R(J)/RRS
      STST(J)=STST(J)/(ABS(STSR(NSTNT)))
      STSA(J)=STSA(J)/(ABS(STSR(NSTNT)))
      STSR(J)=STSR(J)/(ABS(STSR(NSTNT)))
      STNR(J)=STNR(J)/STNR(NSTNT)
      STNT(J)=STNT(J)/STNT(NSTNT)
  992 CONTINUE
      WRITE (3,997)  (I,RC(I),CSTNR(I),CSTNT(I),CSTSR(I),CSTST(I),
     1CSTSA(I),I=1,NSTNC)
  997 FORMAT ('1'//////' ',54X,'TABLE'// ' ',
     1                        40X,'DIMENTIONLESS STRAINS AND STRESSES IN
     1CLADDING'///' ',24X,'STATION',3X,'       R/RO       ER/ERO      ET
     2/ETO     SR/|SRO|     ST/|SRO|     SA/|SRO|    '//(' ',24X,I4,6X,
     34F12.4,2F12.3))
      WRITE (3,2001) RRS,ERO,ETO,SRO
 2001 FORMAT (//' ',23X,'NOTE:   R=RADIUS' ,15X,'RO=RADIUS AT THE FUEL S
     1URFACE=',F6.4,' CM'//' ',31X,'ER=RADIAL STRAIN       ERO=RADIAL ST
     2RAIN AT CLAD OUTER SURFACE=',F10.7//' ',31X,'ET=TANGENTIAL STRAIN
     3  ETO=TANGENTIAL STRAIN AT CLAD SURFACE=',F10.7//' ',31X,'SR=RADIA
     4L STRESS     ST=TANGENTIAL STRESS     SA=AXIAL STRESS'//' ',31X,'
     5|SRO|=ABSOLUTE VALUE OF RADIAL STRESS AT CLAD INNER SURFACE, SRO='
     6,F8.5,'X1000 PSI')
      WRITE (3,999) (I,R(I),STNR(I),STNT(I),STSR(I),STST(I),STSA(I),I=1,
     1NSTNI)
  999 FORMAT ('1'//////' ',54X,'TABLE'// ' ',
     1                        40X,'DIMENTIONLESS STRAINS AND STRESSES IN
     1FUEL'///' ',24X,'STATION',3X,'       R/RO       ER/ERO      ET/ETO
     2    SR/|SRO|     ST/|SRO|     SA/|SRO|    '//(' ',24X,I4,6X,4F12.4,
     32F12.3))
      WRITE (3,2002) RRS,ERF,ETF,SRF
```

```
 2002 FORMAT
     1(//' ',23X,'NOTE:   R=RADIUS',15X,'RO=RADIUS AT THE FUEL SURFACE='
     2,F6.4,' CM'/' ',31X,'ER=RADIAL STRAIN       ERO=RADIAL STRAIN AT F
     3UEL SURFACE=',F10.7/' ',31X,'ET=TANGENTIAL STRAIN   ETO=TANGENTIAL
     4 STRAIN AT FUEL SURFACE=' ,F10.7/' ',31X,'SR=RADIAL STRESS     ST=
     5TANGENTIAL STRESS     SA=AXIAL STRESS' /' ',31X,                  '
     6|SRO|=ABSOLUTE VALUE OF RADIAL STRESS AT FUEL OUTER SURFACE, SRO='
     7,F8.5,'X1000 PSI')
      IF (M.GE.MMAX) GO TO  1000
      M=M+1
      GO TO 1
 1000 STOP
      END
      FUNCTION FCTG4(ES)
C
C        TO OBTAIN EQUIVALENT STRESS IN CLAD
C
      COMMON /FCTC4X/     CCOEFK,CEXPN,CPSNRT, ALSE,CELSMD
      FCTC4=(ALSE-2.*(1.+CPSNRT)*ES/3./CELSMD-CCOEFK*(ES/CELSMD)**CEXPN)
     1*100.
      RETURN
      END
      FUNCTION FCTG1(TX)
C
C        TO CALCULATE FUEL SURFACE TEMPERATURE
C
      DIMENSION RC(11),TC(11),CSTNT(11),STNT(21)
      COMMON /FCTG1X/RC,TC,CSTNT,STNT,            PWRL,STBO,CNTG1,CNTG2,
     1CNTG3,CNTG4,CNTG5,CNTG6/FCT123/IQ,R(21)/HAPPY3/DUMMY2(84),NSTNT,
     2NINT(3)/FCT6X/DIM(3),ABST
      EMIS1=CNTG1+CNTG2*TX
      EMIS2=CNTG3+CNTG4*TC(1)
      GASK=CNTG5*((TC(1)+TX)/2)**CNTG6
      GAPK=GASK+4.*(RC(1)*(1.+CSTNT(1))-R(NSTNT) *(1.+STNT(NSTNT)))*
     1STBO/(1./EMIS1+1./EMIS2-1.)*((TC(1)+TX+2.*ABST)/2.)**3
      FCTG1=TX-TC(1)-ALOG(RC(1)*(1.+CSTNT(1))/(R(NSTNT)*(1.+STNT(NSTNT))
     1))/GAPK*PWRL/(2.*3.14159)
```

```
      RETURN
      END
      FUNCTION FCT1(X)
C
C        TO CALCULATE FUEL TEMPERATURES IN REGION 1
C
      COMMON CNT2,CNT3,CNT4,DENFR(3), PWRV(3)/FCT123/I,R(21)
     1/FCT15/RRV,RR1,TEMP1
      FIK=CNT2*(X-TEMP1)+ALOG(X/TEMP1)/(CNT3-CNT4*DENFR(1))
      FCT1=FIK-PWRV(1)*RR1**2/4.*(1.-(R(I)/RR1)**2+(RRV/RR1)**2*
     1ALOG((R(I)/RR1)**2))
      RETURN
      END
      FUNCTION FCT2(X)
C
C        TO CALCULATE FUEL TEMPERATURES IN REGION 2
C
      COMMON CNT2,CNT3,CNT4,DENFR(3), PWRV(3)/FCT123/I,R(21)
     1                    /FCT24/TEMP2,RR2
      FIK=CNT2*(X-TEMP2)+ALOG(X/TEMP2)/(CNT3-CNT4*DENFR(2))
      FCT2=FIK-PWRV(2)*RR2**2/4.*(1.-(R(I)/RR2)**2+(1.-PWRV(3)/PWRV(2))*
     1ALOG((R(I)/RR2)**2))
      RETURN
      END
      FUNCTION FCT3(X)
C
C        TO CALCULATE FUEL TEMPERATURES IN REGION 3
C
      COMMON CNT2,CNT3,CNT4,DENFR(3), PWRV(3)/FCT123/I,R(21)
     1     /FCT3X/TEMPS                    /FCT34/RRS
      FIK=CNT2*(X-TEMPS)+ALOG(X/TEMPS)/(CNT3-CNT4*DENFR(3))
      FCT3=FIK-PWRV(3)*RRS**2/4.*(1.-(R(I)/RRS)**2)
      RETURN
      END
      FUNCTION FCT4(SIG)
C
C        TO OBTAIN EQUIVALENT STRESS IN FUEL
```

```
C
      DIMENSION  PPTLMT(21),FEXPN(21),FCOEFK(21),EQTSTN(21),ELSMD(21)
      COMMON /FCT4X/ EQTSTN,PPTLMT,ELSMD,FCOEFK,FEXPN,PSNRT ,J
       GOD=(SIG/PPTLMT(J))**(FEXPN(J))
      FCT4=100.*(EQTSTN(J)-FCOEFK(J)*GOD-(2.*PSNRT-1.)*SIG/3./ELSMD(J))
      RETURN
      END
      FUNCTION FCT5(X)
C
C        FOR CALCULATION OF TEMPERATURE IN CENTRAL VOID
C
      COMMON CNT2,CNT3,CNT4,DENFR(3), PWRV(3)
     1/FCT15/RRV,RR1,TEMP1
      FIK=CNT2*(X-TEMP1)+ALOG(X/TEMP1)/(CNT3-CNT4*DENFR(1))
      FCT5=FIK-PWRV(1)*RR1**2/4.*(1.-( RRV/RR1)**2*(1.-ALOG((RRV/RR1)**2
     1)))
      RETURN
      END
      FUNCTION FCT6(X)
C
C        FOR CALCULATION OF T1
C
      COMMON CNT2,CNT3,CNT4,DENFR(3), PWRV(3)
      COMMON /FCT6X/TIME,CNTC,HTVP,      ABST/HAPPY4/BOLZ
      FK=CNT2+1./(X*(CNT3-CNT4*DENFR(3)))
      FCT6=FK-TIME*CNTC*EXP(-HTVP/BOLZ/(X+ABST))/SQRT(X+ABST)**3*PWRV(3)
      RETURN
      END
      FUNCTION FCT7(FRR1)
C
C        FOR CALCULATION OF R1
C
      COMMON CNT2,CNT3,CNT4,DENFR(3), PWRV(3)
      COMMON /FCT24/TEMP2,RR2/FCT15/RX,RY,TEMP1
      FIK=CNT2*(TEMP1-TEMP2)+ALOG(TEMP1/TEMP2)/(CNT3-CNT4*DENFR(2))
      FCT7=FIK-PWRV(2)*RR2**2/4.*(1.-(FRR1/RR2)**2+(1.-PWRV(3)/PWRV(2))*
     1ALOG((FRR1/RR2)**2))
```

```
      RETURN
      END
      FUNCTION FCTD(D)
C
C        TO CALCULATE BUBBLE DIAMETERS
C
      COMMON /FCTDX/COEF(5)
      FCTD=(COEF(5)*D**4+COEF(4)*D**3+COEF(3)*D**2+COEF(2)*D+COEF(1))/
     1(COEF(1)/10.)
      RETURN
      END
      SUBROUTINE QTFE(H,Y,Z,NDIM)
C
C        TO EVALUATE  INTEGRATIONS
C
      DIMENSION Y(1),Z(1)
      SUM2=0.
      IF (NDIM-1)4,3,1
    1 HH=.5*H
      DO 2 I=2,NDIM
      SUM1=SUM2
      SUM2=SUM2+HH*(Y(I)+Y(I-1))
    2 Z(I-1)=SUM1
    3 Z(NDIM)=SUM2
    4 RETURN
      END
      SUBROUTINE THSW
C
C        TO CALCULATE TOTAL THERMAL AND SWELLING STRAINS
C
      EXTERNAL FCTD
      COMMON /FCTDX/COEF(5),MNITR
     2/HAPPY2/AVSTS(21),ATEMP(21),BNU(21),SURT,CNAVST,SGB(21)
     3/HAPPY3/THSWST(21),GATMN(21),BATMN(21),THSTN(21),NSTNT,NINT(3),
     4SGG(21),SGGM(21),VNDWC,SWSLD(21),DB(21)/HAPPY4/BOLZ
      PI=3.14159
      IA=NINT(1)+NINT(2)+1
```

```
      IB=NSTNT
      DO 770 I=IA,IB
      BATMN(I)=GATMN(I)/BNU(I)
      IF (ABS(AVSTS(I)).GT.CNAVST) GO TO 710
      COEF(1)=-6.*BATMN(I)*VNDWC/PI*(1.0E+24)
      COEF(2)=-3.*BATMN(I)*BOLZ*ATEMP(I)/(2.*SURT*PI)*(1.0E+16)
      COEF(3)=0.
      COEF(4)=1.
      COEF(5)=0.
      DY=SQRT(-COEF(2)/3.)
      DX=(-COEF(1)-COEF(2)*1000.)**(1./3.)
      CALL  RTMI(DIAM,FCTDV,FCTD,DY,DX,0.01,     MNITR,IERD1)
      GO TO 720
  710 COEF(1)=24.*SURT*BATMN(I)*VNDWC/PI/AVSTS(I)*(1.0E+32)
      COEF(2)=6.*BATMN(I)*(BOLZ*ATEMP(I)-AVSTS(I)*VNDWC)/PI/AVSTS(I)
     1*(1.0E+24)
      COEF(3)=0.
      COEF(4)=-4.*SURT/AVSTS(I)*(1.0E+08)
      COEF(5)=1.
      IF (AVSTS(I).GT.0.) GO TO 715
      DY=SQRT(COEF(2)/COEF(4)/(-3.))
      DX=100.
      CALL  RTMI(DIAM,FCTDV,FCTD,DY,DX,  0.01,  MNITR,IERD2)
      GO TO 720
  715 DX=-3./4.*COEF(4)
      CALL  RTMI(DIAM,FCTDV,FCTD,0.,DX,  0.01,  MNITR,IERD3)
  720 DB(I)=DIAM*(1.0E-08)
      SGG(I)=1./6.*PI*DB(I)**3*BNU(I)
  770 CONTINUE
      DO 780 I=1,NSTNT
      THSWST(I)=1./3.*(SWSLD(I)+SGG(I)+SGB(I)+SGGM(I))+THSTN(I)
  780 CONTINUE
      RETURN
      END
      SUBROUTINE SGASB(DBGB,KMAX,SGBC,SGBN,I,TIME)
C
C         TO CALCULATE SWELLING AT GRAIN BOUNDARIES
```

```
C
      EXTERNAL FCTD
      DIMENSION          VELB(21), TIMECB(21),VELCB(21),SGBC(KMAX),
     1SGBN(KMAX),DBGB(KMAX),                          DBCB(21)
      COMMON /HAPPY1/  NUTIME,GASNM(21),DTIME(21),TIMECG(21),DG(21),
     1      DBCG(21),CNTE,CNTF,TGDN(21),SCACTE/HAPPY4/BOLZ
     2/HAPPY2/AVSTS(21),ATEMP(21),BNU(21),SURT,CNAVST,SGB(21)
      COMMON /FCTDX/COEF(5),MNITR
  840 DBGB(1)=DBCG(I)
      DO 860 K=2,NUTIME
      IF (AVSTS(I).GT.CNAVST ) GO TO 850
      DBGB(K)=SQRT(DBGB(1)**2+DBGB(K-1)**2)
      GO TO 855
  850 COEF(1)=4.*SURT/AVSTS(I)*(DBGB(1)**2+DBGB(K-1)**2)*(1.0E+24)-
     1(DBGB(1)**3+DBGB(K-1)**3)*(1.0E+24)
      COEF(2)=0.
      COEF(3)=-4.*SURT/AVSTS(I)*(1.0E+08)
      COEF(4)=1.
      COEF(5)=0.
      IF (AVSTS(I).GT.0.) GO TO 853
      DX=6000.
      CALL  RTMI(DIAM,FCTDV,FCTD,0.,DX,  0.01,  MNITR,IERD4)
      WRITE (3,3004)I,IERD4,K
 3004 FORMAT (//' STATION ',I2,,5X,'IERD4=',I1,5X,'K=',I4)
      GO TO 854
  853 DX=-2./3.*COEF(3)
      CALL  RTMI(DIAM,FCTDV,FCTD,0.,DX,  0.01,  MNITR,IERD5)
      WRITE (3,3005)I,IERD5,K
 3005 FORMAT (//' STATION ',I2,5X,'IERD5=',I1,5X,'K=',I4)
  854 DBGB(K)=DIAM*(1.0E-08)
  855 DBCB(I)=CNTF*SQRT(ATEMP(I)/TGDN(I))
      WRITE (3,3007) DBGB(K)
 3007 FORMAT (' DIAMETER OF  BUBBLE AT GRAIN BOUNDARY=',G10.5,'CM')
      IF (DBCB(I).GT.DBGB(K)) GO TO 860
      VELB(I)=CNTE*TGDN(I)/(ATEMP(I)**2*DBCB(I))*EXP(-SCACTE/BOLZ/
     1ATEMP(I))
      TIMECB(I)=DTIME(I)*K+TIMECG(I)
```

```
      VELCB(I)=DG(I)/(TIME-TIMECB(I))
      IF (VELCB(I).GT.VELB(I)) GO TO 860
      KTIMEC=K
      GO TO 870
  860 CONTINUE
      KTIMEC=NUTIME+1
  870 KMAX=NUTIME+2
      PI=3.14159
      SGB(I)=0.
      KC=KTIMEC+2
      GASNM(I)=0.
      BNUS=BNU(I)**(2./3.)
      BNUSPI=BNUS*PI/4.
      SGBC(1)=BNUS
      SGBC(2)=0.
      SGBN(2)=0.
  900 DO 940 K=3,KMAX
      IF (K.LE.KC) GO TO 910
      M=KC-1
      GASNM(I)=GASNM(I)+SGBN(KC-1)*(4.*SURT/DBGB(KC-2)-AVSTS(I))*1./6.*
     1PI*(DBGB(KC-2)**3)/(BOLZ*ATEMP(I))
      GO TO 920
  910 M=K-1
  920 SGBN(M)=SGBC(M-1)+SGBN(M)-SGBC(M)
      SGBC(M)=BNUSPI*(DBGB(1)+DBGB(M-1))**2*SGBN(M)
      M=M-1
      IF (M.GT.1) GO TO 920
      SGBC(K)=0.
      SGBN(K)=0.
      SGBC(1)=BNUS
      DO 930 J=3,K
      SGBC(1)=SGBC(1)-SGBC(J-1)
  930 CONTINUE
  940 CONTINUE
      NMAX=KC-2
      DO 950 N=2,NMAX
  950 SGB(I)=SGB(I)+SGBN(N)*1./6.*PI*DBGB(N-1)**3
```

```
      SGB(I)=SGB(I)/(PI/4.*DG(I))
      RETURN
      END
      SUBROUTINE RTMI(X,F,FCT,XLI,XRI,EPS,IEND,IER)
C
C        TO SOLVE NONLINEAR EQUATIONS
C
      IER=0
      XL=XLI
      XR=XRI
      X=XL
      TOL=X
      F=FCT(TOL)
      IF(F)1,16,1
    1 FL=F
      X=XR
      TOL=X
      F=FCT(TOL)
      IF(F)2,16,2
    2 FR=F
      IF(SIGN(1.,FL)+SIGN(1.,FR))25,3,25
    3 I=0
      TOLF=100.*EPS
    4 I=I+1
      DO 13 K=1,IEND
      X=.5*(XL+XR)
      TOL=X
      F=FCT(TOL)
      IF(F)5,16,5
    5 IF(SIGN(1.,F)+SIGN(1.,FR))7,6,7
    6 TOL=XL
      XL=XR
      XR=TOL
      TOL=FL
      FL=FR
      FR=TOL
    7 TOL=F-FL
```

```
      A=F*TOL
      A=A+A
      IF(A-FR*(FR-FL))8,9,9
    8 IF(I-IEND)17,17,9
    9 XR=X
      FR=F
      TOL=EPS
      A=ABS(XR)
      IF(A-1.)11,11,10
   10 TOL=TOL*A
   11 IF(ABS(XR-XL)-TOL)12,12,13
   12 IF(ABS(FR-FL)-TOLF)14,14,13
   13 CONTINUE
      IER=1
   14 IF(ABS(FR)-ABS(FL))16,16,15
   15 X=XL
      F=FL
   16 RETURN
   17 A=FR-F
      DX=(X-XL)*FL*(1.+F*(A-TOL)/(A*(FR-FL)))/TOL
      XM=X
      FM=F
      X=XL-DX
      TOL=X
      F=FCT(TOL)
      IF(F)18,16,18
   18 TOL=EPS
      A=ABS(X)
      IF(A-1.)20,20,19
   19 TOL=TOL*A
   20 IF(ABS(DX)-TOL)21,21,22
   21 IF(ABS(F)-TOLF)16,16,22
   22 IF(SIGN(1.,F)+SIGN(1.,FL))24,23,24
   23 XR=X
      FR=F
      GO TO 4
   24 XL=X
```

```
      FL=F
      XR=XM
      FR=FM
      GO TO 4
   25 IER=2
      RETURN
      END
```

Table 10.1. Important notations in computer program other than those for input listed in Table 5.1

Notation	Description
ALPH(I)	α, used in stress analysis for fuel
ALPHP(I)	α', "
ATEMP(I)	Absolute temperature
ATGAP	Absolute temperature in fuel-clad gap
AVSTS(I)	Average stress in fuel
BATMN(I)	Number of gas atoms in one bubble
BETA(I)	β, used in stress analysis for fuel
BETAP(I)	β', "
BNCC1	C_1, integral constant for clad stress analysis
BNCC2	C_2, "
BNCG	Calculated constant G in clad stress analysis
BNU(I)	Number of gas bubble
CAVSTS(I)	Average stress in clad
CEPLS1(I)	Equivalent plastic strain in clad
CESTS1(I)	Equivalent stress in clad
CETSTN(I)	Modified equivalent total strain in clad
CEXPN	Exponential constant n_c in the expression for clad stress-strain curves
CPLSTA(I)	Axial plastic strain in clad
CPLSTR(I)	Radial plastic strain in clad
CPLSTT(I)	Tangential plastic strain in clad
CSTNR(I)	Radial strain in clad
CSTNT(I)	Tangential strain in clad

Table 10.1 (Continued)

Notation	Description
CSTSA(I)	Axial stress in clad
CSTSR(I)	Radial stress in clad
CSTST(I)	Tangential stress in clad
CTHSTN(I)	Thermal strain in clad
CTTNDA(I)	Modified axial total strain deviator in clad
CTTNDR(I)	Modified radial total strain deviator in clad
CTTNDT(I)	Modified tangential total strain deviator in clad
DB(I)	Diameter of bubble in grain
DBCB(I)	Critical diameter of bubble for movement at grain boundary
DBCG(I)	Critical diameter of bubble for movement in grain
DBGB(K)	Diameter of bubble at grain boundary after Kth collision
DG(I)	Diameter of grain
DTEMP(I)	Temperature rise with respect to a reference temperature
DTIME(I)	Time interval for swelling calculation after movement of bubbles
ELSMD(I)	Elastic modulus in fuel
EQSTSl(I)	Equivalent stress in fuel
EQTSTN(I)	Modified equivalent total strain in fuel
FCTl	Function subprogram for calculating temperature in region I
FCT2	Function subprogram for calculating temperature in region II

Table 10.1 (Continued)

Notation	Description
FCT3	Function subprogram for calculating temperature in region III
FCT4	Function subprogram for calculating equivalent stress in fuel
FCT5	Function subprogram for calculating central void temperature of fuel
FCT6	Function subprogram for calculating temperature at the outer surface of columnar grain region
FCT7	Function subprogram for calculating temperature at the outer surface of equiaxed grain region
FCTC4	Function subprogram for calculating equivalent stress in clad
FCTD	Function subprogram for calculating diameter of bubble
FCTG1	Function subprogram for calculating temperature at fuel surface
FEXPN	Exponential constant n_f in the expression for fuel stress-strain curves
FSNRT(I)	Fission rate per unit volume
GAMA(I)	γ, used in stress analysis for fuel
GAMAP(I)	γ', used in stress analysis for fuel
GAP	Thickness of fuel-clad gap
GASNM(I)	Number of gas atoms in bubbles moving away from grain boundaries at Ith station
GATMN(I)	Number of gas atoms per unit volume
GATMNM	Total number of gas atoms in bubbles moving away from grain boundaries in region III
NINT(I)	Number of intervals in region I

Table 10.1 (Continued)

Notation	Description
NITR1	Number of iteration for fuel surface temperature
NITR2	Number of iteration for fuel stress analysis
NITR3	Number of iteration for clad stress analysis
NSTN1	Station number at the outer surface of columnar grain region
NSTN2	Station number at the outer surface of equiaxed grain region
NSTN3	Station number at the fuel surface
NSTNC	Total number of stations in clad
NSTNT	Total number of stations in fuel
NUTIME	Number of time intervals for bubble movement
PECLET	Peclet number
PI	3.14159
PLSTA(I)	Axial plastic strain in fuel
PLSTR(I)	Radial plastic strain in fuel
PLSTT(I)	Tangential plastic strain in fuel
PNPL1	P_{N+1}, used in stress analysis for fuel
PORST(I)	Porosity
PPTLMT(I)	Proportional limit
PRESA	Pressure in central void
PRESG	Pressure in fuel-clad gap
PWRV(I)	Volumetric heat power
QNPL1	Q_{N+1}, used in stress analysis for fuel

Table 10.1 (Continued)

Notation	Description
QTEF	Subroutine subprogram to evaluate integrals by trapezoid rule
R(I)	Radius in fuel
RC(I)	Radius in clad
RDC	Radial difference in clad
RDR(J)	Radial difference in region J of fuel
RR1	Radius at outer surface of columnar grain region
RR2	Radius at outer surface of equiaxed grain region
RRS	Radius at fuel surface
RRV	Radius of central void
RTMI	Subroutine subprogram to solve general nonlinear equations of the form f(x)=0 by means of Mueller -S iteration method
SE(I)	The variable e in fuel
SEC(I)	The variable e in clad
SG(I)	The variable g in fuel
SGASB	Subroutine subprogram to calculate fission-gas swelling at grain boundaries
SGB(I)	Fission-gas swelling at grain boundaries
SGBC(M)	The defined variable $C_{i,n}$ in the calculation of fission-gas swelling at grain boundaries
SGBN(M)	The defined variable $N_{i,n}$ in the calculation of fission-gas swelling at grain boundaries
SGC	The variable g in clad
SGGM(I)	Fission-gas swelling due to moving bubbles in grains before reaching a grain boundary

Table 10.1 (Continued)

Notation	Description
STNR(I)	Radial strain in fuel
STNT(I)	Tangential strain in fuel
STSA(I)	Axial stress in fuel
STSR(I)	Radial stress in fuel
STST(I)	Tangential stress in fuel
STSDVA(I)	Axial stress deviator in fuel
STSDVR(I)	Radial stress deviator in fuel
STSDVT(I)	Tangential stress deviator in fuel
SWSLD(I)	Solid fission-product swelling
T(I)	Temperature in fuel
TC(I)	Temperature in clad
TEMP1	Temperature at outer surface of columnar grain region
TEMP2	Temperature at outer surface of equiaxed grain region
TEMPC	Fictitious centerline temperature
TEMPS	Temperature at fuel surface
TEMPV	Temperature in central void
TGDN(I)	Temperature gradient
THSTN(I)	Thermal strain in fuel
THSW	Subroutine subprogram to calculate thermal and irradiation strains
THSWST(I)	Thermal and irradiation dilatation strain
TIME	Irradiation time

Table 10.1 (Continued)

Notation	Description
TIMECB(I)	Critical time for movement of bubbles trapped on grain boundaries
TIMECG(I)	Critical time for movement of bubbles anchored on dislocations in grains
TIMEG(I)	Time required for a bubble to travel across a grain
TIN	Temperature at clad inner surface
TOU	Temperature at clad outer surface
TSTNDA(I)	Modified axial total strain deviator in fuel
TSTNDR(I)	Modified radial total strain deviator in fuel
TSTNDT(I)	Modified tangential total strain deviator in fuel
VELB(I)	Velocity of bubble at grain boundary
VELCB(I)	Critical velocity for bubbles moving away from grain boundaries
VELCG(I)	Critical velocity for bubbles moving away from anchored sites in grains
VELG(I)	Velocity of bubble in grain

XI. APPENDIX B: TABLES OF RESULTS

Table 11.1 Time variations of temperatures and radii at region surfaces, fuel-clad gap, and pressures in central void and gap

Time (hrs)	Temperatures (°C)				radii			fuel-clad gap (mm)	pressures (1000 psi)	
	T_v	T_1	T_2	T_s	R_1/R_s	R_2/R_s	R_v (mm)		void	gap
1	2398.	2340.	2013.	744.9	0.2823	0.5229	0.4086	0.0171	0.1222	0.1614
8	2331.	2149.	1846.	754.8	0.4266	0.6026	0.4833	0.0196	0.1214	0.1417
27	2295.	2050.	1759.	759.8	0.4838	0.6408	0.5181	0.0208	0.1251	0.1335
64	2269.	1985.	1701.	762.0	0.5174	0.6645	0.5396	0.0214	0.1340	0.1302
125	2247.	1936.	1658.	761.7	0.5397	0.6806	0.5541	0.0213	0.1494	0.1306
216	2228.	1898.	1624.	759.0	0.5549	0.6918	0.5643	0.0206	0.1726	0.1347
343	2209.	1867.	1597.	753.7	0.5652	0.6992	0.5712	0.0193	0.2048	0.1437
512	2190.	1841.	1574.	745.4	0.5712	0.7035	0.5753	0.0172	0.2473	0.1603
729	2169.	1819.	1555.	733.8	0.5734	0.7084	0.5768	0.0143	0.3011	0.1914
1000	2145.	1799.	1537.	718.5	0.5719	0.7032	0.5759	0.0106	0.3671	0.2577

Table 11.2. Swelling strain and plastic strains in fuel at time t=1 hour

STATION	SWELLING STRAIN	RADIAL PLASTIC STRAIN	TANGENTIAL PLASTIC STRAIN	AXIAL PLASTIC STRAIN
1	0.0000030	0.0627359	-0.0140391	-0.0486967
2	0.0000030	0.0485200	-0.0000517	-0.0484683
3	0.0000030	0.0401917	0.0077402	-0.0479319
4	0.0000030	0.0344696	0.0126557	-0.0471252
5	0.0000030	0.0300295	0.0160492	-0.0460787
6	0.0000030	0.0245498	0.0195440	-0.0440937
7	0.0000030	0.0197533	0.0220336	-0.0417869
8	0.0000030	0.0152525	0.0239445	-0.0391970
9	0.0000030	0.0109273	0.0254679	-0.0363952
10	0.0000044	0.0067557	0.0266968	-0.0334525
11	0.0000041	0.0020780	0.0280370	-0.0301150
12	0.0000041	-0.0020387	0.0290019	-0.0269632
13	0.0000041	-0.0057765	0.0296806	-0.0239041
14	0.0000041	-0.0091178	0.0300954	-0.0209776
15	0.0000041	-0.0120411	0.0302594	-0.0182184
16	0.0000041	-0.0145244	0.0301793	-0.0156549
17	0.0000041	-0.0165470	0.0298567	-0.0133097
18	0.0000041	-0.0180888	0.0292880	-0.0111992
19	0.0000041	-0.0191282	0.0284623	-0.0093341
20	0.0000041	-0.0196365	0.0273563	-0.0077199
21	0.0000041	-0.0195618	0.0259189	-0.0063571

Table 11.3. Swelling strain and plastic strains in fuel at time t=125 hours

STATION	SWELLING STRAIN	RADIAL PLASTIC STRAIN	TANGENTIAL PLASTIC STRAIN	AXIAL PLASTIC STRAIN
1	0.0003789	0.0523419	-0.0096935	-0.0426484
2	0.0003789	0.0424258	-0.0000174	-0.0424083
3	0.0003789	0.0357488	0.0060696	-0.0418185
4	0.0003789	0.0306597	0.0102647	-0.0409243
5	0.0003789	0.0264041	0.0133614	-0.0397656
6	0.0003789	0.0226091	0.0157697	-0.0383787
7	0.0003789	0.0190826	0.0177160	-0.0367987
8	0.0003789	0.0157275	0.0193319	-0.0350594
9	0.0003789	0.0124979	0.0206961	-0.0331940
10	0.0003789	0.0093783	0.0218563	-0.0312347
11	0.0003712	0.0052408	0.0232455	-0.0284863
12	0.0003712	0.0014292	0.0243255	-0.0257546
13	0.0005696	-0.0017198	0.0249687	-0.0232489
14	0.0005267	-0.0054779	0.0259016	-0.0204237
15	0.0005255	-0.0085830	0.0264917	-0.0179087
16	0.0005243	-0.0112230	0.0267956	-0.0155727
17	0.0005231	-0.0133984	0.0268288	-0.0134303
18	0.0005219	-0.0151067	0.0265987	-0.0114920
19	0.0005208	-0.0163411	0.0261054	-0.0097643
20	0.0005197	-0.0170881	0.0253376	-0.0082495
21	0.0005187	-0.0173167	0.0242628	-0.0069461

Table 11.4. Swelling strain and plastic strains in fuel at time t=729 hours

STATION	SWELLING STRAIN	RADIAL PLASTIC STRAIN	TANGENTIAL PLASTIC STRAIN	AXIAL PLASTIC STRAIN
1	0.0022097	C.0485902	-0.0072334	-0.0413567
2	0.0022097	C.0401558	0.0009890	-0.0411448
3	0.0022097	0.0342863	0.0063371	-C.0406234
4	0.0022097	0.0297220	0.C101094	-0.0398314
5	0.0022097	0.0258628	0.0129400	-0.0388028
6	0.0022097	C.0224026	0.0151669	-0.0375695
7	0.0022097	C.0191802	0.0169818	-0.0361620
8	0.0022097	0.0161114	0.0184982	-0.0346096
9	0.0022097	C.0131557	0.0197854	-0.0329411
10	0.0022097	0.0102985	0.0208862	-0.0311847
11	0.0022097	0.0075399	0.0218273	-C.0293672
12	0.0021651	0.0039297	0.0229702	-0.0268999
13	0.0021651	0.0006914	0.0238239	-0.0245153
14	0.0034125	C.0000115	0.0233666	-0.0233781
15	0.0031483	-0.0041631	0.0245531	-0.0203900
16	0.0031361	-0.0071911	0.0251358	-0.0179446
17	0.0031238	-0.0096854	0.0253876	-0.0157021
18	0.0031118	-0.0116512	0.0253240	-0.0136728
19	0.0031003	-0.0130875	0.0249488	-0.0118613
20	0.0030896	-0.0139841	0.0242498	-0.0102657
21	0.0030803	-0.0143085	0.0231841	-0.0088756

Table 11.5. Swelling strain and plastic strains in fuel at time t=1000 hours

STATION	SWELLING STRAIN	RADIAL PLASTIC STRAIN	TANGENTIAL PLASTIC STRAIN	AXIAL PLASTIC STRAIN
1	0.0030312	0.0476815	-0.0064076	-0.0412740
2	0.0030312	0.0395104	0.0015570	-0.0410673
3	0.0030312	0.0338199	0.0067397	-0.0405595
4	0.0030312	0.0293913	0.0103969	-0.0397881
5	0.0030312	0.0256441	0.0131421	-0.0387862
6	0.0030312	0.0222821	0.0153027	-0.0375848
7	0.0030312	0.0191491	0.0170643	-0.0362133
8	0.0030312	0.0161640	0.0185367	-0.0347007
9	0.0030312	0.0132877	0.0197868	-0.0330745
10	0.0030312	0.0105063	0.0208560	-0.0313624
11	0.0030312	0.0078200	0.0217702	-0.0295903
12	0.0029699	0.0042611	0.0228990	-0.0271602
13	0.0029699	0.0011013	0.0237268	-0.0248281
14	0.0047098	0.0013912	0.0228215	-0.0242128
15	0.0043435	-0.0029958	0.0241528	-0.0211570
16	0.0043253	-0.0060316	0.0247692	-0.0187377
17	0.0043071	-0.0085299	0.0250475	-0.0165177
18	0.0042893	-0.0104976	0.0250039	-0.0145064
19	0.0042723	-0.0119352	0.0246418	-0.0127065
20	0.0042567	-0.0128330	0.0239469	-0.0111139
21	0.0042433	-0.0131575	0.0228698	-0.0097123

Table 11.6. Temperature distribution, temperature gradients and thermal strains in fuel at time t=1 hour

STATION	RADIUS (CM)	TEMPERATURE (C)	TEMPERATURE GRADIENT (C/CM)	THERMAL STRAIN
1	0.039506	2398.05	0.0	0.0493333
2	0.048897	2393.87	862.70	0.0491458
3	0.058288	2382.24	1597.82	0.0486267
4	0.067679	2364.11	2254.94	0.0478247
5	0.077069	2340.06	2858.86	0.0467756
6	0.090205	2294.02	3908.62	0.0448120
7	0.103340	2237.64	4666.64	0.0424865
8	0.116475	2171.65	5373.33	0.0398726
9	0.129610	2096.69	6031.48	0.0370417
10	0.142745	2013.41	6640.60	0.0340635
11	0.154586	1916.66	8428.39	0.0308168
12	0.166428	1813.96	8909.54	0.0276116
13	0.178269	1705.85	9343.13	0.0244934
14	0.190110	1592.91	9721.02	0.0215033
15	0.201952	1475.88	10033.75	0.0186770
16	0.213793	1355.59	10270.40	0.0160436
17	0.225634	1233.00	10418.48	0.0136253
18	0.237476	1109.26	10464.15	0.0114367
19	0.249317	985.65	10392.48	0.0094848
20	0.261158	863.66	10188.45	0.0077689
21	0.273000	744.94	9838.54	0.0062822

Table 11.7. Temperature distribution, temperature gradients and thermal strains in fuel at time t=125 hours

STATION	RADIUS (CM)	TEMPERATURE (C)	TEMPERATURE GRADIENT (C/CM)	THERMAL STRAIN
1	0.053662	2247.25	0.0	0.0428768
2	0.064069	2242.20	944.32	0.0426715
3	0.074476	2228.02	1763.35	0.0420985
4	0.084883	2205.79	2497.97	0.0412106
5	0.095290	2176.24	3170.41	0.0400511
6	0.105698	2139.97	3793.33	0.0386586
7	0.116105	2097.43	4374.09	0.0370691
8	0.126512	2049.06	4916.83	0.0353171
9	0.136919	1995.22	5423.61	0.0334357
10	0.147326	1936.29	5895.14	0.0314574
11	0.160153	1850.18	6987.91	0.0287142
12	0.172979	1757.28	7487.08	0.0259449
13	0.185805	1658.38	7922.97	0.0232044
14	0.196705	1551.51	9960.41	0.0204726
15	0.207604	1441.48	10220.45	0.0178964
16	0.218503	1328.[illegible]	10411.96	0.0154964
17	0.229402	1214.80	10524.77	0.0132879
18	0.240302	1099.87	10547.71	0.0112806
19	0.251201	985.24	10468.93	0.0094787
20	0.262100	872.08	10276.59	0.0078810
21	0.273000	761.68	9959.96	0.0064816

Table 11.8. Temperature distribution, temperature gradients and thermal strains in fuel at time t=729 hours

STATION	RADIUS (CM)	TEMPERATURE (C)	TEMPERATURE GRADIENT (C/CM)	THERMAL STRAIN
1	0.055794	2168.66	0.0	0.0397570
2	0.065870	2163.98	904.40	0.0395765
3	0.075946	2150.81	1694.04	0.0390713
4	0.086021	2130.11	2404.36	0.0382860
5	0.096097	2102.56	3055.25	0.0372582
6	0.106172	2068.70	3658.32	0.0360215
7	0.116248	2028.98	4220.48	0.0346071
8	0.126324	1983.78	4745.71	0.0330452
9	0.136399	1933.46	5236.14	0.0313646
10	0.146475	1878.38	5692.57	0.0295936
11	0.156551	1818.86	6114.91	0.0277591
12	0.168506	1735.98	7166.96	0.0253369
13	0.180462	1647.71	7589.93	0.0229211
14	0.192417	1554.73	7954.12	0.0205516
15	0.203929	1440.77	10037.59	0.0178805
16	0.215441	1323.92	10249.95	0.0153939
17	0.226952	1205.11	10376.25	0.0131105
18	0.238464	1085.40	10403.59	0.0110424
19	0.249976	966.01	9518.29	0.0091950
20	0.261488	848.32	10106.71	0.0075671
21	0.273000	733.85	9756.83	0.0061521

Table 11.9. Temperature distribution, temperature gradients and thermal strains in fuel at time t=1000 hours

STATION	RADIUS (CM)	TEMPERATURE (C)	TEMPERATURE GRADIENT (C/CM)	THERMAL STRAIN
1	0.055659	2145.19	0.0	0.0388569
2	0.065707	2140.56	897.41	0.0386812
3	0.075754	2127.54	1680.95	0.0381891
4	0.085801	2107.05	2385.75	0.0374244
5	0.095848	2079.79	3031.50	0.0364234
6	0.105895	2046.29	3629.73	0.0352188
7	0.115942	2006.99	4187.28	0.0338411
8	0.125989	1962.28	4708.09	0.0323195
9	0.136037	1912.50	5194.26	0.0306823
10	0.146084	1858.01	5646.59	0.0289567
11	0.156131	1799.15	6065.00	0.0271691
12	0.168074	1716.98	7111.99	0.0248029
13	0.180018	1629.48	7531.17	0.0224425
14	0.191962	1537.32	7891.58	0.0201270
15	0.203539	1423.46	9970.91	0.0174965
16	0.215116	1306.74	10179.37	0.0150490
17	0.226692	1188.11	10300.27	0.0128030
18	0.238269	1068.64	10320.53	0.0107705
19	0.249846	949.59	10226.32	0.0089567
20	0.261423	832.36	10004.02	0.0073602
21	0.273000	718.50	9641.85	0.0059741

Table 11.10. Dimensionless strains and stresses in fuel at time t=1 hour

STATION	R/RO	ER/ERO	ET/ETO	SR/|SRO|	ST/|SRO|	SA/|SRO|
1	0.1447	-7.7686	0.9766	-0.7517	-172.172	-129.791
2	0.1791	-6.7554	1.3797	-31.9040	-144.179	-135.770
3	0.2135	-6.1339	1.5927	-48.9873	-127.217	-138.034
4	0.2479	-5.6769	1.7137	-59.1911	-115.508	-138.345
5	0.2823	-5.2937	1.7831	-65.5852	-106.477	-137.504
6	0.3304	-4.7760	1.8292	-70.9153	-96.258	-135.634
7	0.3785	-4.2816	1.8363	-73.5470	-86.062	-131.736
8	0.4266	-3.7886	1.8184	-74.4229	-75.701	-126.685
9	0.4748	-3.2931	1.7833	-74.0095	-64.579	-120.436
10	0.5229	-2.7984	1.7356	-72.6054	-52.336	-112.950
11	0.5663	-2.2494	1.6830	-70.7483	-44.296	-108.952
12	0.6096	-1.7419	1.6222	-68.3144	-28.402	-98.661
13	0.6530	-1.2664	1.5560	-65.0984	-10.808	-86.911
14	0.6964	-0.8270	1.4861	-61.1143	8.920	-73.660
15	0.7397	-0.4273	1.4143	-56.3548	31.544	-58.771
16	0.7831	-0.0708	1.3416	-50.7554	58.320	-41.888
17	0.8265	0.2401	1.2694	-44.1843	91.232	-22.318
18	0.8699	0.5036	1.1984	-36.3994	133.335	1.176
19	0.9132	0.7185	1.1294	-27.0314	189.201	30.544
20	0.9566	0.8843	1.0631	-15.5153	265.746	68.774
21	1.0000	1.0000	1.0000	-1.0000	374.479	120.540

NOTE: R=RADIUS RO=RADIUS AT THE FUEL SURFACE=0.2730 CM
ER=RADIAL STRAIN ERO=RADIAL STRAIN AT FUEL SURFACE=-0.0145211
ET=TANGENTIAL STRAIN ETO=TANGENTIAL STRAIN AT FUEL SURFACE= 0.0350265
SR=RADIAL STRESS ST=TANGENTIAL STRESS SA=AXIAL STRESS
|SRO|=ABSOLUTE VALUE OF RADIAL STRESS AT FUEL OUTER SURFACE, SRO=-0.16109
1000PSI

Table 11.11. Dimensionless strains and stresses in fuel at time t=125 hours

STATION	R/RO	ER/ERO	ET/ETO	SR/|SRO|	ST/|SRO|	SA/|SRO|
1	0.1966	-8.4190	0.9624	-1.1417	-188.035	-150.203
2	0.2347	-7.5139	1.2487	-30.0147	-162.353	-156.560
3	0.2728	-6.8672	1.4158	-47.5550	-144.744	-159.322
4	0.3109	-6.3358	1.5167	-58.7861	-131.277	-159.885
5	0.3490	-5.8558	1.5764	-66.1601	-119.913	-158.940
6	0.3872	-5.3972	1.6085	-70.9897	-109.498	-156.842
7	0.4253	-4.9458	1.6210	-74.0221	-99.295	-153.745
8	0.4634	-4.4957	1.6188	-75.6944	-88.830	-149.690
9	0.5015	-4.0457	1.6054	-76.2891	-77.762	-144.669
10	0.5397	-3.5970	1.5831	-75.9866	-65.831	-138.647
11	0.5866	-2.9909	1.5455	-74.5427	-49.538	-130.085
12	0.6336	-2.4115	1.4986	-71.9758	-29.788	-118.507
13	0.6806	-1.9105	1.4455	-68.3627	-9.046	-106.429
14	0.7205	-1.3324	1.3958	-64.5423	10.780	-94.629
15	0.7605	-0.8299	1.3417	-59.8534	39.304	-77.022
16	0.8004	-0.3829	1.2850	-54.0991	72.402	-57.144
17	0.8403	0.0075	1.2269	-47.1547	112.183	-34.383
18	0.8802	0.3409	1.1686	-38.8181	161.840	-7.603
19	0.9201	0.6174	1.1109	-28.7443	225.998	25.045
20	0.9601	0.8372	1.0545	-16.4003	311.443	66.315
21	1.0000	1.0000	1.0000	-1.0000	428.942	120.327

NOTE: R=RADIUS RO=RADIUS AT THE FUEL SURFACE=0.2730 CM
ER=RADIAL STRAIN ERO=RADIAL STRAIN AT FUEL SURFACE=-0.0114324
ET=TANGENTIAL STRAIN ETO=TANGENTIAL STRAIN AT FUEL SURFACE= 0.0339097
SR=RADIAL STRESS ST=TANGENTIAL STRESS SA=AXIAL STRESS
|SRO|=ABSOLUTE VALUE OF RADIAL STRESS AT FUEL OUTER SURFACE, SRO=-0.12993 1000PSI

Table 11.12. Dimensionless strains and stresses in fuel at time t=729 hours

STATION	R/RO	ER/ERO	ET/ETO	SR/|SRO|	ST/|SRO|	SA/|SRO|
1	0.2044	-14.8813	0.9613	-1.5735	-125.058	-102.484
2	0.2413	-13.4419	1.1958	-19.5546	-108.926	-106.410
3	0.2782	-12.3797	1.3374	-30.8184	-97.601	-108.209
4	0.3151	-11.4914	1.4253	-38.2136	-88.821	-108.690
5	0.3520	-10.6826	1.4789	-43.1826	-81.382	-108.268
6	0.3889	-9.9073	1.5090	-46.5156	-74.568	-107.143
7	0.4258	-9.1434	1.5222	-48.6737	-67.910	-105.396
8	0.4627	-8.3816	1.5227	-49.9548	-61.126	-103.090
9	0.4996	-7.6197	1.5132	-50.5238	-53.983	-100.222
10	0.5365	-6.8595	1.4959	-50.5098	-46.319	-96.766
11	0.5734	-6.1052	1.4723	-49.9808	-37.983	-92.706
12	0.6172	-5.1071	1.4372	-48.7426	-26.630	-86.976
13	0.6610	-4.1781	1.3956	-46.8440	-13.207	-79.667
14	0.7048	-3.8840	1.3525	-44.5165	-5.506	-78.957
15	0.7470	-2.7087	1.3086	-41.7986	13.215	-68.614
16	0.7892	-1.7947	1.2597	-38.2361	37.037	-56.087
17	0.8313	-0.9996	1.2081	-33.7046	65.663	-41.746
18	0.8735	-0.3233	1.1554	-28.0572	101.482	-25.013
19	0.9157	0.2348	1.1025	-21.0349	148.069	-4.842
20	0.9578	0.6759	1.0505	-12.2325	210.851	20.413
21	1.0000	1.0000	1.0000	-1.0000	298.860	53.189

NOTE: R=RADIUS RO=RADIUS AT THE FUEL SURFACE=0.2730 CM
ER=RADIAL STRAIN ERO=RADIAL STRAIN AT FUEL SURFACE=-0.0061277
ET=TANGENTIAL STRAIN ETO=TANGENTIAL STRAIN AT FUEL SURFACE= 0.0352096
SR=RADIAL STRESS ST=TANGENTIAL STRESS SA=AXIAL STRESS
|SRO|=ABSOLUTE VALUE OF RADIAL STRESS AT FUEL OUTER SURFACE, SRO=-0.19090 1000PSI

Table 11.13. Dimensionless strains and stresses in fuel at time t=1000 hours

STATION	R/RO	ER/ERO	ET/ETO	SR/|SRO|	ST/|SRO|	SA/|SRO|
1	0.2039	-22.7198	0.9617	-1.4228	-93.121	-76.721
2	0.2407	-20.5658	1.1842	-14.7692	-81.081	-79.576
3	0.2775	-18.9748	1.3186	-23.1247	-72.650	-80.877
4	0.3143	-17.6432	1.4020	-28.6062	-66.136	-81.221
5	0.3511	-16.4298	1.4528	-32.2877	-60.628	-80.920
6	0.3879	-15.2661	1.4813	-34.7597	-55.595	-80.112
7	0.4247	-14.1189	1.4938	-36.3655	-50.701	-78.873
8	0.4615	-12.9745	1.4941	-37.3239	-45.720	-77.234
9	0.4983	-11.8295	1.4850	-37.7606	-40.490	-75.207
10	0.5351	-10.6868	1.4684	-37.7612	-34.872	-72.761
11	0.5719	-9.5529	1.4459	-37.3876	-28.773	-69.898
12	0.6157	-8.0352	1.4122	-36.4854	-20.346	-65.789
13	0.6594	-6.6353	1.3723	-35.0912	-10.462	-60.629
14	0.7032	-6.5682	1.3322	-33.4641	-7.436	-62.946
15	0.7456	-4.6842	1.2919	-31.5695	7.499	-54.980
16	0.7880	-3.2796	1.2460	-28.9881	25.599	-46.106
17	0.8304	-2.0592	1.1975	-25.6528	47.406	-35.985
18	0.8728	-1.0224	1.1476	-21.4502	74.736	-24.246
19	0.9152	-0.1678	1.0974	-16.1833	110.334	-10.218
20	0.9576	0.5064	1.0480	-9.5342	158.410	7.171
21	1.0000	1.0000	1.0000	-1.0000	226.144	29.448

NOTE: R=RADIUS RO=RADIUS AT THE FUEL SURFACE=0.2730 CM
ER=RADIAL STRAIN ERO=RADIAL STRAIN AT FUEL SURFACE=-0.0039700
ET=TANGENTIAL STRAIN ETO=TANGENTIAL STRAIN AT FUEL SURFACE= 0.0359726
SR=RADIAL STRESS ST=TANGENTIAL STRESS SA=AXIAL STRESS
|SRO|=ABSOLUTE VALUE OF RADIAL STRESS AT FUEL OUTER SURFACE, SRO=-0.25706 1000PSI

Table 11.14. Temperature distribution, thermal strain and plastic strains in cladding at time t=1 hour

STATION	RADIUS (CM)	TEMPERATURE (C)	THERMAL STRAIN	RADIAL PLASTIC STRAIN	TANGENTIAL PLASTIC STRAIN	AXIAL PLASTIC STRAIN
1	0.27900	649.09	0.01202	0.005840	0.004499	-0.010339
2	0.28285	642.68	0.01190	0.005599	0.004605	-0.010203
3	0.28670	636.35	0.01177	0.005367	0.004703	-0.010070
4	0.29055	630.11	0.01165	0.005144	0.004795	-0.009939
5	0.29440	623.95	0.01154	0.004931	0.004880	-0.009811
6	0.29825	617.87	0.01142	0.004725	0.004960	-0.009685
7	0.30210	611.87	0.01130	0.004527	0.005034	-0.009562
8	0.30595	605.94	0.01119	0.004337	0.005104	-0.009440
9	0.30980	600.09	0.01108	0.004154	0.005168	-0.009322
10	0.31365	594.31	0.01096	0.003977	0.005228	-0.009205
11	0.31750	588.60	0.01085	0.003807	0.005284	-0.009091

Table 11.15. Temperature distribution, thermal strain and plastic strains in cladding at time t=125 hours

STATION	RADIUS (CM)	TEMPERATURE (C)	THERMAL STRAIN	RADIAL PLASTIC STRAIN	TANGENTIAL PLASTIC STRAIN	AXIAL PLASTIC STRAIN
1	0.27900	649.09	0.01202	0.005860	0.004478	-0.010338
2	0.28285	642.68	0.01190	0.005618	0.004583	-0.010202
3	0.28670	636.35	0.01177	0.005386	0.004682	-0.010068
4	0.29055	630.11	0.01165	0.005163	0.004775	-0.009938
5	0.29440	623.95	0.01154	0.004948	0.004861	-0.009809
6	0.29825	617.87	0.01142	0.004742	0.004941	-0.009683
7	0.30210	611.87	0.01130	0.004544	0.005016	-0.009560
8	0.30595	605.94	0.01119	0.004353	0.005086	-0.009439
9	0.30980	600.09	0.01108	0.004169	0.005151	-0.009320
10	0.31365	594.31	0.01096	0.003992	0.005211	-0.009203
11	0.31750	588.60	0.01085	0.003822	0.005268	-0.009089

Table 11.16. Temperature distribution, thermal strain and plastic strains in cladding at time t=729 hours

STATION	RADIUS (CM)	TEMPERATURE (C)	THERMAL STRAIN	RADIAL PLASTIC STRAIN	TANGENTIAL PLASTIC STRAIN	AXIAL PLASTIC STRAIN
1	0.27900	649.09	0.01202	0.005820	0.004521	-0.010341
2	0.28285	642.68	0.01190	0.005580	0.004625	-0.010205
3	0.28670	636.35	0.01177	0.005349	0.004723	-0.010072
4	0.29055	630.11	0.01165	0.005127	0.004814	-0.009941
5	0.29440	623.95	0.01154	0.004913	0.004899	-0.009812
6	0.29825	617.87	0.01142	0.004708	0.004978	-0.009687
7	0.30210	611.87	0.01130	0.004511	0.005052	-0.009563
8	0.30595	605.94	0.01119	0.004321	0.005121	-0.009442
9	0.30980	600.09	0.01108	0.004138	0.005185	-0.009324
10	0.31365	594.31	0.01096	0.003962	0.005245	-0.009207
11	0.31750	588.60	0.01085	0.003793	0.005300	-0.009093

Table 11.17. Temperature distribution, thermal strain and plastic strains in cladding at time t=1000 hours

STATION	RADIUS (CM)	TEMPERATURE (C)	THERMAL STRAIN	RADIAL PLASTIC STRAIN	TANGENTIAL PLASTIC STRAIN	AXIAL PLASTIC STRAIN
1	0.27900	649.09	0.01202	0.005776	0.004567	-0.010344
2	0.28285	642.68	0.01190	0.005537	0.004671	-0.010208
3	0.28670	636.35	0.01177	0.005308	0.004767	-0.010075
4	0.29055	630.11	0.01165	0.005087	0.004857	-0.009944
5	0.29440	623.95	0.01154	0.004875	0.004941	-0.009816
6	0.29825	617.87	0.01142	0.004671	0.005019	-0.009690
7	0.30210	611.87	0.01130	0.004475	0.005092	-0.009567
8	0.30595	605.94	0.01119	0.004286	0.005160	-0.009446
9	0.30980	600.09	0.01108	0.004105	0.005223	-0.009328
10	0.31365	594.31	0.01096	0.003930	0.005282	-0.009211
11	0.31750	588.60	0.01085	0.003761	0.005336	-0.009097

Table 11.18. Dimensionless strains and stresses in cladding at time t=1 hour

STATION	R/RO	ER/ERO	ET/ETO	SR/|SRO|	ST/|SRO|	SA/|SRO|
1	1.0220	1.2191	1.0016	-1.0000	-20.417	-256.787
2	1.0361	1.1942	1.0027	-1.2261	-15.202	-257.148
3	1.0502	1.1701	1.0034	-1.3760	-9.930	-257.333
4	1.0643	1.1466	1.0038	-1.4515	-4.601	-257.339
5	1.0784	1.1239	1.0040	-1.4554	0.776	-257.172
6	1.0925	1.1018	1.0039	-1.3897	6.194	-256.833
7	1.1066	1.0803	1.0036	-1.2555	11.647	-256.325
8	1.1207	1.0594	1.0030	-1.0577	17.130	-255.650
9	1.1348	1.0390	1.0022	-0.7954	22.637	-254.813
10	1.1489	1.0193	1.0012	-0.4721	28.162	-253.818
11	1.1630	1.0000	1.0000	-0.0894	33.702	-252.668

NOTE: R=RADIUS RO=RADIUS AT THE FUEL SURFACE=0.2730 CM

ER=RADIAL STRAIN ERO=RADIAL STRAIN AT CLAD OUTER SURFACE= 0.0151023

ET=TANGENTIAL STRAIN ETO=TANGENTIAL STRAIN AT CLAD SURFACE= 0.0168744

SR=RADIAL STRESS ST=TANGENTIAL STRESS SA=AXIAL STRESS

|SRO|=ABSOLUTE VALUE OF RADIAL STRESS AT CLAD INNER SURFACE, SRO=-0.16111 1000PSI

Table 11.19. Dimensionless strains and stresses in cladding at time t=125 hours

STATION	R/RO	ER/ERO	ET/ETO	SR/|SRO|	ST/|SRO|	SA/|SRO|
1	1.0220	1.2193	1.0012	-1.0000	-27.020	-318.240
2	1.0361	1.1944	1.0023	-1.3074	-20.559	-318.705
3	1.0502	1.1702	1.0031	-1.5193	-14.026	-318.949
4	1.0643	1.1467	1.0036	-1.6371	-7.426	-318.974
5	1.0784	1.1240	1.0038	-1.6671	-0.767	-318.782
6	1.0925	1.1018	1.0037	-1.6102	5.945	-318.377
7	1.1066	1.0803	1.0034	-1.4684	12.700	-317.763
8	1.1207	1.0594	1.0029	-1.2446	19.491	-316.942
9	1.1348	1.0391	1.0021	-0.9418	26.314	-315.919
10	1.1489	1.0193	1.0012	-0.5627	33.158	-314.700
11	1.1630	1.0000	1.0000	-0.1110	40.020	-313.289

NOTE: R=RADIUS RO=RADIUS AT THE FUEL SURFACE=0.2730 CM

ER=RADIAL STRAIN ERO=RADIAL STRAIN AT CLAD OUTER SURFACE= 0.0151211

ET=TANGENTIAL STRAIN ETO=TANGENTIAL STRAIN AT CLAD SURFACE= 0.0168502

SR=RADIAL STRESS ST=TANGENTIAL STRESS SA=AXIAL STRESS

|SRO|=ABSOLUTE VALUE OF RADIAL STRESS AT CLAD INNER SURFACE, SRO=-0.13029 1000PSI

Table 11.20. Dimensionless strains and stresses in cladding at time t=729 hours

STATION	R/RO	ER/ERO	ET/ETO	SR/|SRO|	ST/|SRO|	SA/|SRO|
1	1.0220	1.2189	1.0020	-1.0000	-16.025	-215.872
2	1.0361	1.1941	1.0030	-1.1724	-11.639	-216.165
3	1.0502	1.1699	1.0037	-1.2809	-7.203	-216.309
4	1.0643	1.1465	1.0041	-1.3278	-2.721	-216.303
5	1.0784	1.1238	1.0042	-1.3139	1.800	-216.152
6	1.0925	1.1017	1.0041	-1.2433	6.357	-215.857
7	1.1066	1.0802	1.0037	-1.1157	10.944	-215.419
8	1.1207	1.0593	1.0031	-0.9332	15.555	-214.842
9	1.1348	1.0390	1.0022	-0.6978	20.188	-214.129
10	1.1489	1.0192	1.0012	-0.4114	24.835	-213.282
11	1.1630	1.0000	1.0000	-0.0757	29.494	-212.306

NOTE: R=RADIUS RO=RADIUS AT THE FUEL SURFACE=0.2730 CM

ER=RADIAL STRAIN ERO=RADIAL STRAIN AT CLAD OUTER SURFACE= 0.0150841

ET=TANGENTIAL STRAIN ETO=TANGENTIAL STRAIN AT CLAD SURFACE= 0.0168980

SR=RADIAL STRESS ST=TANGENTIAL STRESS SA=AXIAL STRESS

|SRO|=ABSOLUTE VALUE OF RADIAL STRESS AT CLAD INNER SURFACE, SRO=-0.19122 1000PSI

Table 11.21. Dimensionless strains and stresses in cladding at time t=1000 hours

STATION	R/RO	ER/ERO	ET/ETO	SR/|SRO|	ST/|SRO|	SA/|SRO|
1	1.0220	1.2185	1.0028	-1.0000	-9.971	-159.549
2	1.0361	1.1937	1.0037	-1.0984	-6.726	-159.747
3	1.0502	1.1696	1.0043	-1.1504	-3.444	-159.834
4	1.0643	1.1463	1.0046	-1.1568	-0.127	-159.813
5	1.0784	1.1236	1.0046	-1.1206	3.218	-159.683
6	1.0925	1.1015	1.0044	-1.0418	6.589	-159.448
7	1.1066	1.0801	1.0040	-0.9216	9.983	-159.108
8	1.1207	1.0592	1.0033	-0.7619	13.395	-158.665
9	1.1348	1.0390	1.0024	-0.5635	16.822	-158.123
10	1.1489	1.0192	1.0013	-0.3276	20.260	-157.482
11	1.1630	1.0000	1.0000	-0.0563	23.706	-156.745

NOTE: R=RADIUS RO=RADIUS AT THE FUEL SURFACE=0.2730 CM

ER=RADIAL STRAIN ERO=RADIAL STRAIN AT CLAD OUTER SURFACE= 0.0150437

ET=TANGENTIAL STRAIN ETO=TANGENTIAL STRAIN AT CLAD SURFACE= 0.0169502

SR=RADIAL STRESS ST=TANGENTIAL STRESS SA=AXIAL STRESS

|SRO|=ABSOLUTE VALUE OF RADIAL STRESS AT CLAD INNER SURFACE, SRO=-0.25745 1000PSI